

THE PROTEIN TYROSINE PHOSPHATASE, SHP2, FUNCTIONS IN MULTIPLE
CELLULAR COMPARTMENTS IN FLT3-ITD+ LEUKEMIA

Briana Marie Richine

Submitted to the faculty of the University Graduate School

in partial fulfillment of the requirements

for the degree

Doctor of Philosophy

in the Department of Medical and Molecular Genetics,

Indiana University

June 2016

Accepted by the Graduate Faculty, Indiana University, in partial fulfillment of the requirements for the degree of Doctor of Philosophy.

Rebecca J. Chan, MD, PhD, Chair

Doctoral Committee

Nadia Carlesso, MD, PhD

March 9, 2016

Karen E. Pollok, PhD

Kenneth E. White, PhD

DEDICATION

I would like to dedicate my doctoral dissertation to my late father, Stephen C. Richine. You always encouraged me to follow my dreams and passions, and I wish you could be here to see me accomplish this one.

ACKNOWLEDGMENTS

First and foremost, I would like to sincerely thank my mentor, Dr. Rebecca Chan. Her unwavering support, encouragement, and guidance helped shape me into a better scientist and a better person. I am so thankful to have had an opportunity to work in her laboratory and learn from her every day. I will carry her wisdom with me as I embark on the next chapter of my career.

I would next like to thank my advisory and research committee, members both past and present, for their continuous support and insight, which helped shape both my project and myself. To Drs. Karen Pollok, Kenneth White, Nadia Carlesso, Mingjiang Xu, Xin Zhang, and Brenda Grimes: thank you for selflessness and willingness to be a member of my committee. Meeting with you all helped strengthen my skills as a scientist and as a public speaker.

Additionally, I would like to thank all the members of the Chan Lab who have helped develop me as a research scientist. Dr. Sarah Nabinger, Dr. Xingjun Li, Dr. Libby Virts, Dr. Charles Goodwin, Lisa Deng, Joshua Bowling, and Tirajeh Saadatzaadeh: your friendship and camaraderie have been priceless and I couldn't have asked for a better group to have alongside of me during this journey.

Moreover, I would like to thank the members and administration of the Hematologic Malignancies and Stem Cell Biology group at IUSM for their collaboration and assistance whenever needed. I would also like to thank the IUSM *In Vivo* Therapeutics Core for their assistance with all of the mouse transplants in my dissertation

work. Additionally, I would like to thank Dr. Scott Boswell for providing AML patient samples for this study.

I would like to thank the following sources for funding my studies and research during my time as a graduate student: National Institute of Health (NIH), IU Simon Cancer Center (IUSCC), and the National Cancer Institute (NCI).

Finally, I would like to acknowledge my parents, Maureen and Stephen Richine. Thank you for instilling a strong work ethic in me early on in my educational career. Your unwavering support and love has meant the world to me. I look up to you both and thank you endlessly for your presence in my life. To my sister, Caitlin, and all my friends, thank you for always providing great advice, stress relief, and humor when I needed it most.

THE PROTEIN TYROSINE PHOSPHATASE, SHP2, FUNCTIONS IN MULTIPLE
CELLULAR COMPARTMENTS IN FLT3-ITD+ LEUKEMIA

FMS-like tyrosine receptor kinase-internal tandem duplications (FLT3-ITDs) are the most frequent deleterious mutations found in acute myeloid leukemia (AML) and portend a poor prognosis. Currently, AML patients typically achieve disease remission, yet undergo high rates of disease relapse, implying a residual post-treatment reservoir of resistant malignancy-initiating cells. This begs for new therapeutic approaches to be discovered, and suggests that targeting multiple cellular compartments is needed for improved therapeutic approaches. We have shown that the protein tyrosine phosphatase, Shp2, associates physically FLT3-ITD at tyrosine 599 (Y599) and positively regulates aberrant STAT5 activation and leukemogenesis. We also demonstrated that genetic disruption of *Ptpn11*, the gene encoding Shp2, increased malignancy specific survival of animals transplanted with FLT3-ITD-transduced cells, suggesting that Shp2 may regulate the function of the malignancy-initiating cell. Taken together, I hypothesized that inhibiting Shp2 can target both FLT3-ITD+ AML tumor cells as well as FLT3-ITD-expressing hematopoietic stem cells. To study this hypothesis, I employed two validation models including genetic inhibition of Shp2 interaction with FLT3-ITD in 32D cells or genetic disruption of Shp2 in FLT3-ITD-expressing HSCs.

Using FLT3-ITD-expressing 32D cells as an AML tumor model, I found that mutating the Shp2 binding site on FLT3-ITD (Y599) reduced proliferation *in vitro* and increased latency to leukemia onset *in vivo*. Further, pharmacologic inhibition of Shp2 preferentially reduced proliferation of FLT3-ITD+ primary AML samples compared to FLT3-ITD- samples, and cooperated with inhibition of the lipid kinase, phospho-inositol-3-kinase (PI3K), and of the tyrosine kinase, Syk, to reduce proliferation of both FLT3-ITD+ and FLT3-ITD- AML samples.

To evaluate the stem cell compartment, I crossed a murine locus-specific knock-in of FLT3-ITD with Shp2^{flox/flox}; Mx1-Cre mice to generate FLT3-ITD; Shp2+/- mice and found that Shp2 heterozygosity dramatically inhibits hematopoietic stem cell engraftment in competitive transplant assays. Further, I found that lineage negative cells from FLT3-ITD; Shp2+/- mice demonstrated increased senescence compared to control mice, suggesting that Shp2 may regulate senescence in FLT3-ITD-expressing hematopoietic stem cells.

Together, these findings indicate a cooperative relationship between the tyrosine phosphatase, Shp2, and the kinases PI3K and Syk in AML tumor cells, and indicate that Shp2 plays a positive role in the stem cell compartment to promote stem cell function of the malignancy-initiating cell in AML. Therefore, targeting Shp2 may hold therapeutic benefit for patients with FLT3-ITD+ AML.

Rebecca J. Chan, MD, PhD, Chair

TABLE OF CONTENTS

LIST OF TABLES	xi
LIST OF FIGURES	xii
LIST OF ABBREVIATIONS.....	xviii
CHAPTER ONE	1
INTRODUCTION	1
Acute Myeloid Leukemia	1
Normal Hematopoiesis.....	6
The Receptor Tyrosine Kinase, FLT3	8
Protein Tyrosine Phosphatase, Shp2.....	9
FLT3-ITD Mutations in AML	13
Treatment for FLT3-ITD+ AML	17
Shp2- and FLT3-ITD-induced Leukemogenesis	18
Spleen Tyrosine Kinase, Syk	20
Summary	23
Significance.....	25
CHAPTER TWO	28
MATERIALS AND METHODS.....	28
Materials	28
Plasmids	28
Primers	28
Patient Samples.....	30

Mice	30
Antibodies	31
Inhibitors	33
Biochemical Assays	33
Methods.....	34
Cell Culture.....	34
Transfection	35
Retroviral Transduction	36
Cell Sorting.....	36
³ H-Thymidine Incorporation Assay	36
Total Cellular Protein Extraction	37
Immunoblot Analysis.....	37
Immunoprecipitation Analysis.....	38
Apoptosis Assay.....	38
β-Galactosidase Staining Assay	39
Transplants	39
Chromatin Immunoprecipitation Assay	41
Statistical Analysis.....	42
CHAPTER THREE	43
SHP2 FUNCTIONS AT TYR599 AND TYR768 ON THE FLT3-ITD RECEPTOR TO POSTIVELY REGULATE SIGNALING AND LEUKEMOGENESIS	43
Introduction.....	43
Results.....	50

Discussion.....	97
CHAPTER FOUR.....	102
REGULATION OF SENESCENCE IN FLT3-ITD-EXPRESSING MALIGNANCY-INITIATING CELLS BY SHP2	102
Introduction.....	102
Results.....	107
Discussion.....	152
CHAPTER FIVE	159
OVERALL CONCLUSIONS AND IMPLICATIONS	159
REFERENCES	165
CURRICULUM VITAE	

LIST OF TABLES

Table 2.1: Genotyping primers	28
Table 2.2: Real Time-PCR primers	29
Table 2.3: Chromatin Immunoprecipitation Primers	30
Table 2.4: Primary Antibodies	31
Table 2.5: Secondary Antibodies	33
Table 2.6: Inhibitors	33
Table 2.7: Biochemical and Functional Assays	33
Table 3.1: Inhibitors and their IC ₅₀ values used in pharmacologic studies	68

LIST OF FIGURES

Figure 1.1. Simplified schematic of hematopoiesis versus leukemogenesis	2
Figure 1.2. Evolution of leukemogenesis, highlighting the role of pre-leukemic stem cells in the development of disease	5
Figure 1.3. Hierarchy of hematopoietic cell lineages in mouse and human	7
Figure 1.4. Schematic of the protein tyrosine phosphatase, Shp2	12
Figure 1.5. Schematic of the FLT3 receptor and known internal tandem duplications (ITDs).....	15
Figure 1.6. Overall survival curve of AML patients with or without FLT3-ITD mutations.....	16
Figure 1.7. Schematic depicting Shp2 signaling from WT FLT3 and FLT3-ITD.....	19
Figure 1.8. Schematic of the tyrosine kinase, Syk.....	22
Figure 3.1. Knockdown of Shp2 reduces STAT5 activity at the Bcl-X _L promoter, <i>BCL2L1</i>	45
Figure 3.2. Mutation of Tyr599 results in reduced hyperproliferation and STAT5 activation.....	46
Figure 3.3. Hypothesis of the signaling transduction pathways that promote FLT3-ITD-mediated hyperproliferation and leukemogenesis	49
Figure 3.4. Constructs used to examine the role of N51-FLT3 Tyr599 and Tyr768.....	51
Figure 3.5. Stable 32D cell lines highly express WT, N51, or N51-mutant constructs..	52

Figure 3.6. Mutation of duplicated Tyr599 and Tyr768 reduces the interaction between Shp2 and FLT3-ITD	55
Figure 3.7. Mutation of duplicated Tyr599 and Tyr768 significantly reduces the hyperproliferation of N51-FLT3 cells	56
Figure 3.8. Neither Tyr599 nor Tyr768 mutations result in lower eGFP levels in the peripheral blood compared to N51-FLT3 mice	60
Figure 3.9. N51-FLT3, N51-Y599F1/2, and N51-Y768F mice all display elevated white blood cell counts in the peripheral blood.....	61
Figure 3.10. N51-Y599F1/2 mice exhibit delayed progression to MPD, while N51-Y768F does not alter progression.....	62
Figure 3.11. FLT3-ITD Tyr599 is important for STAT5 activation, while FLT3-ITD Tyr768 is important for Erk activation.....	66
Figure 3.12. Schematic representation of the hypothesis that inhibition of Shp2/Syk and Shp2/PI3K will act to reduce FLT3-ITD-induced hyperproliferation.....	68
Figure 3.13. WT FLT3-expressing 32D cells did not respond to II-B08 or R406, and the combination had a minimal effect on proliferation	70
Figure 3.14. N51-FLT3-expressing 32D cells exhibit a significant response to both II-B08 and R406 treatment alone, and there was a cooperative effect of II-B08 and R406 on proliferation.	71
Figure 3.15. Shp2 inhibition and Syk inhibition work cooperatively to reduce the proliferation of AML patient samples.....	74
Figure 3.16. FLT3-ITD+ and FLT3-ITD- AML patient samples display cooperativity of Shp2 and Syk inhibition.	75

Figure 3.17. Inhibition of Shp2 and Syk results in lower levels of STAT5, Akt, and Erk phosphorylation in N51-, but not WT, FLT3 cells.....	77
Figure 3.18. Inhibition of Shp2 and Syk lower the level of active STAT5 in N51-FLT3-expressing 32D cells.....	78
Figure 3.19. Primary AML patient samples are sensitive to the inhibition of PI3K and cooperate with Shp2 inhibition to reduce proliferation.	81
Figure 3.20. FLT3-ITD+ primary AML patient samples are more sensitive to Shp2 or PI3K inhibition alone compared to FLT3-ITD- primary AML patient samples.....	82
Figure 3.21. Inhibition of Shp2 and PI3K lower the levels of STAT5, Akt, and Erk phosphorylation in N51-, but not WT, FLT3 cells.....	83
Figure 3.22. FLT3-ITD+ AML patient samples are uniquely sensitive to Shp2 inhibition by II-B08	85
Figure 3.23. II-B08 markedly reduced the clonal expansion of N51-FLT3-ITD-expressing cells	87
Figure 3.24. Schematic overview depicting the experimental procedure for analysis of II-B08 and/or GDC-0941 in preventing FLT3-ITD-induced leukemogenesis <i>in vivo</i>	89
Figure 3.25. Combination treatment of II-B08 and GDC-0941 reduces the level of eGFP positive cells in the peripheral blood.....	92
Figure 3.26. Combination treatment of II-B08 and GDC-0941 trends toward a reduction in elevated WBC counts in the peripheral blood	93

Figure 3.27. N51-FLT3-expressing mice treated with II-B08 and/or GDC-0941 all display splenomegaly upon morbidity	94
Figure 3.28. Shp2 inhibition and/or PI3K inhibition did not prevent progression to MPD in N51-FLT3-expressing mice.	95
Figure 3.29. II-B08 and GDC-0941 treatment increases the median survival of N51-FLT3-expressing mice	96
Figure 4.1. Deletion of Shp2 in FLT3-ITD-expressing mice leads to bone marrow failure.....	104
Figure 4.2. Mice transplanted with FLT3-ITD-transduced cells uniquely display lower chimerism upon Shp2 deletion.....	105
Figure 4.3. Deletion of Shp2 in FLT3-ITD-expressing cells does not result in increased apoptosis	109
Figure 4.4. Mice transplanted with WT FLT3 and FLT3-ITD do not display increased apoptosis upon the loss of Shp2.....	110
Figure 4.5. FLT3-ITD-transduced cells display increased senescence compared to WT FLT3-transduced cells.	113
Figure 4.6. Lineage depleted FLT3-ITD-expressing cells display increased senescence upon the loss of Shp2.	114
Figure 4.7. FLT3-ITD-expressing cells rapidly reduce Bmi1 expression levels upon the loss of Shp2 compared to WT FLT3-expressing cells.	116
Figure 4.8. Schematic of the FLT3-ITD mouse model used to study the function of Shp2 on senescence and HSC function	118

Figure 4.9. Examples of PCR reactions used to determine the genotypes of experimental mice.....	119
Figure 4.10. Shp2 heterozygosity in FLT3-ITD expressing LDMNCs leads to a reduction in proliferation.	122
Figure 4.11. Shp2 heterozygosity leads to elevated senescence in FLT3-ITD-expressing cells.....	124
Figure 4.12. Shp2 heterozygosity in Lin- bone marrow cells result in increased senescence in FLT3-ITD-expressing cells only.....	125
Figure 4.13. Shp2 heterozygosity corresponds to slightly reduced Bmi1 levels and elevated p16 mRNA levels.....	127
Figure 4.14. Shp2 heterozygosity does not affect Hoxa7 but lowers Hoxa9 mRNA levels.....	129
Figure 4.15. The murine and human <i>BMII</i> locus have a conserved MYC consensus sequence 181 bp upstream of the transcription start site.	131
Figure 4.16. MYC binding to the <i>BMII</i> promoter is increased in the presence of FLT3-ITD.	131
Figure 4.17. The human <i>BMII</i> locus contains four STAT5 consensus sequences that are conserved in the murine <i>Bmi1</i> locus.	134
Figure 4.18. STAT5 binding to the <i>BMII</i> locus is slightly elevated in FLT3-ITD-expressing MV411 cells.....	135
Figure 4.19. Schematic overview of the Shp2 phosphatase-mediated mechanism that regulates senescence in FLT3-ITD-expressing cells.	136

Figure 4.20. Experimental method for competitive transplants to examine the effect of Shp2 heterozygosity on FLT3-ITD+ HSC engraftment.	138
Figure 4.21. Shp2 heterozygosity severely reduces engraftment potential of FLT3-ITD-expressing cells in a competitive transplant model.	140
Figure 4.22. Shp2 heterozygosity continues to reduce the engraftment potential of FLT3-ITD-expressing cells in a secondary transplant model.	142
Figure 4.23. Experimental method for competitive transplants to examine the effect of Shp2 heterozygosity on FLT3-ITD+ HSC engraftment in comparison to WT, Shp2 heterozygosity alone, and ITD alone.....	144
Figure 4.24. FLT3-ITD; Shp2 ^{+/-} mice display the lowest level of chimerism in a competitive transplant model.	146
Figure 4.25. Deletion of one allele of Shp2 significantly alters differentiation of FLT3-ITD-expressing cells, but not WT FLT3-expressing cells	150
Figure 4.26. Shp2 heterozygosity in FLT3-ITD donor cells have an expanded mature myeloid and reduced B cell population	151

LIST OF ABBREVIATIONS

AML.....	Acute Myeloid Leukemia
HSC.....	Hematopoietic Stem Cell
FLT3.....	<i>FMS</i> -like Tyrosine Kinase 3
FL.....	FLT3 ligand
WT.....	Wild Type
ITD.....	Internal Tandem Duplication
eGFP.....	enhanced Green Fluorescent Protein
FBS.....	Fetal Bovine Serum
LDMNC.....	Low Density Mononuclear Cells
CBC.....	Complete Blood Count
ChIP.....	Chromatin Immunoprecipitation
S.D.....	Standard Deviation
SEM.....	Standard Error of the Mean
MPD.....	Myeloproliferative Disease
WBC.....	White Blood Cell
RT-PCR.....	Real Time-Polymerase Chain Reaction

CHAPTER ONE

INTRODUCTION

Acute Myeloid Leukemia

Acute Myeloid Leukemia (AML) is a clonal malignancy of the bone marrow resulting from a block in the differentiation of myeloid progenitor cells. This block results in an accumulation of hyperproliferative myeloblasts that are unable to fully mature, thereby preventing their development into terminally differentiated hematopoietic cells, such as monocytes, neutrophils, and macrophages (Figure 1.1). Additionally, these myeloblasts overtake the bone marrow and crowd out any remaining mature blood cells. Together, this causes patients diagnosed with AML to present with fatigue due to anemia, bleeding due to thrombocytopenia, and increased risk of infection due to leukopenia (Estey and Döhner 2006).

AML is the one of the most frequently diagnosed types of leukemia, afflicting both children and adults. AML presents most often in adults over the age of 55, with a median age at diagnosis of 65 (Siegel, Miller et al. 2015). The 5-year survival rate is only 34.4% in patients under the age of 65 and dramatically lower at 4.3% in patients over 65 years of age (Deschler and Lubbert 2006). While incidence of leukemia increases with age, leukemia is still the most common cancer in children ages 15 years and younger. Both adults and children show low cure rates and sustain high levels of therapy-related morbidity due to harsh treatment regimens: radiation, rigorous and toxic high-dose chemotherapy, and allogeneic bone marrow transplantation.

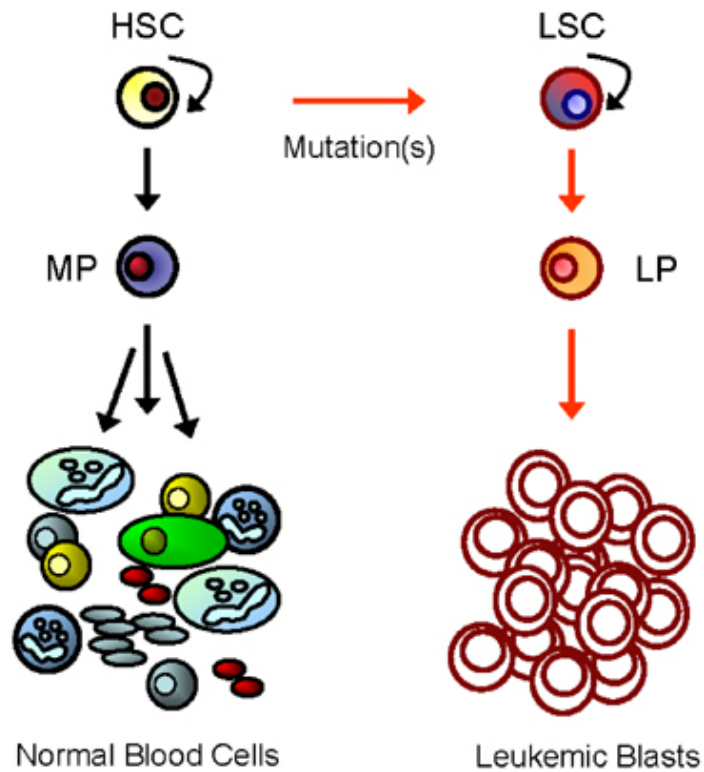


Figure 1.1. Simplified schematic of hematopoiesis versus leukemogenesis.

In normal hematopoiesis, stem cells self-renew, differentiate to multipotent progenitors (MPs), and then to terminally differentiated blood cells. In AML, leukemia stem cells (LSCs) differentiate to leukemia progenitors (LPs) and leukemic blasts which hyperproliferate and crowd out the normal blood cells. Figure adapted from Jordan et al. (Jordan and Guzman 2004).

As mentioned, AML remains difficult to treat; in adults, there is only a 19% cure rate for AML at 5 years post-diagnosis (Koh, Nakamae et al. 2011). Because of the low survival rate, low cure rate, and harsh treatment options, older patients are often treated with supportive, palliative therapies rather than curative therapies. Moreover, the survival rate of AML in older adults has not changed significantly. This becomes a concern when one considers the increasing lifespan of adults in the United States. Incidence of diagnosed AML is likely to increase greatly for this reason. Additionally, a high rate of relapse in patients after treatment suggests that we are not targeting all the essential populations of cells responsible for the development of disease.

On average, diagnosed AML has approximately five mutations, suggesting a serial acquisition of mutations in specific clones of hematopoietic stem cells (HSCs) (Cancer Genome Atlas Research 2013). Recently, the idea of pre-leukemic stem cells has emerged. These cells are characterized by acquiring early mutations, typically in genes regulating epigenetics, such as DNA methylation and chromatin modification (Chan and Majeti 2013). Mutations in ten-eleven translocation methylcytosine dioxygenase 2 (*TET2*), for example, result in an increase in HSC function, giving them a competitive advantage. Not surprisingly, TET2 protein is highly mutated in pre-leukemic HSCs (Moran-Crusio, Reavie et al. 2011). This suggests that early mutations allow for further mutations to acquire in genes responsible for signaling (such as the FLT3-ITD mutation), providing the clone a self-renewal and proliferative advantage and thereby promoting development into a full blown leukemic clone (Figure 1.2).

In essence, effective and less toxic therapies are needed that target not only bulk tumor cells but also the pre-leukemic, malignancy-initiating stem cells. As we are

interested in the signaling that goes awry leading to leukemogenesis, we first need to consider what occurs in normal hematopoiesis.

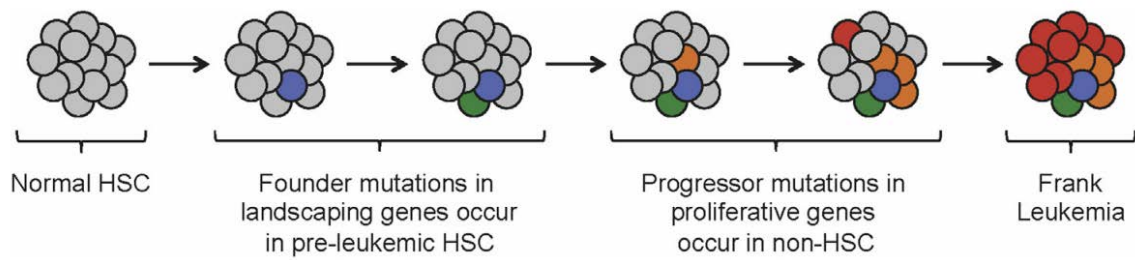


Figure 1.2. Evolution of leukemogenesis, highlighting the role of pre-leukemic stem cells in the development of disease.

Normal HSCs acquire epigenetic mutations, resulting in a pre-leukemic HSC. Further mutations acquired in these pre-leukemic HSC lead to frank leukemia. Figure adapted from Majeti 2014. (Majeti 2014).

Normal Hematopoiesis

Hematopoiesis is the generation of all fully differentiated blood cells in the body. Prior to birth, hematopoiesis occurs in the yolk sac and fetal liver (Yoder, Hiatt et al. 1997, Kumaravelu, Hook et al. 2002, Li, Johnson et al. 2003), and moves to the spleen and bone marrow after birth. The hematopoietic hierarchy begins with the smallest population and most primitive cell type, the Long Term- Hematopoietic Stem Cell (LT-HSC). These LT-HSCs undergo symmetric and asymmetric cell division, allowing for their self-renewal as well as differentiation into more mature lineage-specific cells. LT-HSCs differentiate into lineage-specific progenitors called the common myeloid progenitor (CMP) and the common lymphoid progenitor (CLP). CMPs give rise to monocytes/macrophages, granulocytes, and erythrocytes, while CLPs give rise to B cells, T cells, and NK cells (Figure 1.3).

Cell surface markers provide a precise way to distinguish the different hematopoietic lineages and to analyze individual populations (Figure 1.3). For example, one population of cells enriched for HSCs and progenitors are defined as lineage negative (Lin⁻, meaning cells lack mature markers, such as Mac-1 and Gr-1), Sca1⁺, and c-Kit⁺. Each terminally differentiated cell type expresses a unique set of markers that allow one to identify the hematopoietic composition of the blood and bone marrow. *FMS*-like tyrosine kinase 3 (FLT3), also referred to as CD135, is not expressed in most LT-HSCs, but is seen in the multipotent progenitor (MPP) compartment in mice and the CMP compartment in humans.

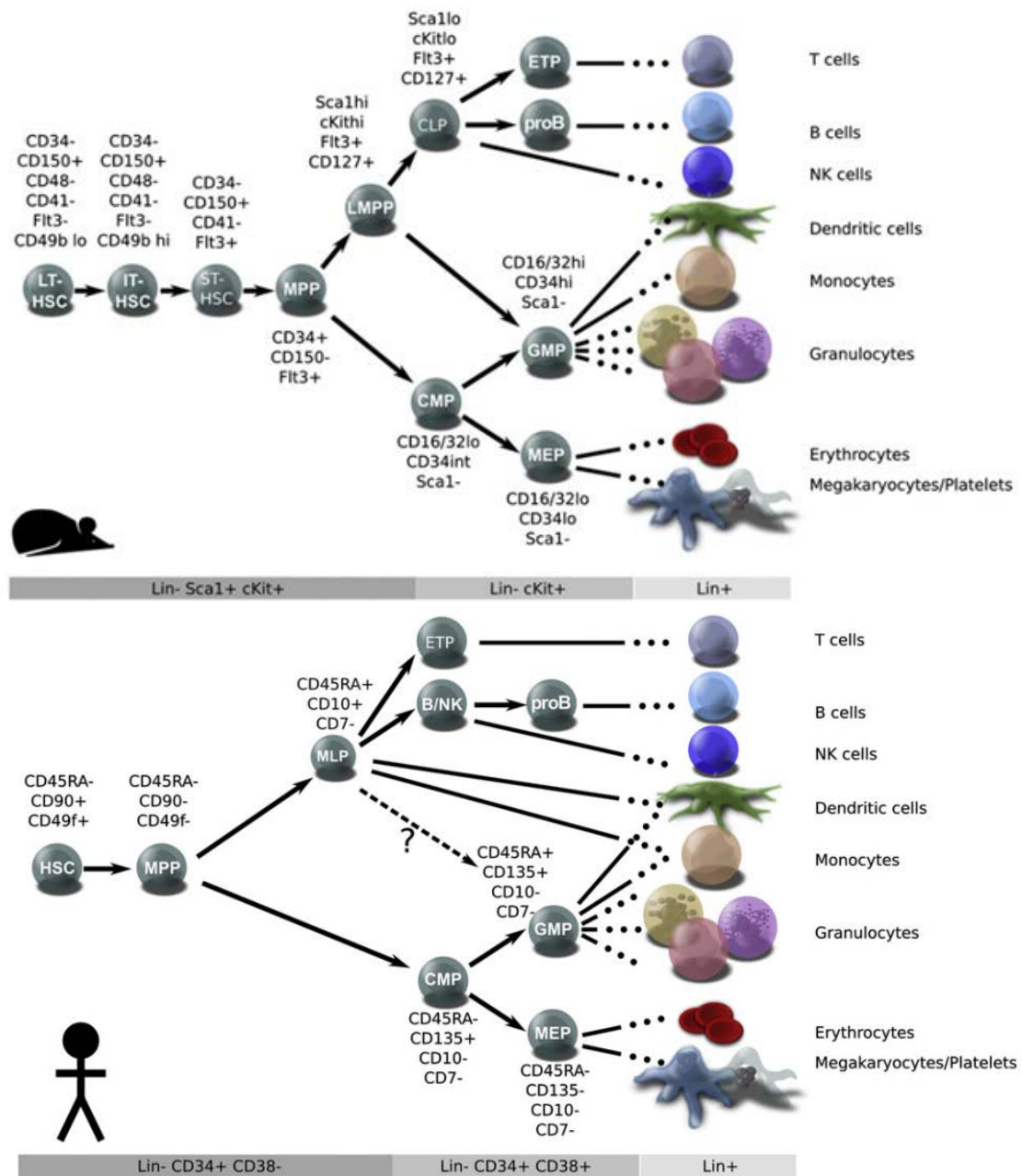


Figure 1.3. Hierarchy of hematopoietic cell lineages in mouse and human.

Schematic of normal hematopoiesis in *mus musculus* (mice) and humans. Each cell population is defined by different combinations of cell surface markers, allowing for the isolation, quantitation, and analysis of individual populations. Figure adapted from Doulatov et al. (Doulatov, Notta et al. 2012).

The Receptor Tyrosine Kinase, FLT3

The receptor tyrosine kinase, FLT3, is a member of the class III subfamily of receptor tyrosine kinases and is composed of an extracellular (EC) portion containing 5 immunoglobulin-like repeats, a transmembrane (TM) domain, a juxtamembrane (JM) domain, and cytoplasmic tyrosine kinase domains (TK1 and TK2) split by an insert sequence (Figure 1.5) (Reilly 2002). *FLT3* gene encodes a 993 amino acid protein that weighs approximately 130 and 160 kDA (depending on its glycosylation status). FLT3 is expressed on immature hematopoietic multi-potent progenitors and FLT3 levels decrease as progenitor cells differentiate. While FLT3 is expressed in short-term HSCs, it does not appear to be expressed in LT-HSCs. FLT3 is an important regulator of cell proliferation, survival, and differentiation in a variety of hematopoietic cell types. For example, while mice lacking FLT3 fail to produce normal levels of T cells and myeloid cells, only minor defects were evident in the most primitive HSC compartment (Mackarehtschian 1995).

Upon FLT3 ligand (FL) stimulation, WT FLT3 dimerizes and autophosphorylates specific tyrosine residues in the juxtamembrane domain, resulting in a conformational change that permits further autophosphorylation. Griffith et al. determined the crystal structure of the autoinhibited form of FLT3 and showed that Tyr589 and Tyr591 are located between the JM-S and C lobe of the receptor and are important tyrosines for the orientation switch allowing for further transphosphorylation and activation of FLT3 (Griffith, Black et al. 2004). Once phosphorylated, residues on the FLT3 receptor are able to recruit various signaling molecules linked within multiple transduction pathways, such as the Mitogen-Activated Protein Kinase (MAPK)/Erk and

Phosphatidylinositide 3-Kinase (PI3K)/Akt pathways. In a study done by Heiss et al., tyrosine residues 572, 589, 591, and 599 in the juxtamembrane domain were identified as autophosphorylation sites of FLT3 *in vivo*. These studies also demonstrated tyrosine 599 (Tyr599, Y599) to be critical for the activation of Erk, as mutation of Tyr599 to phenylalanine (F) (Y599F), resulted in lower phospho-Erk levels. Also, in a glutathione S-transferase (GST) assay, the mutation of Tyr599 led to decreased binding of the protein tyrosine phosphatase, Shp2, a known activator of Erk (Heiss, Masson et al. 2006, Chan, Cheung et al. 2011). A representative schematic of FLT3 signaling in normal hematopoiesis is shown in Figure 1.7, left panel.

Protein Tyrosine Phosphatase, Shp2

The non-receptor protein tyrosine phosphatase, Shp2, is encoded by the gene *Ptpn11*. Shp2 contains two Src homology 2 (SH2) domains (N-SH2 and C-SH2) at the amino-terminal end and a phosphatase domain at the carboxy-terminal end (Figure 1.4) (Chan and Feng 2007). Shp2 is ubiquitously expressed and has been shown to be important in major cellular processes, such as proliferation, differentiation, and migration. Under normal conditions, Shp2 phosphatase activity has been shown to be required for Ras, a regulator of the MAPK/Erk pathway, although the exact mechanism remains unclear (Neel, Gu et al. 2003, Mohi and Neel 2007). It is thought that Shp2 dephosphorylates and inactivates inhibitors of the Ras/Erk pathway. SPRED1 has been shown to be a substrate of Shp2, and that dephosphorylation of SPRED1 lead to increased Ras/Erk activation (Quintanar-Audelo, Yusoff et al. 2011). Another possible substrate of Shp2 in normal signaling is Sprouty. Like SPRED1, Sprouty has been

shown to be able to be dephosphorylated by Shp2 and this reversed the inhibitory effect on MAPK (Erk) activation (Hanafusa, Torii et al. 2004).

Somatic mutations in *PTPN11*, the human gene encoding for Shp2, have been identified in approximately 4% of AML cases, and are commonly found in the fatal childhood disease, juvenile myelomonocytic leukemia (JMML) (Tartaglia, Niemeyer et al. 2003, Loh, Reynolds et al. 2004, Loh, Vattikuti et al. 2004, Tartaglia, Martinelli et al. 2004, Kratz, Niemeyer et al. 2005).

The necessity of Shp2 is exemplified in Shp2 knockout mice, which are embryonic lethal (Saxton, Henkemeyer et al. 1997). These mice, with an internal deletion of approximately 60 amino acid residues in the N-SH2 domain, fail to gastrulate properly, which prevents normal development. Additionally, the laboratory of Gen-Sheng Feng developed a conditional Shp2 knockout animal in which two loxP sites were introduced into the introns flanking exon 4 of the *Ptpn11* allele. Upon induction of Cre expression, recombination of the *Ptpn11* allele occurs, resulting in the deletion of exon 4 and generation of a stop codon, rendering the Shp2 protein non-functional (Zhang, Chapeau et al. 2004).

This Shp2^{flox/flox} mouse was crossed with Mx1-Cre to examine the importance of Shp2 in hematopoietic cells. The Mx1 promoter, in response to interferon alpha or double stranded RNA (such as polyI:C), will turn on Cre recombinase expression in hematopoietic cells. Using this conditional *Ptpn11* knockout model, the importance of Shp2 in the maintenance of adult HSCs was demonstrated. In the context of Mx1-Cre; Shp2^{flox/flox}, mice displayed cytopenia in the bone marrow, spleen, and peripheral blood as well as poor HSC function (Zhu, Ji et al. 2011). Additionally, other investigators

showed that mice transplanted with bone marrow cells in which Shp2 was deletion exhibited decreased chimerism, and these Shp2 knockout bone marrows cells display increased apoptosis, and decreased Erk and Akt upon loss of Shp2. Conversely, deletion of Shp2 in recipient mouse had no effect on transplantation of wild-type HSCs, showing a cell autonomous dependence on Shp2 (Chan, Cheung et al. 2011).

Shp2 functions in the hematopoietic stem and progenitor cell (HSPC) compartment, as evidenced by the fact that Shp2 heterozygous (+/-) HSCs exhibit decreased self-renewal, decreased quiescence, and decreased engraftment compared to wild-type HSCs, despite having normal hematopoiesis and peripheral blood counts overall (Chan, Li et al. 2006). Because of the necessity of Shp2 in normal hematopoiesis, its recruitment to WT FLT3, and the fact that WT Shp2 has been shown to be overexpressed in AML (Xu, Yu et al. 2005), the Chan lab previously hypothesized that Shp2 also plays a role in FLT3-dependent oncogenic leukemogenesis.



Figure 1.4. Schematic of the protein tyrosine phosphatase, Shp2.

The non-receptor protein tyrosine phosphatase contains two Src homology 2 (SH2) and the enzymatic phosphatase domain. The protein is 597 amino acids in length, corresponding to a molecular weight of approximately 72 kDa.

FLT3-ITD Mutations in AML

The *FLT3* gene is a proto-oncogene in hematopoietic cells and mutations in the receptor enhance survival and promote hyperproliferation of the leukemic blasts. Within the FLT3 receptor, two types of mutations are common in patients diagnosed with AML. First, approximately 7% of FLT3 mutations are point mutations in the activation loop of the tyrosine kinase domain (TKD). These point mutations alter the conformation of the FLT3 receptor and stabilize the open conformation (Parcells, Ikeda et al. 2006). The vast majority of AML patients have a mutation in exon 14 of the FLT3 juxtamembrane domain called internal tandem duplications (ITDs), which are in-frame insertions of several amino acids into the juxtamembrane domain of the receptor (Figure 1.5). ITDs result in ligand-independent dimerization and phosphorylation, and therefore, constitutive activation of FLT3 and downstream signaling pathways (Kiyoi, Ohno et al. 2002). As mentioned previously, Tyr589 and Tyr591 located in the JM membrane are important tyrosines for the autoinhibition of FLT3. It is hypothesized that the presence of an ITD may alter the structure of the receptor and allow for the constant exposure of these tyrosines, resulting in the constitutive phosphorylation of the JM membrane and activation of the FLT3 receptor (Rocnik, Okabe et al. 2006).

FLT3-ITDs have been shown to promote aberrant signaling pathways, leading to the constitutive activation of the pro-survival transcription factor Signal Transducer and Activator of Transcription 5, STAT5 (Hayakawa, Towatari et al. 2000, Mizuki, Fenski et al. 2000, Spiekermann, Bagrintseva et al. 2003, Choudhary, Brandts et al. 2007). STAT5-target genes, including pro-survival genes such as Bcl-X_L, Cyclin D1, and Pim-1 (Bowman, Garcia et al. 2000, Kim, Baird et al. 2005), are active in the presence of FLT3-

ITD, again supporting the growth-promoting functions of this mutation. Multiple studies have been conducted in order to tease out the mechanism through which FLT3-ITD aberrantly leads to STAT5 activation, however, an exact mechanism is still unknown. Src kinases have been shown to positively correlate with STAT5 phosphorylation and activation (Leischner, Albers et al. 2012). Conversely, a direct FLT3-ITD-mediated activation of STAT5 has been demonstrated, in addition to being a target of Src and Jak kinases, can also be a direct target of FLT3-ITD (Choudhary, Brandts et al. 2007).

Clinically, FLT3-ITDs are prevalent in approximately 25% of both pediatric and adult AML patients and portend a poor prognosis (Nakao M 1996, Thiede, Steudel et al. 2002) (Figure 1.6). Patients presenting with FLT3-ITD have shorter remission time and higher rates of relapse compared to other patients with AML, due in part to the aggressiveness and hyperproliferation caused by this mutation.

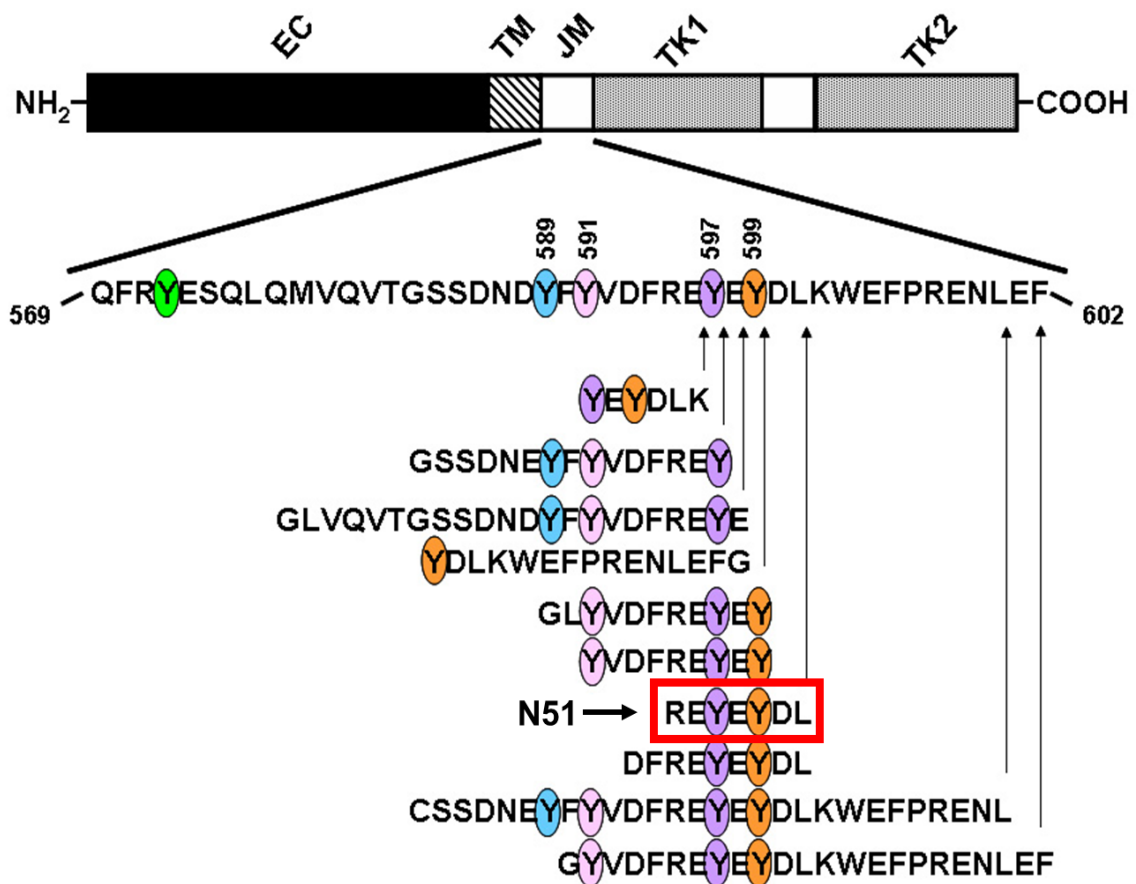


Figure 1.5. Schematic of the FLT3 receptor and known internal tandem duplications (ITDs).

The FLT3 receptor contains an extracellular domain (EC), transmembrane domain (TM), a juxtamembrane domain (JM), and two tyrosine kinase domains (TK). The FLT3 protein is 993 amino acids in length and approximately 130 and 160 kDa, depending on its glycosylation status. The expanded JM amino acid sequence of WT FLT3 is shown, with described ITDs highlighted below. N51, an ITD of 7 amino acids, is the ITD studied in this dissertation. [Figure adapted from Nabinger. (Nabinger 2012)].

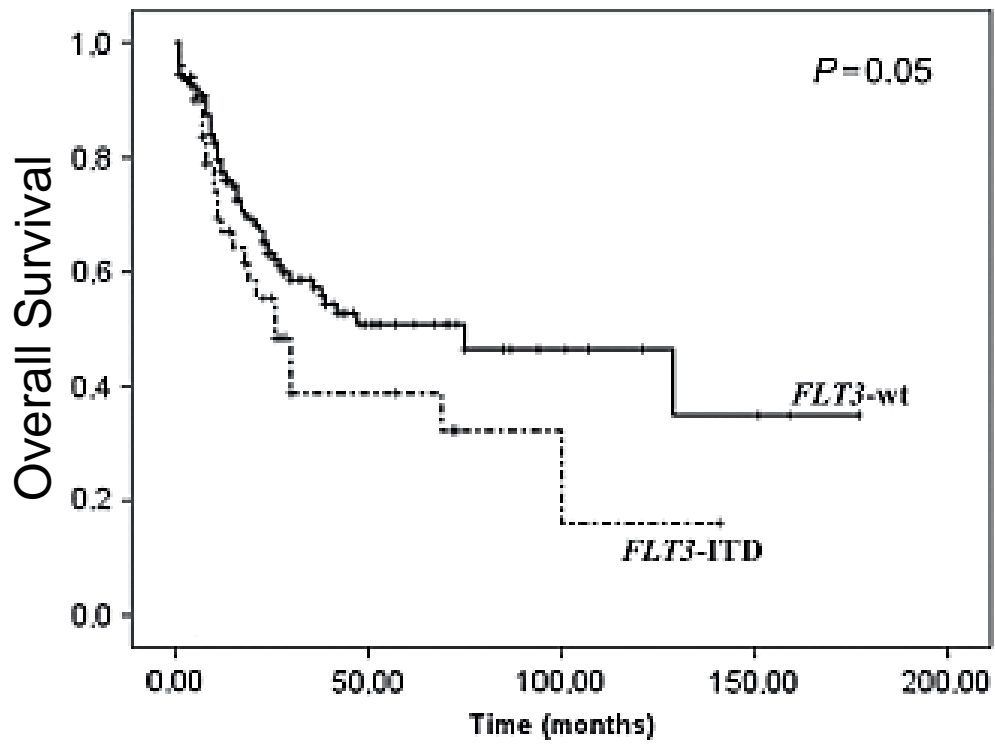


Figure 1.6. Overall survival curve for AML patients with or without FLT3-ITD mutations.

Adapted from Blau et al. (Blau, Berenstein et al. 2013).

Treatment for FLT3-ITD+ AML

As mentioned previously, current therapy for AML utilizes harsh cytotoxic therapy often coupled with HSC transplant. Although there has been much research done to seek improved therapies, the overall approach to AML treatment has been essentially unchanged for decades. The standard treatment regimen is colloquially referred to as “7+3” induction therapy, which is used to induce remission. Within this treatment protocol, the patient undergoes 7 days of treatment with cytarabine, a cytosine derivative that is incorporated into DNA and results in death of the cell, along with 3 days of an anthracycline (such as daunorubicin), which inhibits DNA synthesis by inhibiting topoisomerase II. To date, there is no conclusive evidence that increasing the doses of either drug in the 7+3 regimen improves overall survival (OS). Following the initial induction therapy, the patient undergoes consolidation therapy to help prevent relapse, which may include more rounds of cytarabine and/or a HSC transplant. However, older patients cannot tolerate this harsh treatment regimen and therefore, studies continue to be performed to identify improved and more targeted therapies.

Since FLT3 is highly mutated in AML, much dedication has gone into developing a FLT3 inhibitor. Midostaurin in combination with 7+3 provide promising results in a phase III clinical trial of newly diagnosed FLT3-ITD+ patients, but it is still too early to declare definitively (Dombret and Gardin 2016). A phase I trial suggests that sorafenib administration after HSC transplant may be effective for FLT3-ITD+ patients (Dombret and Gardin 2016). While targeting FLT3 is an attractive option, relapse is still highly prevalent because of acquired resistance in a sub-clone. Taken together, new therapies

that are less cytotoxic and more selective for all clones (including the pre-leukemic clones) are needed.

Shp2- and FLT3-ITD-induced Leukemogenesis

As Shp2 has previously been shown to be recruited to Tyr599 (Heiss, Masson et al. 2006), a commonly duplicated tyrosine in reported FLT3-ITDs, the Chan lab hypothesized that Shp2 positively regulates FLT3-ITD-induced leukemogenesis. Indeed, the Chan lab has shown that Shp2 is constitutively associated with FLT3-ITD at Tyr599 and positively regulates the aberrant STAT5 activation in FLT3-ITD+ cells (Figure 1.7, right panel) (Nabinger, Li et al. 2013). Additionally, treatment of FLT3-ITD-expressing cells with the novel Shp2 phosphatase inhibitor, II-B08, reduced phosphorylation of Shp2 and STAT5, suggesting that Shp2 phosphatase promotes STAT5 activation via the dephosphorylation, and thus activation, of a STAT5-activating kinase. However, how Shp2 functions at the FLT3 receptor to regulate STAT5 remains to be elucidated. In Chapter 3 of this dissertation, we will examine different kinases that may serve as intermediates that link Shp2 signaling to STAT5, as well as to promote FLT3-ITD-induced leukemogenesis.

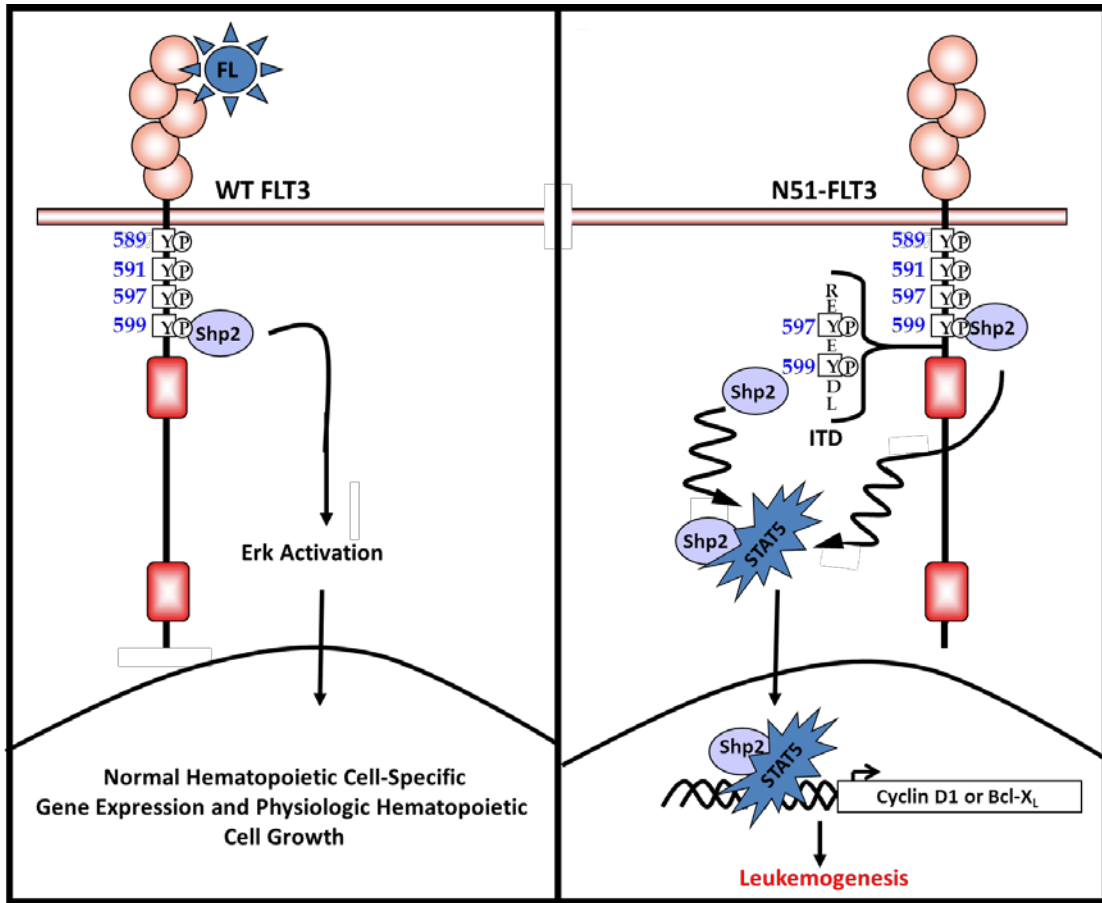


Figure 1.7. Schematic depicting Shp2 signaling from WT FLT3 and FLT3-ITD.

On the left, in physiologic conditions, FL binds to WT FLT3 promoting FLT3 dimerization and autophosphorylation with subsequent recruitment of Shp2 to Tyr599, where it can signal to Erk. In the context of FLT3-ITD (right panel), Shp2 is constitutively recruited to the duplicated Tyr599, where it binds to and leads to the activation of STAT5, promoting transcription of STAT5-target genes and leukemogenesis.

Spleen Tyrosine Kinase, Syk

Spleen tyrosine kinase, Syk, is a non-receptor protein tyrosine kinase highly expressed in hematopoietic cells and contains two SH2 domains and a kinase domain (Figure 1.8). Syk kinase has classically been known to play a prominent role in immunoreceptor signaling in adaptive immunity (Mocsai, Ruland et al. 2010). Syk kinase is important for leukocyte formation. Syk knockout mice die shortly after birth from a defect in vascular tissue and lymphatic system (Turner, Mee et al. 1995). Examination of the fetal liver cells showed a reduction in mature B cells resulting from a block in the pro-B to pre-B transition (Turner, Mee et al. 1995). To better characterize the resultant vascular alteration and lymphatic defects, Böhmer et al. used genetic mapping to identify Syk in vascular endothelial growth factor (VEGF)-producing myeloid cells. Upon the loss of Syk, they found an accumulation of VEGF that resulted in lymphatic hyperplasia (Bohmer, Neuhaus et al. 2010). Therefore, they concluded that Syk plays a role in both myeloid and lymphoid cells and directs lymphopoiesis.

Interestingly, Hahn et al. found that gefitinib, an endothelial growth factor receptor (EGFR) inhibitor was effective on AML cells. However, EGFR is not expressed in AML cells, prompting delimitation of another target. They found that Syk activation was reduced upon treatment with gefitinib, and that reduction in Syk induces myeloid differentiation (Hahn, Berchuck et al. 2009). In parallel, another RNAi screen was done and showed that Syk is a crucial mediator of Integrin- β 3 signaling in leukemic stem cells (LSCs) (Miller, Al-Shahrour et al. 2013). Treatment with the Syk inhibitor, R406, decreased leukemic growth *in vivo* (Miller, Al-Shahrour et al. 2013). Moreover,

as Syk is highly expressed in hematopoietic cells, it is an attractive therapeutic target for hematologic malignancies.

In a recent study of FLT3-ITD-induced leukemogenesis, Puissant et al. found that Syk interacts with FLT3 at tyrosine residues Y589, Y591, Y597, and Y599 in the juxtamembrane of both WT and FLT3-ITD receptors. Additionally, these investigators found that Syk enhances the phosphorylation of Tyr768 and Tyr955 on WT and FLT3-ITD receptors (Puissant, Fenouille et al. 2014). Considering the shared binding site with Shp2 on FLT3-ITD, and the fact that Syk has been shown to bind to STAT5 in the context of Integrin- β 2 signaling (Oellerich, Oellerich et al. 2013), in Chapter 3 of this dissertation, we will examine the cooperativity of Shp2 and Syk on STAT5 activation and FLT3-ITD-induced leukemogenesis.



Figure 1.8. Schematic of the tyrosine kinase, Syk.

The non-receptor tyrosine kinase contains two Src homology 2 (SH2) and the enzymatic kinase domain. The protein is 629 amino acids in length, corresponding to a molecular weight of approximately 72 kDa.

Summary

FMS-like tyrosine receptor kinase-internal tandem duplications (FLT3-ITDs) are the most frequent mutation found in acute myeloid leukemia (AML) and portend a poor prognosis. Currently, AML patients undergo high rates of relapse, suggesting that crucial populations of cells, including the pre-leukemic, malignancy-initiating stem cells, are not being properly eradicated. These findings support the concept for development of a new therapeutic strategy.

The protein tyrosine phosphatase, Shp2, is a cytosolic signaling molecule crucial for many cellular processes, and has been shown to be important for normal hematopoietic stem cell function (Chan, Li et al. 2006, Chan, Cheung et al. 2011, Zhu, Ji et al. 2011). Shp2 phosphatase is often overexpressed in AML (Xu, Yu et al. 2005) and has been shown to interact with Tyr599 in WT FLT3 (Heiss, Masson et al. 2006), a commonly duplicated amino acid in reported FLT3-ITDs. Additionally, Shp2 has been previously shown by our lab to be constitutively associated with FLT3-ITD, leading to the activation of STAT5 and the hyperproliferation of these cells (Nabinger, Li et al. 2013). We also demonstrated that genetic disruption of *Ptpn11*, the gene encoding Shp2, prevented malignancy and increased survival of animals transplanted with FLT3-ITD-transduced cells, suggesting that Shp2 may regulate the function of the malignancy-initiating cells following transplant. Taken together, we hypothesized that inhibiting Shp2 can target both the bulk tumor cells and the malignancy-initiating stem cells. More specifically, we hypothesized that Shp2 inhibition can cooperate with inhibition of other kinases to further reduce leukemogenesis in bulk tumor cells. Furthermore, we

hypothesized that FLT3-ITD-expressing stem cells are dependent on Shp2 signaling, and that loss of Shp2 will lead to altered signaling and reduced stem cell function.

As mentioned previously, Shp2 regulates FLT3-ITD-mediated leukemogenesis; however, the mechanism through which Shp2 functions at the receptor remains unclear. As Shp2 is a phosphatase, it itself cannot phosphorylate STAT5, so we set out to delineate a pathway in which Shp2 is working at FLT3-ITD to promote STAT5 activation, as well as other FLT3-ITD-effectors. Based on the findings that Syk kinase has been shown to interact with and positively regulate STAT5 (Leischner, Albers et al. 2012, Oellerich, Oellerich et al. 2013, Sprissler, Belenki et al. 2014), and that Syk kinase has also been shown to be recruited to Tyr599 on FLT3 to phosphorylate Tyr768 on the inter-kinase domain of FLT3 (Puissant, Fenouille et al. 2014), we ***hypothesized that the duplicated Tyr599 on N51-FLT3-ITD permits increased Shp2 recruitment, allowing Shp2 to dephosphorylate, and thus activate, Syk kinase, leading to constitutive phosphorylation and activation of STAT5, as well as promoting Tyr768-dependent activation of PI3K, thereby promoting leukemogenesis (Figure 3.3).*** Indeed, we provide evidence that Shp2 cooperates with Syk to promote STAT5 activation and hyperproliferation of N51-FLT3-ITD-expressing 32D cells and primary AML samples, as seen through both pharmacologic and genetic studies. Inhibition with Syk was also able to reduce activation of Akt and Erk. Moreover, we show that Shp2 and PI3K inhibition cooperate to reduce Akt and Erk signaling and normalize hyperproliferation, again through pharmacologic and genetic studies.

As Shp2 phosphatase functions in FLT3-ITD-induced leukemogenesis, and that Shp2 is important for HSC function, such that Shp2 heterozygosity results in decreased

quiescence and repopulating ability in competitive transplant models (Chan, Li et al. 2006), we reasoned that Shp2 may also be critical for the malignancy-initiating HSC function. *We hypothesized that FLT3-ITD HSPCs are dependent on Shp2, and that deletion of Shp2 in this compartment would lead to reduced stem cell function, causing increased senescence and bone marrow failure in transplant mice.* In the following work, we show that loss of Shp2 in cells expressing FLT3-ITD, but not WT FLT3, leads to bone marrow failure *in vivo* due to an increase in senescence and reduction in stem cell function, as seen through competitive transplant models. Moreover, we outlined a pathway in which Shp2 function is linked to STAT5, Myc, and/or Hoxa9 to regulate Bmi1 and senescence.

Collectively, we show that there is an increased dependence of FLT3-ITD-expressing HSPCs on Shp2, and that Shp2 plays a positive regulatory role at FLT3-ITD to induce leukemogenesis. We believe targeting Shp2 may hold therapeutic benefit for FLT3-ITD+ AML patients, as it may be a key effector that can affect both the pre-leukemic, malignancy-initiating stem cells as well as the bulk tumor cells.

Significance

Standard treatment for AML utilizes rigorous and toxic chemotherapy agents that the majority of older patients cannot tolerate (Deschler and Lubbert 2006), and produces lifelong morbidities suffered by childhood AML survivors. In essence, more targeted, effective and less toxic therapies are needed.

FLT3-ITD positivity results in the aberrant activation of STAT5, hyperproliferation, and results in a poor prognosis for AML patients. FLT3-ITDs are commonly studied mutations and have generated intense interest as drug targets for drug development. Unfortunately little success has been achieved using FLT3 inhibitors as a monotherapy (Pratz and Levis 2010); therefore, the identification of novel pharmacologic agents that preferentially target FLT3-ITD+ AML are needed. Shp2 may serve as a novel therapeutic option, as Shp2 inhibition can lead to a decrease in hyperproliferation and a reduction in phospho-STAT5 levels, potentially bearing clinical relevance for FLT3-ITD+ AML patients.

In the following work, we delineated a pathway by which the interaction between Shp2 and FLT3-ITD can lead to aberrant STAT5 and Erk activation, which ultimately leads to leukemogenesis. Through the following experiments, we provide support for a novel targeted therapy of Shp2 inhibition in combination with PI3K or Syk inhibition to treat patients diagnosed with FLT3-ITD+ AML. These improved treatment strategies will allow physicians to bypass the standard, harsh regimens currently in practice. Additionally, these studies are timely and innovative, as Shp2 phosphatase inhibitors for potential clinical use are in development, and may provide a novel approach to FLT3-ITD+ AML.

AML is a clonal disorder, giving rise to the idea that hematopoietic stem cells harboring somatic mutations bear a competitive advantage, thereby becoming leukemic stem cells (Skoda 2007, Ding, Ley et al. 2012). By investigating the role of Shp2 in FLT3-ITD+ stem cells, we provide evidence that Shp2 is essential for malignant stem cell function and that targeting Shp2 in FLT3-ITD+ AML may target the primitive

malignancy-initiating cell population. It is thought that AML has a high rate of relapse in part because we are not targeting the correct population of cells. We provide support for targeting Shp2 in FLT3-ITD+ patients, as FLT3-ITD-expressing stem cells are more sensitive to the loss of Shp2 than WT FLT3 cells.

Taken together, we believe that Shp2 is essential for both bulk tumor cells as well as the malignancy-initiating stem cells. By targeting Shp2, one can target multiple cellular compartments necessary for FLT3-ITD-induced leukemogenesis.

CHAPTER TWO

MATERIALS AND METHODS

Materials

Plasmids

WT FLT3, FLAG-WT FLT3, N51-FLT3, FLAG-N51-FLT3, FLAG-N51-FLT3-Y599F1/2, and FLAG-N51-FLT3-Y768F constructs obtained from human patient cDNA were expressed using the bicistronic Murine Stem Cell Virus (pMSCV) vector, co-expressing enhanced Green Fluorescent Protein (eGFP) as a selection marker. FLAG-FLT3 fusion constructs were first generated in the pFLAG vector, and then sub-cloned into the pMSCV vector. N51-FLT3 is characterized by the duplication of the following amino acid sequence: REYEYDL.

Primers

All PCR reactions were performed using oligonucleotides synthesized by Invitrogen.

Table 2.1: Genotyping Primers

Gene	Forward Primer (5' → 3')	Reverse Primer (3' → 5')
Shp2 ^{lox}	ACGTCATGATCCGCTGTCAG	ATGGGAGGGACAGTGCAGTG
Mx1-Cre	GCCTGCATTACCGGTCGATGC AACGAGTG	CTGGCAATTTCCGGCTATACG TAACAGGGTG
Shp2 ^{null}	AAGAGGAAATAGGAAGCATT GAGGA	TAGGGAATGTGACAAGAAAG CAGTC

Gene	Forward Primer (5' → 3')	Reverse Primer (3' → 5')
WT FLT3	TCTGGTTCCATCCATCTTCC	AGGAAGTCGATGTTGGCACT
FLT3 ITD	TCTGGTTCCATCCATCTTCC	TGGCTACCCGTGATATTGCT

Table 2.2: Real Time-PCR Primers

Gene	Forward Primer (5' → 3')	Reverse Primer (3' → 5')
b-actin	TACAATGAGCTGCGTGTGG	ACATGGCTGGGGTGTGA
S16	TGCGGTGTGGAGCTCGTGC TTGT	GCTACCAGGCCTTTGAGATG GA
Shp2	GATGGTTTCACCCCAACAT C	GCAAACCTTCTCCCCACCATA
Bmi1	TGGCTCGCATTTCATTTTATG	AGGAGTGGTCTGGTTTTGTG
Hoxa7	TATGTGAACGCGCTTTTTA GCA	GGGGCTGTTGACATTGTAT AA
Hoxa9	CCCCGACTTCAGTCCTTGC	GATGCACGTAGGGGTGGTG
p16	GAACTCTTTCGGTTCGTACC C	GAATCTGCACCGTAGTTGAG C

Table 2.3: Chromatin Immunoprecipitation Primers

Gene	Forward Primer (5' → 3')	Reverse Primer (3' → 5')
STAT5_1	CAGAGAGCGAATAGAACTG TTT	GCCTCAGCTTGACACCTTAT A
STAT5_2	TCACTTGGGCTTGACAGTG A	CACTAAGCCCACTAAATCCT TT
STAT5_3	ACTTCGTGATCGGTGGTTTT	GAACAGCCTTCTTGGTGCTT
STAT5_4	ACTTCAGTGAGGTCTGGAA	AACAATACACCAGCCGACA
Myc	ACGGGCCTGACTACACCGA CACT	CTGAAGGCAGAGTGGAAC TGACAC

Patient Samples

Primary patient peripheral blood samples were obtained with prior patient consent and given to us through collaborations with Drs. Scott Boswell and Heiko Konig (under the Institutional Review Board (IRB) #9812-11, Principle investigator: Dr. Larry Cripe), as well as Dr. Kent Robertson.

Mice

C3H/HeJ

C3H/HeJ transplant recipient mice were purchased from Jackson Laboratory at approximately 5-6 weeks of age.

BoyJ

BoyJ transplant recipient mice were purchased from the Indiana University School of Medicine *In Vivo* Therapeutics Core at approximately 5-6 weeks of age.

C57/BoyJ F1

F1 transplant recipient mice were purchased from the Indiana University School of Medicine *In Vivo* Therapeutics Core.

Shp2^{flox}

Shp2^{flox/flox} animals were generous gift from Dr. Gen-Sheng Feng (Zhang, Eric E et al, 2004).

Mx1-Cre

Mx1-Cre mice were a generous gift from Dr. Reuben Kapur and crossed with Shp2^{flox} mice to generate Shp2^{flox}; Mx1-Cre mice.

FLT3-ITD

FLT3-ITD knock-in mice were purchased from Jackson Laboratory (B6.129-*Flt3^{tm1Dgg}/J*) and crossed with the Shp2^{flox}; Mx1-Cre mice.

Antibodies

Table 2.4: Primary Antibodies

Primary Antibody	Vendor	Clone
Total-FLT3	Santa Cruz	C-20

Primary Antibody	Vendor	Clone
FLAG	Sigma-Aldrich	M2
Phospho-STAT5 (Y594)	Cell Signaling	N/A
Total-STAT5	Cell Signaling	N/A
Total-STAT5 (ChIP)	Santa Cruz	N-20
Total-Myc (ChIP)	Santa Cruz	9E10
Phospho-Shp2 (Y580)	Cell Signaling	N/A
Total-Shp2	Santa Cruz	C-18
Phospho-Erk	Cell Signaling	N/A
Total-Erk	Cell Signaling	N/A
Phospho-Akt (S473)	Cell Signaling	587F11
Total-Akt	Cell Signaling	N/A
GAPDH	Biodesign International	6C5
Acetyl-Histone H4	Millipore	N/A
Normal Rabbit IgG	Millipore	N/A
CD45.1-FITC	BD Pharmigen	A20
CD45.2-APC	eBioscience	104

Table 2.5: Secondary Antibodies

Secondary Antibody	Vendor	Clone
Goat Anti-Rabbit IgG-HRP	Santa Cruz	N/A
Goat Anti-Mouse IgG-HRP	Santa Cruz	N/A
Rabbit TrueBlot	Rockland	eB182
Mouse TrueBlot	Rockland	eB144

Inhibitors**Table 2.6: Inhibitors**

Inhibitor	Target	Vendor
II-B08	Shp2	Zhong-Yin Zhang, Medicinal and Synthetic Chemistry Core, IUSM
GDC-0941	PI3K	Selleckchem
R406	Syk	Selleckchem

Biochemical Assays**Table 2.7: Biochemical and Functional Assays**

Kit	Vendor	Catalog Number
Plasmid Mini-Prep Kit	Qiagen	27106
Plasmid Maxi-Prep Kit	Invitrogen	K210007

Kit	Vendor	Catalog Number
Amaya Cell Line Nucleofector Kit V	Lonza	VCA-1003
Profection Mammalian Transfection System	Promega	E1200
SuperSignal West Dura Extended Duration Substrate	Thermo Scientific	34076
ChIP Assay Kit	Millipore	17-295
Hematopoietic Progenitor and Stem Cell Enrichment Kit	EasySep, Stem Cell Technologies	19756
Senescence β -Galactosidase Staining Kit	Cell Signaling	9860
Absolutely RNA RT-PCR Miniprep Kit	Agilent Technologies	400800
Superscript III First-Strand Synthesis System for RT-PCR	Invitrogen	18080-051

Methods

Cell Culture

32D Cells

32D cells, American Type Culture Collection (ATCC), were cultured in IMDM (Gibco) containing 10% fetal bovine serum (FBS) (HyClone), 2% Penicillin/Streptomycin (Gibco), and 10 ng/mL Interleukin-3 (IL-3) (PeproTech). Cells were grown at 37°C and 5% CO₂ and split every 2 days.

MV411 Cells

MV411 cells were cultured in IMDM containing 10% FBS and 2% Penicillin/Streptomycin. Cells were grown at 37°C and 5% CO₂ and split every 2-4 days.

HL60 Cells

HL60 cells were cultured in IMDM containing 10% FBS and 2% Penicillin/Streptomycin. Cells were grown at 37°C and 5% CO₂ and split every 2-4 days.

Primary Murine Low Density Mononuclear Cells (LDMNCs)

Primary murine LDMNCs were isolated from total bone marrow using a Histopaque-ficoll gradient (Sigma-Aldrich). LDMNCs were cultured in IMDM containing 20% FBS, 2% Penicillin/Streptomycin, Granulocyte-Colony-Stimulating Factor (G-CSF), Stem Cell Factor (SCF), and Thrombopoietin (TPO) (100 ng/mL each) (Peprotech). LDMNCs were maintained at 37°C and 5% CO₂.

Transfection

Nascent 32D cells (1.5×10^6) were transfected with MSCV-FLAG-WT, MSCV-FLAG-N51-FLT3, FLAG-FLT3-Y599F1/2, or FLAG-FLT3-Y768F plasmid (3 µg) via electroporation using Amaxa Nucleofector Kit V and placed in a 6-well non-tissue culture plate. Cells were subjected to cell sorting using fluorescence-activated cell

sorting (FACS) analysis, collecting eGFP positive cells to create an enriched, pure population of transfected cells.

Retroviral Transduction

Low density mononuclear (LDMNCs) cells were transduced with 2 mL pMSCV-WT FLT3 or pMSCV-N51-FLT3 retroviral supernatant, supplemented with TPO, SCF, and G-CSF (100 ng/mL) in retronectin-coated, 6 cm non-tissue culture plates for 24 hours at 37°C. After 24 hours, cells were collected, transduced again, (fresh retroviral supernatant and growth factors), and incubated overnight at 37°C. The following morning, cells were collected and plated back into prestimulation media for 24 hours before collection.

Cell Sorting

Retrovirally transduced cells are collected and sorted using fluorescence-activated cell sorting (FACS) analysis, collecting enhanced green fluorescent protein positive (eGFP+) cells.

³H-Thymidine Incorporation Assay

Cells were starved for 4 hours (primary AML patient samples) or 6 hours (32D cells) in IMDM containing 0.2% Bovine Serum Albumin (BSA) (Roche) and plated in a 96-well non-tissue culture plate (200 µL IMDM with 10% FBS and 2%

Penicillin/Streptomycin/well) for ^3H -thymidine incorporation assays ($3-4 \times 10^4$ cells/well) either at baseline (no growth factor) or in the presence of FLT3 Ligand (FL) (50 ng/mL), with or without indicated inhibitors and incubated overnight at 37°C and 5% CO_2 . The following morning, cells were pulsed with tritiated (^3H) thymidine (Perkin Elmer) (1 μCi) and incubated for 5-6 hours at 37°C . ^3H -thymidine incorporation was measured using an automated 96-well cell harvester and scintillation counter (Brandel, Gaithersburg, MD).

Total Cellular Protein Extraction

Cells were collected and washed twice with cold PBS and incubated on ice for 30 minutes on ice in a lysis buffer containing Hepes (50 mM), NaCl (150 mM), Glycerol (10% v/v), Triton X (1% v/v), MgCl_2 (1.5 mM), EGTA (1 mM), NaF (100 mM), and NaPP_i (10 mM) with fresh inhibitors: sodium orthovanadate, ZnCl_2 , PMSF, and protease inhibitor cocktail (Sigma). Protein lysates were then centrifuged at 13000 rpm for 15 minutes at 4°C and the supernatant was collected and transferred to a chilled tube. Lysates were quantified using Bradford reagent.

Immunoblot Analysis

Protein lysates (30 μg) were separated by Sodium Dodecyl Sulfate-Polyacrylamide Gel Electrophoresis (SDS-PAGE) and transferred to a nitrocellulose membrane. Membranes were incubated in primary antibody (Table 2.3) overnight at 4°C , while gently rocking. The following day, the membrane was washed using Tris-Buffered

Saline-Tween 20 (TBST), incubated with the appropriate HRP-conjugated secondary antibody (Table 2.4) for 1 hour, developed with enhanced chemiluminescence (SuperSignal), and exposed using a BioRad Imager.

Immunoprecipitation (IP) Assay

Exponentially growing cells were plated overnight (2 x 10⁶/10 cm non-TC plate) and total protein extraction was conducted the following day. Anti-FLAG M2 gel (Sigma) was resuspended and aliquoted (40 μ L per IP) into a 1.5 mL tube. Gel was washed twice by: gently spinning (5000 g for 30 seconds) down the gel, aspirating the supernatant, washing with TBS (500 μ L) incubating for 15 minutes at 4°C. Protein lysate (1 mg) was added to the washed resin and buffer was added to equal volume (1 mL). Gel resin-protein mixture rotated overnight at 4°C. The following day, samples were gently spun (5000 g for 30 seconds). Supernatant was aspirated and resin was washed 3 times with TBS (500 μ L). Buffer and reducing agent (27 μ L and 3 μ L, respectively) were added to each sample. Samples were then run following the immunoblot analysis protocol.

Apoptosis Assay

Three days after LDMNCs were isolated (and sorted if transduced), cells were counted and plated in a 24 well non-Tissue Culture plate (2.5 x 10⁴/well). Media (various concentrations of FBS) was added to obtain an equal volume (1.0 mL). The following day (approximately 24 hours after plating), cells were collected into

Eppendorf tubes. The well was washed with PBS (500 μ L) and added to the tube. Cells were collected by centrifugation (1 minute, maximum speed using microcentrifuge). Media was aspirated; cells were washed again with PBS and collected. Cells were then resuspended in binding buffer (100 μ L). Annexin V-APC and propidium iodine (PI)-PE (5 μ L each) were added to the tube. Cells were vortexed, covered in foil, and incubated (15 minutes at room temperature). Binding buffer was once again added (200 μ L). Cells were analyzed by flow cytometry using the Accuri Flow Machine.

β -Galactosidase Staining Assay

Four days after LDMNCs were isolated, cells were counted and plated on poly-L-lysine coated 4-well chamber slides (Lab-Tek) ($1-4 \times 10^4$ /well) in IMDM containing 2% FBS (500 μ L). Slides were incubated overnight at 37°C and 5% CO₂. The following day, slides were spun down at 1500 rpm for 5 minutes at room temperature, washed with PBS, fixed, and stained with X-Gal staining solution (pH 6.0). Plates were incubated overnight at 37°C without CO₂. The following day, senescent cells were quantitated by counting the number of blue cells in 6 distinct fields of view.

Transplants

Syngeneic Transplants

WT FLT3, N51-FLT3, or N51-FLT3-mutant 32D cells were expanded in 10 cm non-tissue culture plates (approximately $2-3 \times 10^6$ cells/plate) for about two weeks prior to transplant. Viability was measured periodically using flow cytometry and cell viability was kept above 90%. Additionally, cells were analyzed via ^3H -thymidine incorporation assays to ensure hyperproliferation of the N51-FLT3 cells compared to WT FLT3. On the day of the transplant, cells were collected and resuspended in fresh growth media. After a few hours, cells were again collected, counted, and resuspended in filter-sterile transplant media (IMDM containing 0.2% BSA) ($2-3 \times 10^6$ cells per 300 μL). Cells were transplanted via intravenous injection. Mice were followed for 12-16 weeks after transplant and peripheral blood eGFP and complete blood counts (CBCs) were examined every 3-4 weeks. Mouse endpoint was determined based on the following characteristics: loss of greater than 10% body weight, scruffy fur, and labored breath and movement. Upon euthanasia, evaluation of spleen size and histopathological diagnosis was performed.

Competitive Transplants

Donor $\text{Shp2}^{\text{flox/+}}$; Mx1-Cre (+ or -); FLT3-ITD (+/- or -/-) mice (C57Bl/6 background, CD45.2 marker) were treated with polyI:C to delete one allele of Shp2. 5 weeks post-treatment, peripheral blood was collected and analyzed to ensure the deletion of Shp2. Bone marrow LDMNCs were isolated and counted. Donor cells ($1-2 \times 10^6$),

along with competitor cells (2×10^6) (BoyJ background, CD45.1 marker) were resuspended in transplant media (IMDM containing 0.2% BSA, 300 μ L) and transplanted into lethally irradiated BoyJ recipient mice (1100 cGy, split dose). Mice were followed for 12-16 weeks after transplant. Chimerism was examined every 4 weeks by staining for CD45.1 and CD45.2 (Table 2.4), as well as an evaluation of spleen size and histopathological diagnosis at the time of death.

Chromatin Immunoprecipitation Assay

Chromatin immunoprecipitation (ChIP) assays were performed using a ChIP assay kit (Millipore). HL60 and MV411 cells were treated with formaldehyde (1%) and lysed using a lysis buffer containing SDS (1%), EDTA (10 mM), and Tris-HCL (50 mM) at pH 8.1. Extracts were sonicated (15 replicates of 5 seconds on, 20 seconds off at 20% power) to produce 500–1000 bp DNA fragments. Input (20 μ L) was saved and stored at -80°C . The remaining was split equally into Eppendorf tubes and incubated with one of the following antibodies: anti-Rabbit IgG, anti-acetyl-histone H4, anti-STAT5, or anti-Myc (Table 2.4) and salmon sperm DNA/Protein A agarose in ChIP dilution buffer (SDS (0.01%), Triton X-100 (1.1%), EDTA (1.2 mM), Tris-HCl (16.7 mM), NaCl (167 mM) at pH 8.1) and rotated overnight at 4°C . The next day, immunoprecipitates were collected by gentle centrifugation, washed with low and high immune complex buffers, and eluted using elution buffer (SDS (1%) and NaHCO_3 (0.1 M)). Histone-DNA crosslinks were reversed by heating samples at 65°C overnight. Proteins were digested by treatment with proteinase K for 1 hour at 45°C , and DNA was recovered using phenol/chloroform extraction. Quantitative

PCR was performed using SYBR green reagent, appropriate target primers on the human *BMI1* promoter (Table 2.6), and the Applied Biosystems 7500 instrument. Amplified fragments were expressed as a percentage of the total chromatin used in the sample (input) and normalized to the rabbit IgG negative control.

Statistical Analysis

Survival curves are represented as Kaplan-Meier curves and statistics were performed using log-rank test, in collaboration with Ziyue Liu (Assistant Professor of Biostatistics, Department of Biostatistics, IU Richard M. Fairbanks School of Public Health).

For the remaining experiments, statistics were performed using paired or unpaired, two-tailed student's *t* test, and figures shown as mean +/- standard deviation (S.D.) or mean +/- standard error of the mean (SEM), as indicated in each respective figure.

CHAPTER THREE

SHP2 FUNCTIONS AT TYR599 AND TYR768 ON THE FLT3-ITD RECEPTOR TO POSITIVELY REGULATE SIGNALING AND LEUKEMOGENESIS

Introduction

The protein tyrosine phosphatase, Shp2, has been shown to be important for FLT3-ITD-induced leukemogenesis. Shp2 is constitutively associated with FLT3-ITD and leads to the increased phosphorylation of STAT5 (Nabinger, Li et al. 2013). Moreover, pharmacologic inhibition of Shp2 partially reverses aberrant Shp2-mediated signaling. Using immunoprecipitation assays, the Chan lab showed that Shp2 and STAT5 are found in a complex together both in the cytoplasm and nucleus (Nabinger, Li et al. 2013), and subsequently hypothesized that both Shp2 and STAT5 play a role in the activation of STAT5-target genes, such as BCL-X_L. To examine this hypothesis, Shp2 RNA was knocked down using shRNA and the activity of the BCL-X_L promoter, *BCL2L1*, was measured by a luciferase assay. Indeed, we found that the transcription of STAT5-target genes in the presence of N51-FLT3-ITD is dependent on Shp2 protein, as evidenced by lower *BCL2L1* promoter-mediated luciferase expression in the absence of Shp2 (Figure 3.1) (Nabinger, Li et al. 2013). Collectively, these data suggest a crucial role for Shp2 in mediating FLT3-ITD signaling to STAT5.

The Chan Lab previously hypothesized that eliminating the ability of Shp2 to interact with FLT3 will reduce the hyperproliferation of FLT3-ITD-expressing cells to levels similar to that of WT FLT3-expressing cells. To test this, we generated constructs bearing tyrosine (Y) to phenylalanine (F) mutations at amino acid 599 in order to

eliminate the phosphorylation potential, which is necessary for binding of Shp2. In one experimental construct, only the native Tyr599 was mutated (Y599F1). In another experimental construct, both the native and duplicated Tyr599 were mutated (Y599F1/2). These constructs were transduced into murine low density mononuclear cells (LDMNCs) and analyzed both for proliferation via ³H-thymidine incorporation and for STAT5 activation via western blot analysis. While both constructs reduced the hyperproliferation compared to that of N51-FLT3-expressing cells at baseline, the Y599F1/2 mutation most significantly reduced hyperproliferation at baseline and after FL stimulation (Figure 3.2A), as well as FLT3-ITD-induced STAT5 hyperactivation (Figure 3.2B) (Nabinger, Li et al. 2013). These findings suggest that signaling from Tyr599, the binding residue of Shp2, positively regulates proliferation and aberrant STAT5 activation. For our future studies, we will focus on the mutation of both the original and duplicated Tyr599 (Y599F1/2) to study the importance of signaling from this residue.

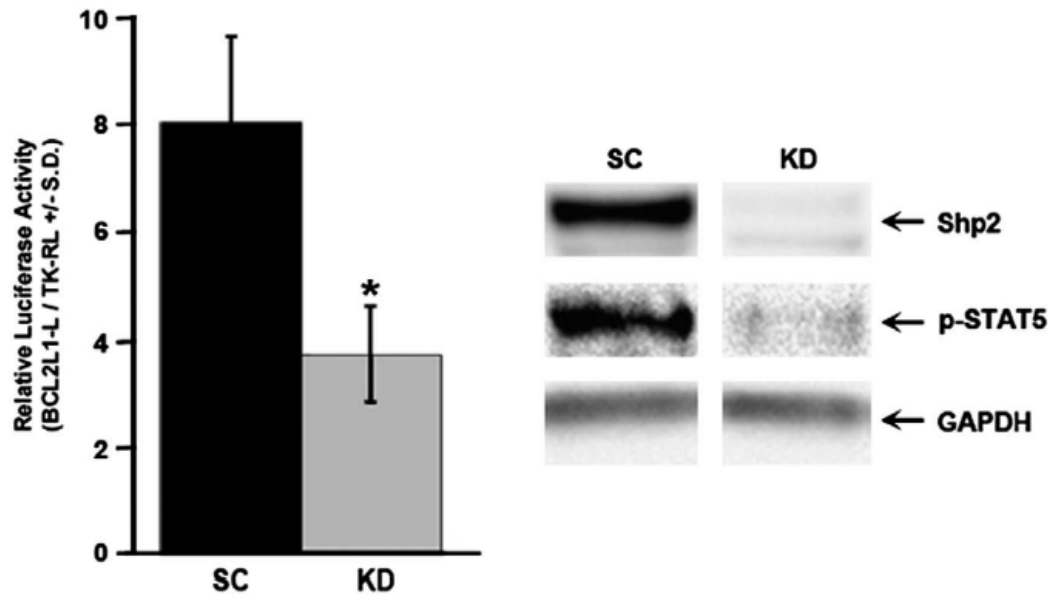


Figure 3.1. Knockdown of Shp2 reduces STAT5 activity at the Bcl-X_L promoter, *BCL2L1*.

FLT3-ITD+ MV411 cells (scrambled, SC or Shp2 knockdown, KD) were transfected with pBCL2L1-L and pTK-RL. Protein lysates were assayed for luciferase and Renilla luciferase activity (left panel). n=3, *p<0.05 for KD vs SC. Protein lysates were also analyzed for Shp2 expression and phospho-STAT5 levels (right panel). Adapted from Nabinger et al. (Nabinger, Li et al. 2013).

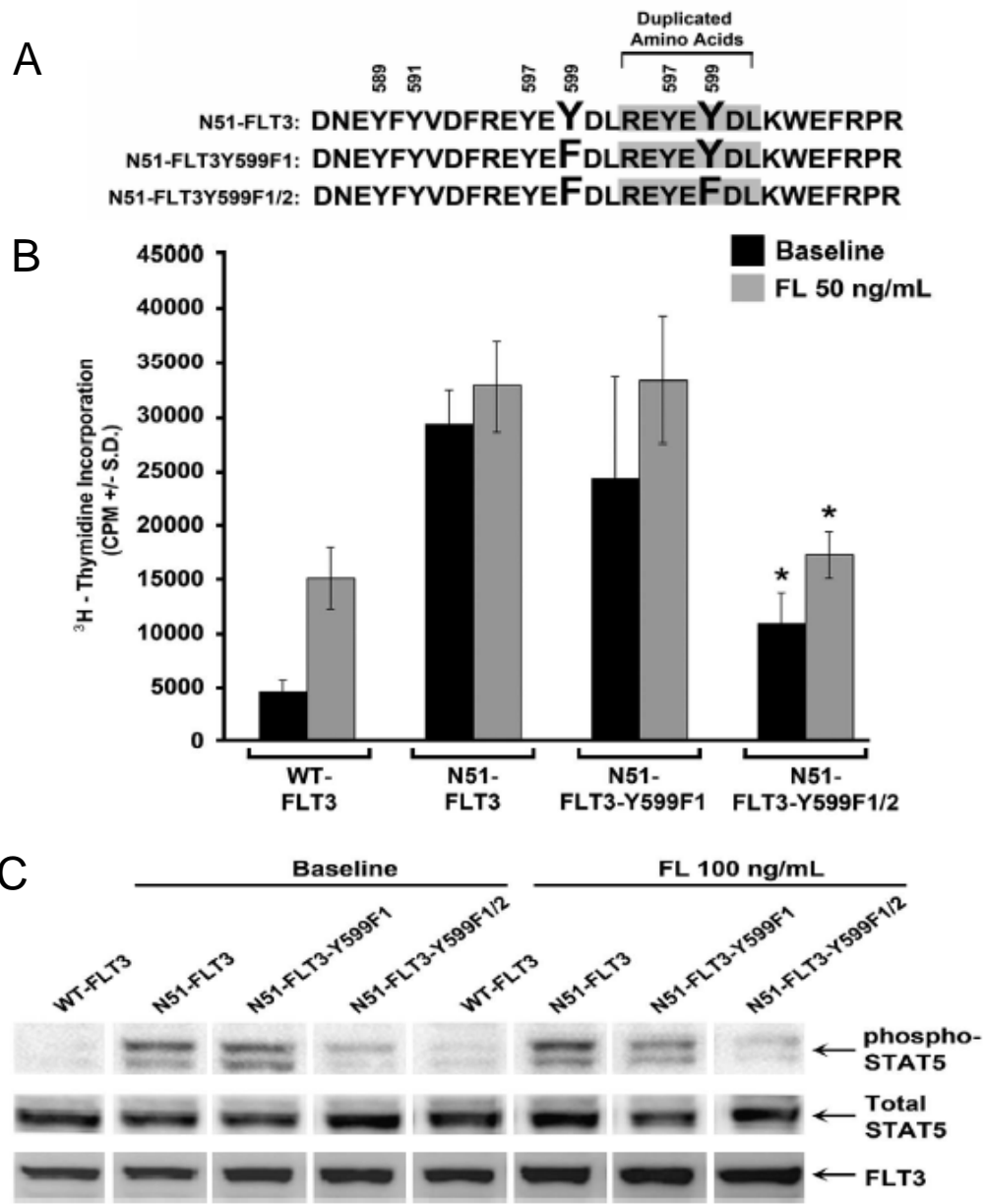


Figure 3.2. Mutation of Tyr599 results in reduced hyperproliferation and STAT5 activation.

(A) Murine bone marrow LDMNCs were transduced with FLT3 constructs, sorted by FACS, and subjected to ³H-thymidine incorporation assay in the absence and presence of FL (50 ng/mL). n=5–8, *p<0.05 for N51-Y599F1/2 vs N51-FLT3 at baseline and FL stimulation, statistical analysis using unpaired, two-tailed student's *t* test; (B) Immunoblot analysis of STAT5 phosphorylation, total STAT5, and FLT3 expression in retrovirally transduced and sorted WT FLT3-, N51-FLT3-, N51-Y599F1- or N51-Y599F1/2-expressing bone marrow-derived macrophages in the absence and presence of FL. Adapted from Nabinger et al. (Nabinger, Li et al. 2013).

While we know that Shp2 activity at the FLT3-ITD receptor correlates with aberrant STAT5 activation, Shp2 phosphatase itself cannot directly phosphorylate STAT5. Therefore, we anticipated that Shp2 cooperates with a STAT5-activating kinase to promote cellular hyperproliferation. The spleen tyrosine kinase, Syk, has been found to interact with Tyr599 on FLT3-ITD and can phosphorylate inter-kinase domain Tyr768 (Puissant, Fenouille et al. 2014). Therefore, we **hypothesized that Shp2 interacts in a complex with Syk kinase and STAT5 at Tyr599 on FLT3-ITD, and that Shp2 and Syk cooperate to activate STAT5.**

There is evidence that Shp2 may promote signal transduction as a scaffolding protein via its two SH2 domains, rather than using its catalytic domain for enzymatic function. Shp2 is known to interact with a number of proteins involved in signaling, including the GM-CSF receptor, adapter molecules such as Gab2 and Grb2, and signaling molecules such as the p85 α regulatory subunit of Phosphatidylinositide 3-Kinase (PI3K) (Neel, Gu et al. 2003, Mohi, Williams et al. 2005, Yu, Daino et al. 2006). PI3K is a known regulator of Akt signaling, and has been shown to positively regulate MAP kinase (Erk) in the context of gain of function (GOF) Shp2 mutations (Goodwin, Li et al. 2014). Additionally, the PI3K/Akt pathway has been shown to be constitutively active in approximately 70% of reported AML cases (Kornblau, Womble et al. 2006).

In the context of WT FLT3, Shp2 has been reported to participate in multi-protein complexes containing Gab2 and p85 α at the FLT3 receptor upon FL stimulation (Zhang and Broxmeyer 1999, Zhang, Mantel et al. 1999, Zhang and Broxmeyer 2000). Additionally, Tyr768 on WT FLT3 has been shown to recruit Grb2, Gab2, and p85 α , and mutation of Y768F mutation results in lower STAT5 and Akt phosphorylation (Masson,

Liu et al. 2009). Taken together, we **hypothesized that an additional means of Shp2 interaction with FLT3-ITD may be via p85 α -containing complexes at FLT3-ITD Tyr768, and that Shp2 and PI3K work cooperatively to promote FLT3-ITD-induced hyperproliferation.** We believe that increased Shp2 recruitment to duplicated Tyr599 on FLT3-ITD cooperates with Syk to enhance constitutive STAT5 phosphorylation and to promote Tyr768-dependent Erk and Akt phosphorylation via PI3K (Figure 3.3). Consequently, we predicted that mutation of duplicated Tyr599 or of Tyr768 to phenylalanine would lead to reduced proliferation *in vitro* and reduced FLT3-ITD-induced myeloproliferative disease (MPD) *in vivo*. Therefore, in the following studies, we investigated both Shp2/Syk function and Shp2/PI3K function in FLT3-ITD-induced leukemogenesis.

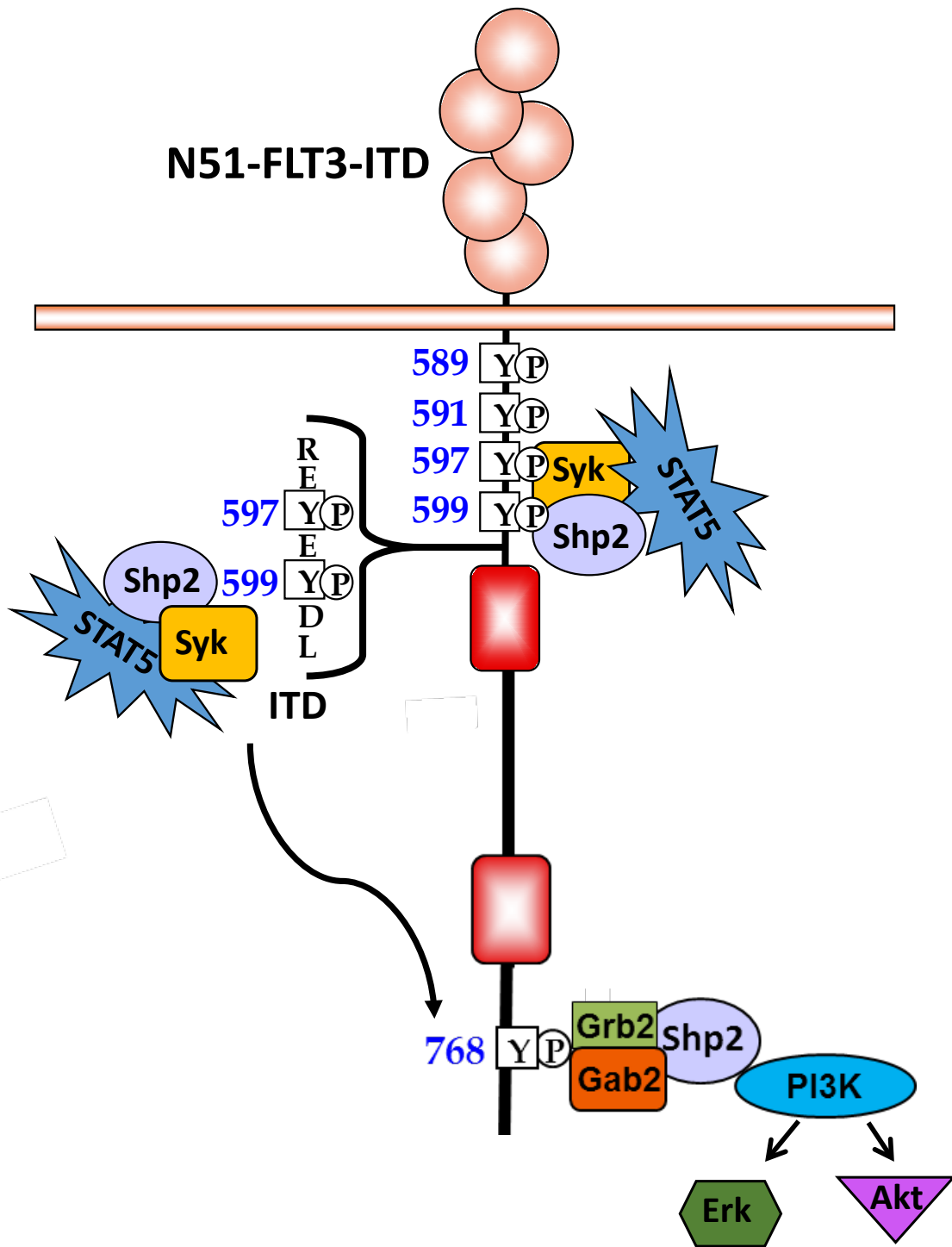


Figure 3.3. Hypothesis of the signaling transduction pathways that promote FLT3-ITD-mediated hyperproliferation and leukemogenesis.

Results

Genetic Disruption of FLT3-ITD/ Shp2 Interaction

To study the importance of Shp2 interaction with FLT3-ITD, we first began by generating 32D cells transfected with WT FLT3, N51-FLT3, and modified N51-FLT3 constructs bearing mutation of the duplicated juxtamembrane tyrosine 599 residues to phenylalanine (N51-FLT3-Y599F1/2) (Nabinger, Li et al. 2013) or of tyrosine 768 to phenylalanine (N51-FLT3-Y768F) (Figure 3.4A). For ease of biochemical studies, these FLT3-ITD mutant constructs were cloned with an N-terminal FLAG tag (Figure 3.4B). 32D cells were enriched based on eGFP positivity to create stable cell lines (Figure 3.5). We chose to use the murine myeloid 32D cell line as opposed to the murine myeloid Baf3 cell line for ease of syngeneic transplants studies later. Both 32D cells and C3H/HeJ both express the MHC H2 haplotype *k*, eliminating the possibility of rejection of the transplanted cells by the recipient immune system.

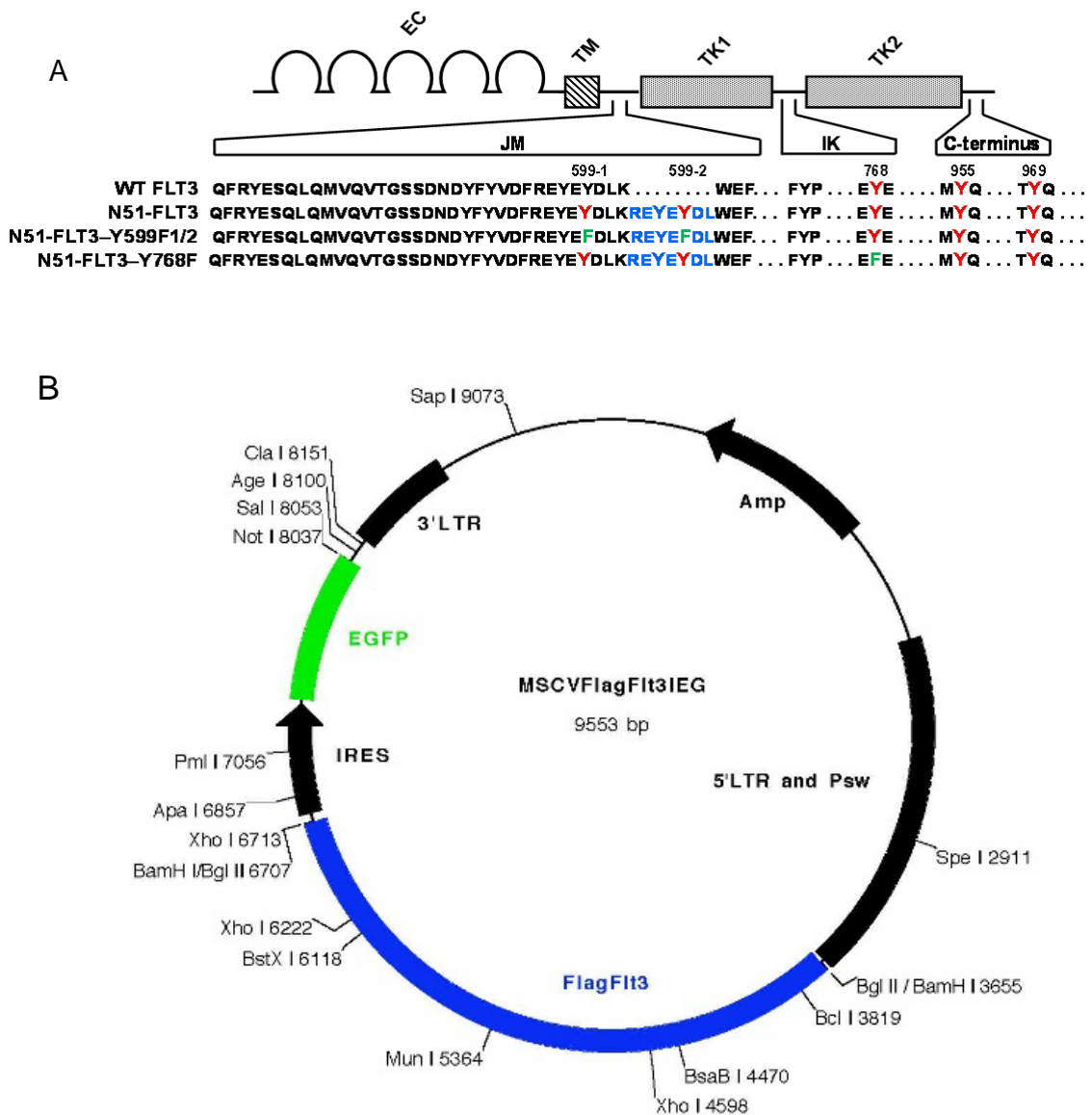


Figure 3.4. Constructs used to examine the role of N51-FLT3 Tyr599 and Tyr768.

(A) Schematic of the FLT3 constructs used in these studies. To look at Tyr599, both the original tyrosine and duplicated tyrosine were mutated to phenylalanine. Additionally, another FLT3-ITD construct was created in which Tyr768 was mutated to phenylalanine; (B) The FLT3 constructs were cloned into a pMSCV backbone co-expressing eGFP. Additionally, each FLT3 construct has an N-terminal FLAG tag.

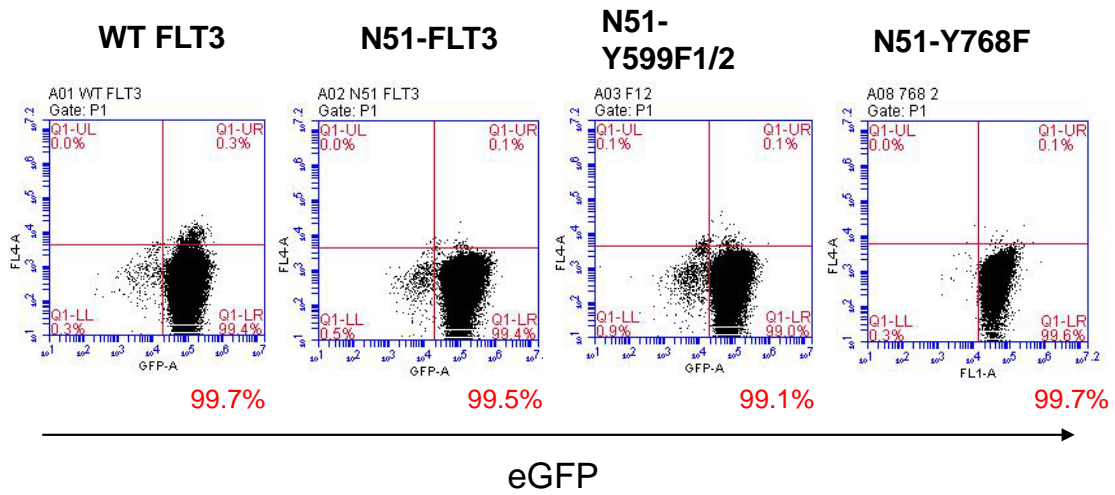


Figure 3.5. Stable 32D cell lines highly express WT, N51, or N51-mutant constructs.

Transfected cells were enriched by sorting for eGFP positivity using fluorescence activated cell sorting (FACS).

Because both Shp2 and STAT5 are present in FLT3-containing protein complexes in FLT3-ITD-expressing Baf3 cells (Nabinger, Li et al. 2013), we hypothesized that mutating Tyr599 would decrease the interaction of Shp2 with FLT3-ITD. Additionally, as Shp2 has been shown to be incorporated in protein complexes with Grb2, Gab2, and p85 α at Tyr768, we hypothesized that mutating Tyr768 would also decrease the interaction of Shp2 with FLT3-ITD. To test this hypothesis, each of the FLT3-ITD experimental (N51-Y599F1/2 and N51-Y768F) and control (WT and N51-FLT3) constructs were introduced into 32D cells and cells were enriched for transfected cells based on their eGFP positivity (Figure 3.5). Lysates were collected and subjected to immunoprecipitation analysis to investigate the FLT3-Shp2 interaction. Mutation of duplicated Y599 or of Y768 resulted in reduced Shp2 interaction with FLT3 compared to N51-FLT3 in immunoprecipitation assays (Figure 3.6, compare lanes 3 and 4 to lane 2). We next examined how reducing the Shp2/FLT3-ITD interaction at these residues would affect FLT3-ITD-induced hyperproliferation and leukemogenesis.

To examine the hyperproliferative capability of N51-FLT3 upon mutation of the various tyrosine residues, we subjected our 32D cell lines with various constructs to ³H-thymidine incorporation assays. Radioactive thymidine is incorporated into the DNA of dividing cells, and therefore is a direct measure of proliferation. Cells were incubated in starvation media (0.2% BSA-IMDM) for 6 hours, plated in equal numbers, and incubated overnight in normal growth media (10% FBS, 2% Penicillin/Streptomycin) in the absence and presence of FLT3 Ligand (FL, 50 ng/mL). Cells were pulsed with ³H-thymidine and harvested 6 hours later. We hypothesized that Y599F1/2 mutation, as we saw with LDMNCs (Figure 3.2A), should prevent baseline and FL-induced hyperproliferation.

Additionally, we hypothesized that Y768F should also prevent baseline and FL-induced hyperproliferation, as a result of abrogated signaling from the mutated tyrosine residues. We saw that cells expressing N51-Y599F1/2 or N51-Y768F demonstrated a significant reduction in proliferation compared to cells expressing N51-FLT3, both at baseline and in the presence of FL (Figure 3.7). Notably, in the presence of FL, the Y599F1/2 mutation significantly reduced hyperproliferation compared to Y768F mutation in 32D cells. These findings suggest that the signaling occurring at both Tyr599 and Tyr768 are important for the hyperproliferation of FLT3-ITD-expressing cells; therefore, targeting the FLT3-ITD-effector proteins should also reduce the hyperproliferation of FLT3-ITD-expressing cells. Moreover, interference of the signaling pathways emanating from Tyr599 and Tyr768 should increase the latency to disease *in vivo*. Our functional analysis of mutated Tyr599 versus mutated Tyr768 on FLT3-ITD indicated differential effects on hyperproliferation, with mutated Tyr599 resulting in less proliferation compared to mutation of Tyr768. These observations are consistent with the idea that signaling from Tyr599 may be more important to FLT3-ITD signaling and leukemogenesis compared to Tyr768.

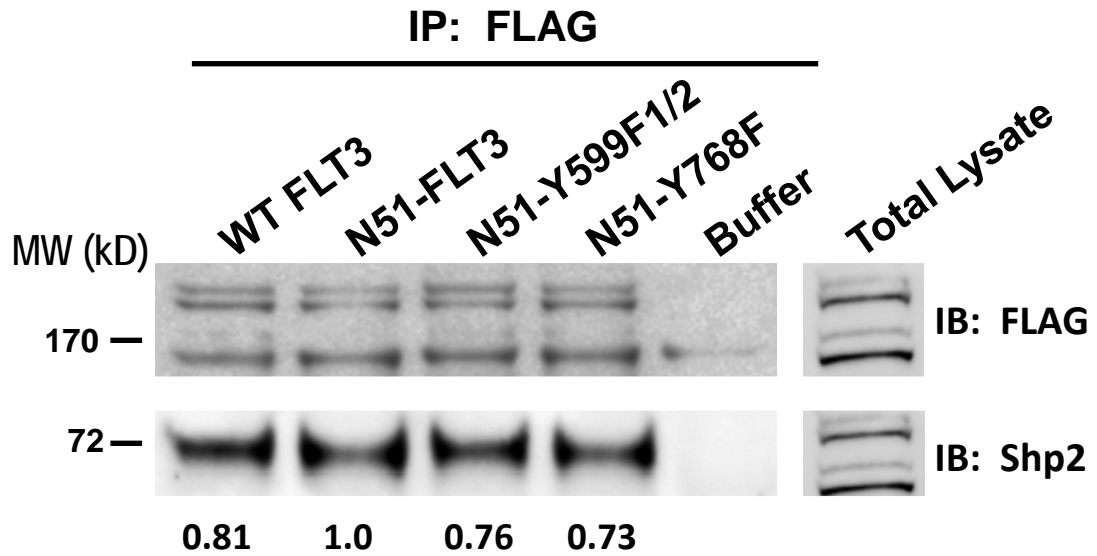


Figure 3.6. Mutation of duplicated Tyr599 and of Tyr768 reduces the interaction between Shp2 and FLT3-ITD.

Total cellular proteins from exponentially growing 32D cells transfected with respective constructs were immunoprecipitated (IP) with anti-FLAG and immunoblotted (IB) with anti-Shp2 or anti-FLAG, experiment performed on two independent occasions.

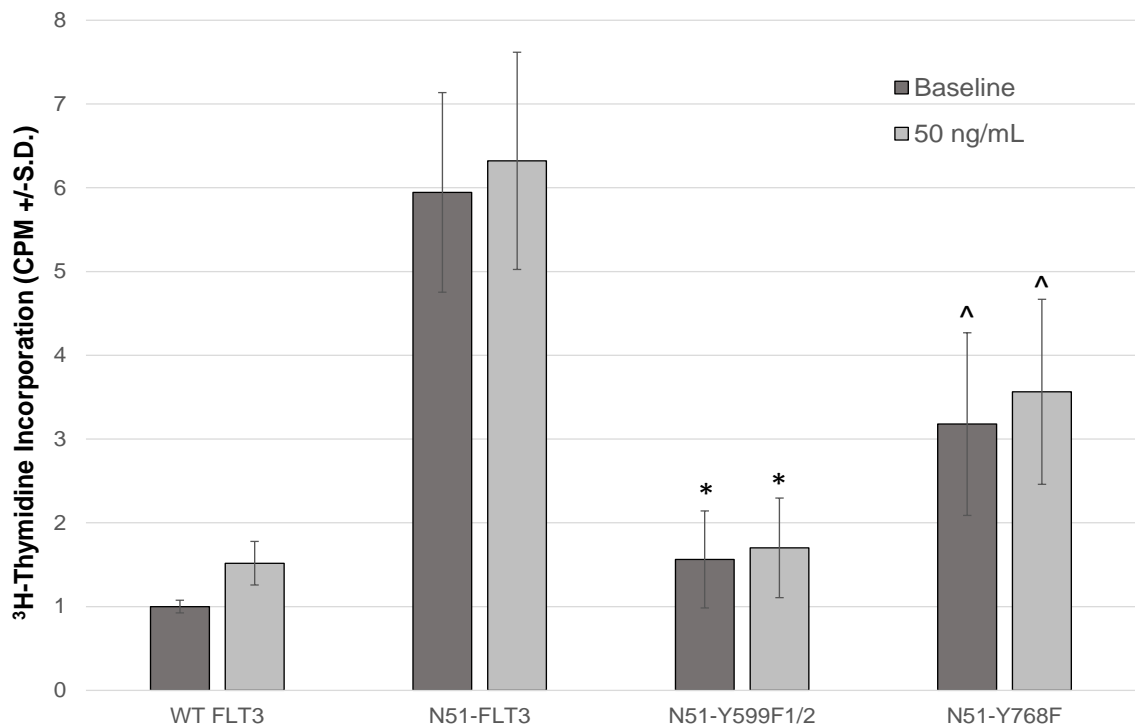


Figure 3.7. Mutation of duplicated Tyr599 and Tyr768 significantly reduces the hyperproliferation of N51-FLT3 cells.

32D cells were transfected with WT FLT3, N51-FLT3, N51-Y599F1/2, or N51-Y768F and sorted for eGFP+ cells and proliferation was evaluated by ^3H -thymidine incorporation. Data shown is compiled from 4 independent experiments and normalized to average WT FLT3 baseline within each experiment. *n=4, $p < 0.005$ comparing N51-Y599F1/2 to N51-FLT3 in the absence or presence of FL, ^n=4, $p < 0.05$ comparing N51-Y768F to N51-FLT3 in the absence or presence of FL and comparing N51-Y768F to N51-Y599F1/2 in the presence of FL, statistics performed using unpaired, two-tailed student's *t* test.

Since both Tyr599 and Tyr768 reduce the hyperproliferation of N51-FLT3-expressing cells, we hypothesized that mice transplanted with cells expressing mutated Tyr599 (N51-Y599F1/2) and mutated Tyr768 (N51-Y768F) should display increased latency to the onset of MPD compared to mice transplanted with N51-FLT3-expressing 32D cells. It should be noted that these mice do not develop AML, as FLT3-ITD alone is not sufficient to cause AML in a mouse model (Kelly, Liu et al. 2001). MPD is an indicator of disease, however, because it exhibits the same hallmarks of AML: clonal hyperproliferation, splenomegaly (as a result from extramedullary hematopoiesis), and altered hematopoiesis in the bone marrow. For these studies, we employed a syngeneic transplant model to study the progression to disease. A syngeneic transplant is one in which the donor cells express the same major histocompatibility class (MHC) antigens as the cells in the recipient mice. This genetic similarity prevents the mice from undergoing an immune response and rejecting the foreign cells. Because of this, the recipient mice do not need to be lethally irradiated (for myeloablation) before transplant. As mentioned previously, 32D cells have the same MHC haplotype, k, as C3H/HeJ mice, so C3H/HeJ mice will be used as recipients in our studies.

32D cell lines expressing the various FLT3 constructs were expanded, and viability and eGFP positivity of at least 90% was confirmed using flow cytometry. C3H/HeJ mice were transplanted with 32D cells (3×10^6) and survival was followed over time. Peripheral blood was collected from the mice via tail vein periodically for analysis of complete blood counts (CBCs) and eGFP positivity as signs of progression to MPD. At the time of euthanasia, tissues were saved in formalin for staining with hematoxylin

and eosin. Additionally, the spleen was examined for splenomegaly and bone marrow was analyzed for eGFP positivity.

Mice transplanted with WT FLT3 did not show any eGFP in the peripheral blood and rarely developed MPD (data not shown). At three weeks post-transplant, of transplanted animals showing greater than 0.5% eGFP positive circulating cells, mice transplanted with N51-FLT3-transfected cells showed the highest level of eGFP positivity (Figure 3.8). This suggests that while each cell type is able to expand *in vivo*, it may be slower in the mutant cell types. However, when analyzing peripheral blood white blood cell (WBC) counts, another indicator of MPD progression, we found that N51-FLT3 mice displayed high WBC counts, but the WBC counts were not reduced in either of the mutant cell types (Figure 3.9). In fact, while it appears that the N51-Y768F mutant mice had lower eGFP levels, they demonstrated elevated WBC counts. In retrospect, we believe that the observed eGFP levels in the N51-Y768F mice at three weeks post-transplant may be due to the rapid death of N51-Y768F mice prior to the three week peripheral blood assessment (Figure 3.10).

In contrast to what we observed with the N51-Y768F mice, N51-Y599F1/2 mice exhibiting greater than 0.5% peripheral blood eGFP positivity at three weeks post-transplant demonstrated a prolonged overall survival compared to the N51-FLT3 mice (Figure 3.10). These findings suggest that STAT5 activation through Shp2 at Tyr599 is critical for the aggressiveness of the disease. Taking into account the hyperproliferation of these cells *in vitro* and the progression to MPD *in vivo*, it appears that duplicated Tyr599 and Tyr768 have differential effects on FLT3-ITD-induced leukemogenesis, most likely due to signaling to different effectors. Additionally, duplicated Tyr599 may play a

more prominent role, but is not the only factor contributing to disease, as its mutation reduces but does not completely ablate leukemia onset and progression.

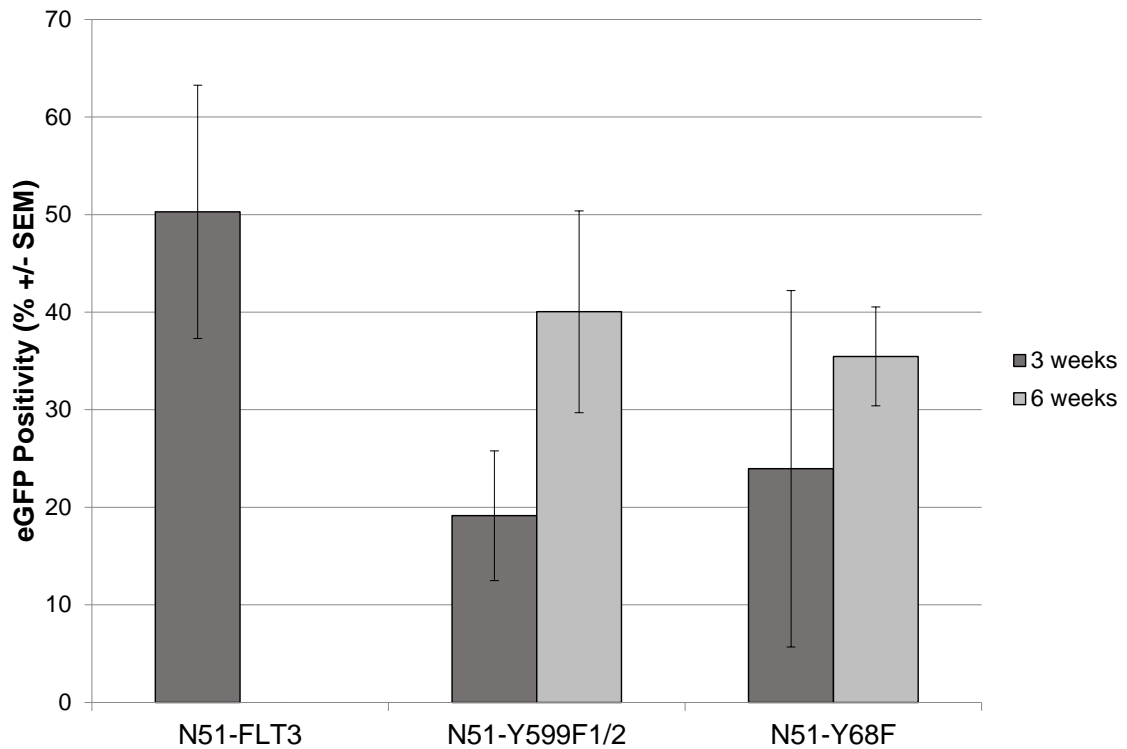


Figure 3.8. Neither Tyr599 nor Tyr768 mutations result in lower eGFP levels in the peripheral blood compared to N51-FLT3 mice.

C3H/HeJ mice were transplanted with 32D cells expressing various FLT3 constructs. eGFP expansion in the peripheral blood was followed over time. Peripheral blood was collected, underwent red blood cell lysis, and analyzed by flow cytometry. $n=5$ for N51-FLT3, $n=15$ for N51-Y599F1/2, and $n=4$ for N51-Y768F at 3 weeks, and $n=0$ for N51-FLT3, $n=5$ for N51-Y599F1/2, and $n=3$ for N51-Y768F at 6 weeks. $p=0.07$ comparing N51-FLT3 vs. N51-Y599F1/2 at 3 weeks using unpaired, two-tailed student's t test.

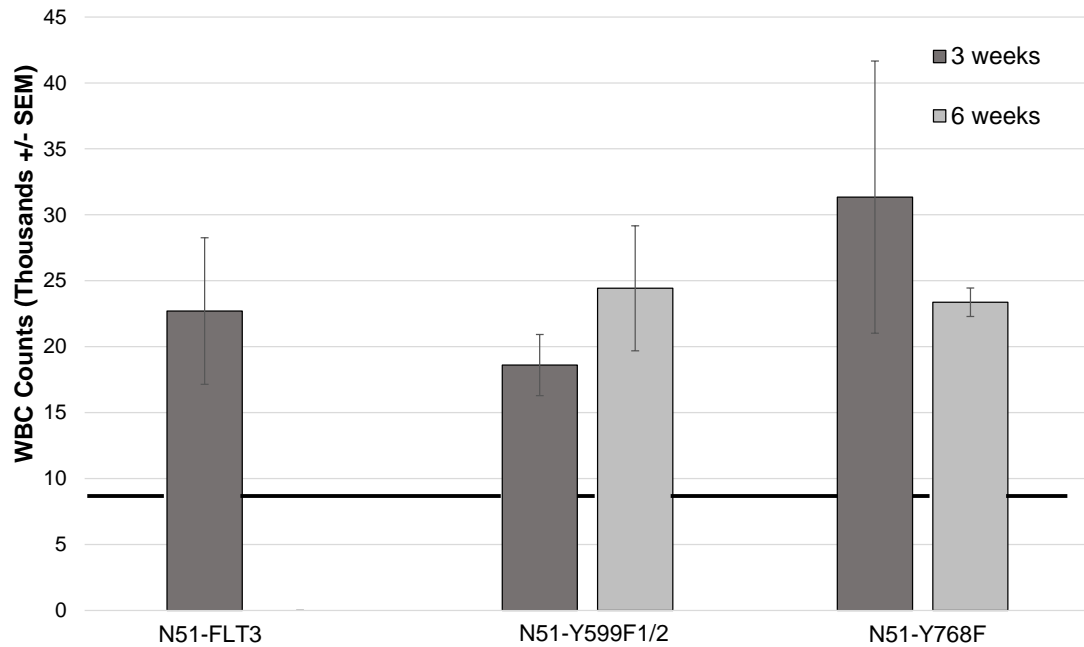


Figure 3.9. N51-FLT3, N51-Y599F1/2, and N51-Y768F mice all display elevated white blood cell counts in the peripheral blood.

C3H/HeJ mice were transplanted with 32D cells expressing various FLT3 constructs. WBC counts in the peripheral blood were followed over time. Peripheral blood was collected and analyzed for complete blood counts (CBCs) using a Hemavet. n=8 for N51-FLT3, n=15 for N51-Y599F1/2, and n=8 for N51-Y768F.

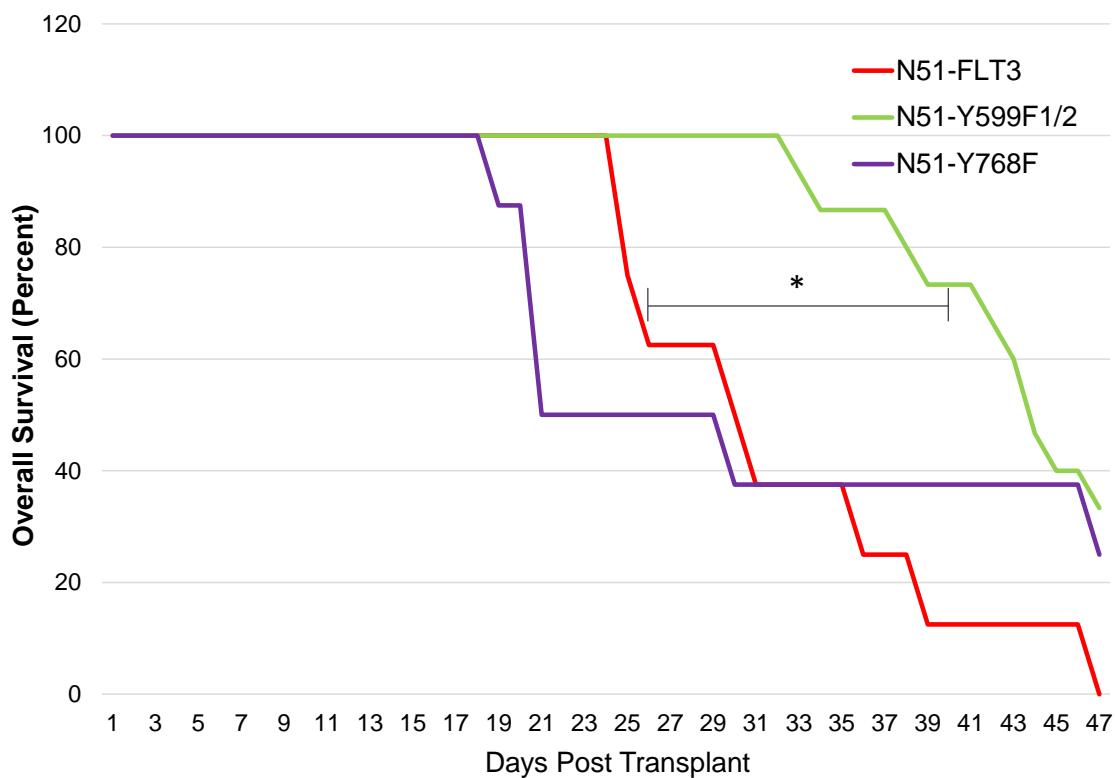


Figure 3.10. N51-Y599F1/2 mice exhibit delayed progression to MPD, while N51-Y768F does not alter progression.

C3H/HeJ mice were transplanted with 32D cells expressing various FLT3 constructs. Survival was followed over time. n=8 for N51-FLT3, n=15 for N51-Y599F1/2, and n=8 for N51-Y768F, *p<0.01 for N51-FLT3 vs. N51-Y599F1/2 using log-rank test.

Because of the difference in progression to MPD *in vivo*, we hypothesized that the underlying reason was due to differential signaling from each tyrosine in FLT3-ITD. Therefore, we examined the altered signaling seen as a result of mutation of duplicated Tyr599 and Tyr768. We subjected our 32D cell lines to starvation for different time points (3 hours and overnight) and examined the activation of candidate effector proteins downstream of FLT3-ITD, including STAT5, Erk, and Akt. Interestingly, we saw differences in activation of constitutive STAT5 and Erk depending on the starvation length. We therefore looked at the effect of Tyr599 or Tyr768 mutation at the time points post-starvation where N51-FLT3-expressing cells demonstrated elevated phospho-STAT5 or phospho-Erk compared to WT FLT3-expressing cells.

Others have demonstrated that STAT5 is hyperactivated in FLT3-ITD (Hayakawa, Towatari et al. 2000, Choudhary, Brandts et al. 2007). In our 32D model, we saw hyperactivation of STAT5 in cells starved for 3 hours, but not in cultures starved overnight. Therefore, we used the 3 hour starvation to monitor the effect of each tyrosine mutation on STAT5 activity. Since we saw that mutation of duplicated Tyr599 resulted in prolonged overall survival (Figure 3.10), we therefore hypothesized we would see reduced phospho-STAT5 levels. Indeed, consistent with previous findings, we saw that N51-Y599F1/2 mutation trended towards lower STAT5 activation compared to N51-FLT3 (Figure 3.11), although not statistically significant. Additionally, N51-Y599F1/2 did not completely normalize phospho-STAT5 to WT levels, consistent with the prolonged survival, but not complete ablation of N51-FLT3-mediated leukemia *in vivo*. We next examined STAT5 in the N51-Y768F mutant cells. Consistent with the *in vivo*

findings, we did not see that N51-Y768F mutation reduced STAT5 activation, as phosphorylation levels were similar to that of the N51-FLT3 cells (Figure 3.11).

We next examined Erk and Akt activation in our mutant cells. Since we hypothesize that the Shp2/Syk/STAT5 protein complex at Tyr599 is critical for the phosphorylation of Tyr768 and therefore the recruitment and activation of the protein complex at Tyr768, we hypothesized that Tyr599 mutation would also result in lower Akt and Erk activation. In regards to Akt activation, we never observed increased Akt activation in the N51-FLT3 compared to WT FLT3 control cells (Figure 3.11).

Interestingly, there have been inconsistencies in the literature about hyperactivation of Akt in FLT3-ITD+ AML. While the PI3K/Akt pathway is known to be highly active in AML (Kornblau, Womble et al. 2006), others have shown that in the context of FLT3-ITD, Akt is only slightly elevated (Mizuki, Fenski et al. 2000), while others see no difference in Akt activation (Janke, Pastore et al. 2014). Therefore, further studies will be required to definitively conclude if N51-Y599F1/2 or N51-Y768F play a role in downstream Akt activation.

Erk has been shown to be hyperactive in FLT3-ITD-expressing cells, so we hypothesized that our N51-FLT3 cells would display increased Erk activation compared to WT FLT3, and that mutation of either Tyr599 or Tyr768 could normalize it. Upon overnight growth factor and serum deprivation, N51-FLT3-expressing 32D cells exhibited elevated phospho-Erk levels compared to WT FLT3; this elevation was not seen at the shorter, 3 hour time point. As the overnight time point in our model showed elevation consistent with the literature for Erk activation, we used the overnight time point to examine the effect of our various tyrosine mutants on Erk activation. While we

expected N51-Y599F1/2 would prevent Erk activation, this was not the case in our analyses (Figure 3.11), suggesting Tyr599 alone is not sufficient to normalize Erk activation. Upon mutation of Tyr768, we did observe a reduction in Erk activation (Figure 3.11). Collectively, these findings suggest that the inter-kinase domain Tyr768 is most relevant for hyperactivation of Erk, and that STAT5 activation is regulated by signaling through Tyr599 of the FLT3-ITD.

The findings from our *in vitro* proliferation and *in vivo* transplantation studies collectively suggest that signaling of STAT5 at Tyr599 is more important to FLT3-ITD-induced leukemogenesis compared to the signaling through Erk at Tyr768, as evidenced by proliferation assays and our syngeneic transplant model.

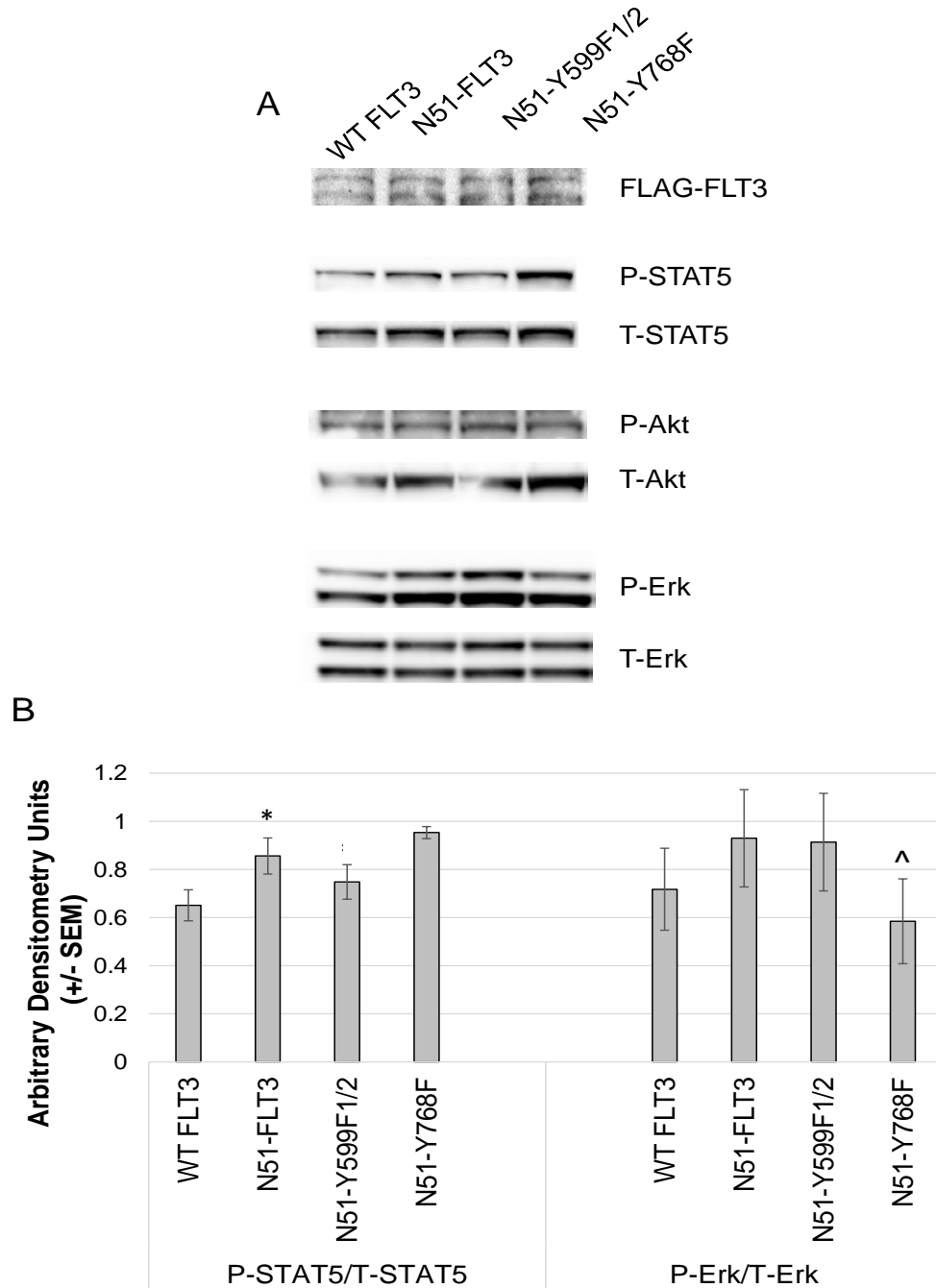


Figure 3.11. FLT3-ITD Tyr599 is important for STAT5 activation, while FLT3-ITD Tyr768 is important for Erk activation.

Total cellular lysates were collected from 32D cells bearing various FLT3 constructs after starvation for either 3 hours or overnight. Samples were analyzed via western blot analysis (**A**) and quantitated using densitometry (**B**). * $n=3$, $p<0.05$ for WT FLT3 vs N51-FLT3; ^ $n=5$, $p=0.05$ for N51-FLT3 vs N51-Y768F, using paired, two-tailed student's *t* test.

Pharmacologic Inhibition of FLT3-ITD Effector Proteins

Given our hypothesis that Shp2 functions both at duplicated Tyr599 in the juxtamembrane domain with Syk and at Tyr768 in the inter-kinase domain with PI3K, and that normalization of STAT5 and Erk activation (Figure 3.11) significantly modulated FLT3-ITD-induced proliferation *in vitro* (Figure 3.7) and altered disease development *in vivo* (in the case of Y599F1/2) (Figure 3.10), we predicted that inhibition of Shp2 phosphatase would cooperate with inhibition of Syk or PI3K to reduce proliferation of leukemogenic cells. For the following studies, we used the Shp2 inhibitor, II-B08 (Zhang, He et al. 2010), the Syk inhibitor, R406 (Braselmann, Taylor et al. 2006), and the PI3K inhibitor, GDC-0941 (Folkes, Ahmadi et al. 2008) (Table 3.1). We treated both WT FLT3 and N51-FLT3 32D cells, as well as primary AML samples, to examine the effect on proliferation and determine cooperativity. We hypothesized that Shp2 will act cooperatively with both Syk and PI3K to reduce FLT3-ITD-induced hyperproliferation (Figure 3.12).

Table 3.1. Inhibitors and their IC₅₀ values used for pharmacologic studies.

IC₅₀ values are based on cell-free assays

Drug	Target	Shp2	PTP1B	Shp1	FAP1	Lyp	CD45	LMWPTP
II-B08	Target	Shp2	PTP1B	Shp1	FAP1	Lyp	CD45	LMWPTP
	IC ₅₀	5 μM	14.3 μM	15.7 μM	20.3 μM	25.0 μM	30 μM	31.1 μM
R406	Target	Syk	FLT3					
	IC ₅₀	40 nM	~200 nM**					
GDC-0941	Target	p110α/δ	p110β	p110γ	mTOR	C2β	DNA-PK	Vps34
	IC ₅₀	3 nM	33 nM	75 nM	0.58 μM*	0.67 μM	1.23 μM	>10 μM

. **Value given is K_i value instead of IC₅₀.

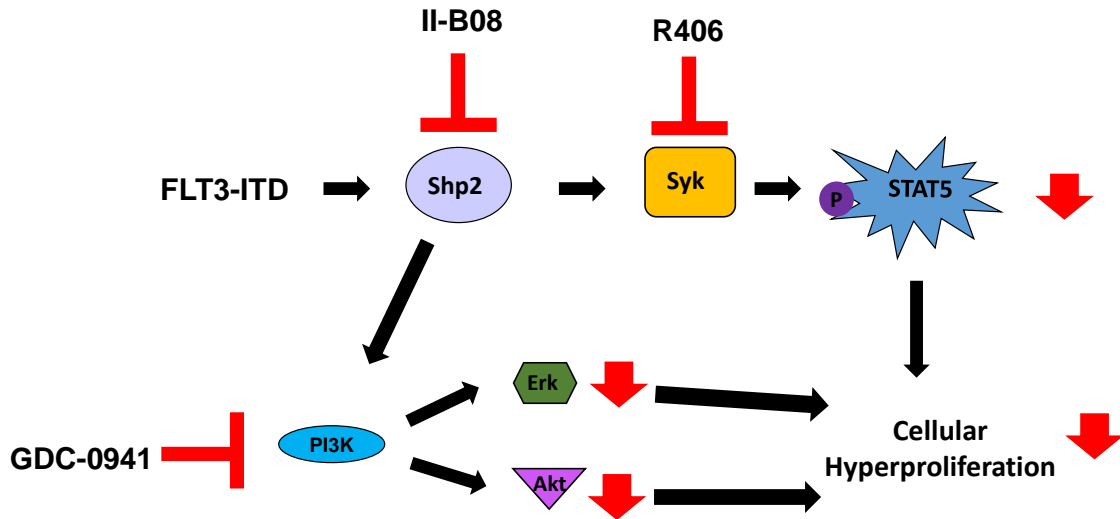


Figure 3.12. Schematic representation of the hypothesis that inhibition of Shp2/Syk and Shp2/PI3K will act to reduce FLT3-ITD-induced hyperproliferation.

We first examined the hypothesis that Shp2 and Syk inhibition could work cooperatively to reduce STAT5 activation and cellular hyperproliferation of FLT3-ITD-expressing cells. Additionally, since STAT5 is hyperactivated in FLT3-ITD-expressing cells, we hypothesized that FLT3-ITD-expressing cells would be uniquely sensitive to Shp2/Syk inhibition due to reduced STAT5 activation, and that there would be little effect on WT FLT3-expressing cells. To test this hypothesis, we first looked at our 32D cells expressing either WT FLT3 or N51-FLT3. Cells were starved for 6 hours in starvation media (0.2% BSA-IMDM), counted, plated (3×10^4 cells/well), and incubated overnight in normal growth media (10% FBS, 2% Pen/Strep) in the presence of: no drug (baseline), II-B08 (25 μ M) alone, increasing doses of R406 (5, 10, 25 nM) alone, or II-B08 in combination with the same increasing doses of R406. The following day, cells were pulsed with ^3H -thymidine, incubated for 6 hours, harvested, and read for ^3H -thymidine incorporation. Cells expressing WT FLT3 did not significantly respond to drug treatment, such that only at high doses of the combination treatment of R406 and II-B08 was there an effect on proliferation (Figure 3.13). However, this finding was in stark contrast to that seen in N51-FLT3 cells. N51-FLT3-expressing cells respond to II-B08 alone and have a dose dependent decrease in proliferation in response to R406 treatment. Most notably, there is a significant cooperativity in R406 and II-B08 treatment (Figure 3.14). This suggests that FLT3-ITD-expressing cells are uniquely dependent on Shp2 and Syk activity.

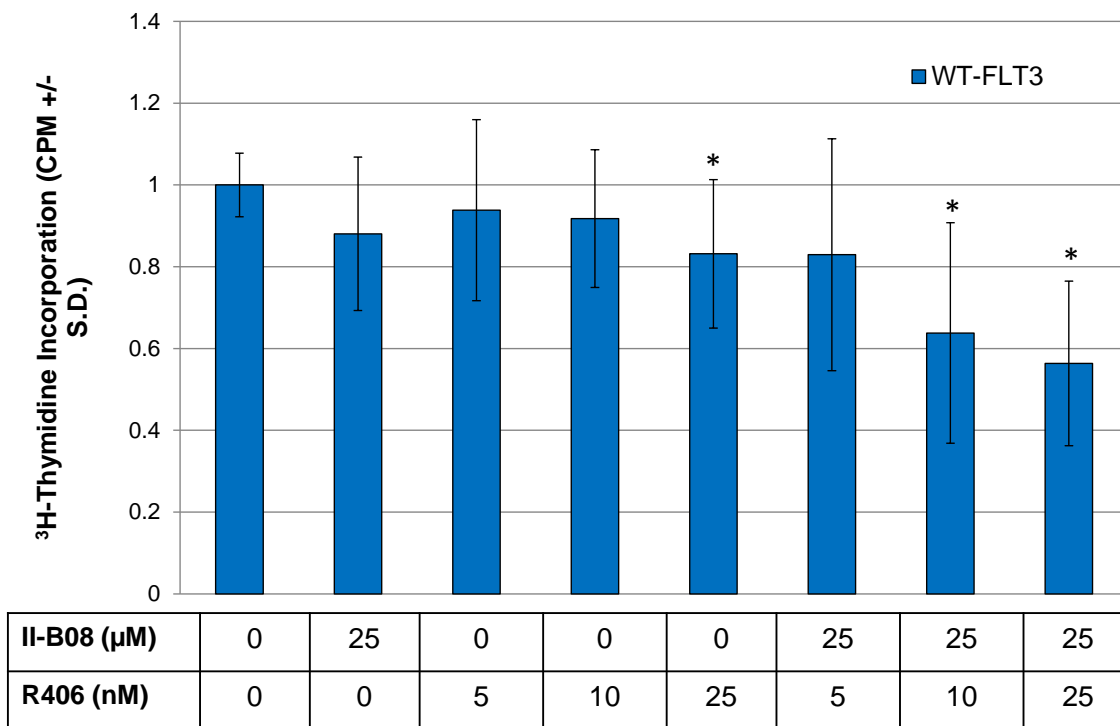


Figure 3.13. WT FLT3-expressing 32D cells did not respond to II-B08 or R406, and the combination had a minimal effect on proliferation.

32D cells expressing WT FLT3 were starved and treated with Shp2 inhibitor, II-B08, and/or Syk inhibitor, R406, overnight and subjected to a ^3H -thymidine incorporation assay. Data represented as percent average proliferation in the absence of drug for each independent sample. Compiled from 3 independent experiments, * $p < 0.05$ by students, unpaired, two-tailed student's t test.

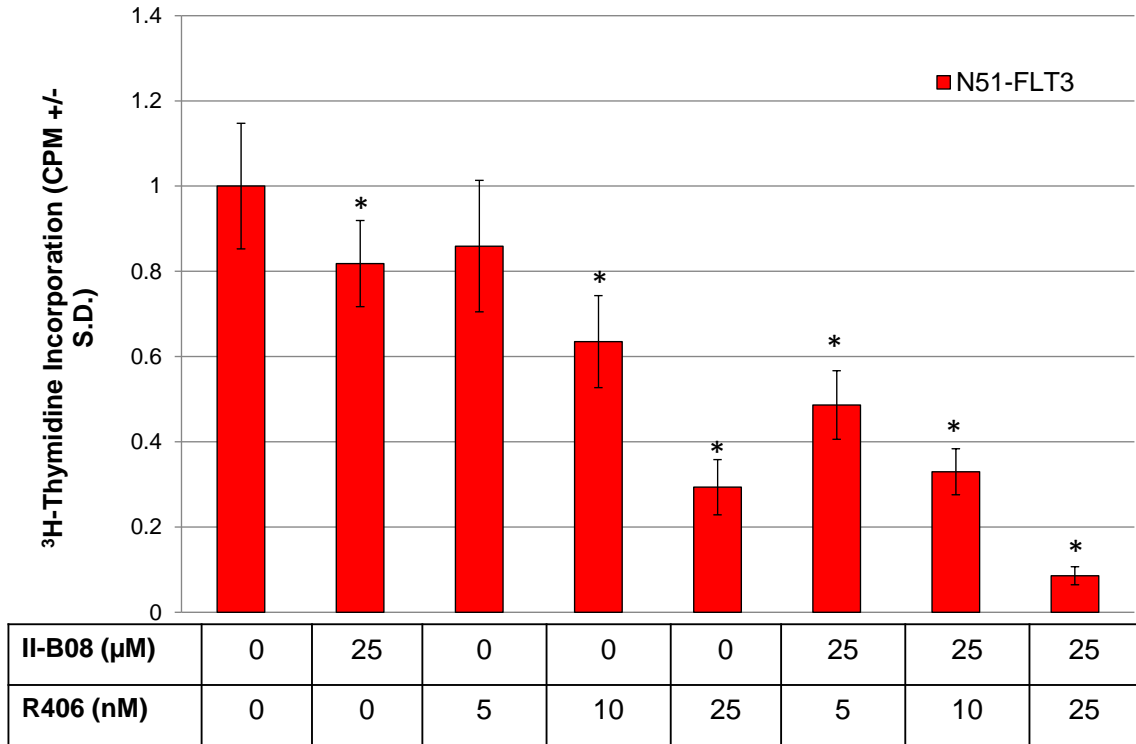


Figure 3.14. N51-FLT3-expressing 32D cells exhibit a significant response to both II-B08 and R406 treatment alone, and there was a cooperative effect of II-B08 and R406 on proliferation.

32D cells expressing N51-FLT3 were starved and treated with Shp2 inhibitor, II-B08, and/or Syk inhibitor, R406, overnight and subjected to a ³H-thymidine incorporation assay. Data represented as percent average proliferation in the absence of drug for each independent sample. Compiled from 3 independent experiments, *p<0.01 using unpaired, two-tailed student's *t* test.

Next, we examined primary AML patient samples, both all samples collectively as well as separated out based on FLT3-ITD mutational status, for their response to R406 and the combination treatment of II-B08 and R406. Primary AML patient peripheral blood samples were obtained, a gradient density was used to obtain mononuclear cells, and cells were incubated overnight in growth media (10% FBS, 2% Pen/Strep supplemented with 10 ng/mL FL and 10 ng/mL GM-CSF). We hypothesized that, similar to the N51-FLT3-expressing 32D cells, we would see a cooperative effect of Shp2 and Syk inhibition in primary AML patient samples. R406 alone had a profound effect on reducing the proliferation of these cells, as measured by ³H-thymidine incorporation (Figure 3.15). At the lowest dose of R406 (0.5 μM), addition of II-B08 (25 μM) further reduced proliferation, indicating a cooperative effect of R406 and II-B08 on patient sample proliferation (Figure 3.15). Of these AML samples, we compared the differential response of FLT3-ITD- AML patient samples to FLT3-ITD+ AML patient samples to determine if FLT3-ITD+ AML patient samples are sensitive to the loss of Shp2 and Syk signaling. FLT3-ITD+ cells trended toward lower proliferation in response to R406 alone, but due to variability and low sample size, we did not see a significant difference between the FLT3-ITD+ and FLT3-ITD- samples (Figure 3.16). Furthermore, both the FLT3-ITD+ and FLT3-ITD- cells appear to be similarly sensitive to the cooperative effect of R406 and II-B08. At low doses of R406 in combination with II-B08, however, there was a trend toward selectivity for FLT3-ITD+ samples over FLT3-ITD- (p=0.06). This differential effect may be due to the fact that Shp2 and Syk both function at the juxtamembrane domain, which is mutant in FLT3-ITD+ samples. This suggests that while Shp2 inhibition may be more selective for FLT3-ITD+ samples, Syk inhibition

targets both FLT3-ITD+ and FLT3-ITD- patient samples, making it a potential general therapeutic target for AML.

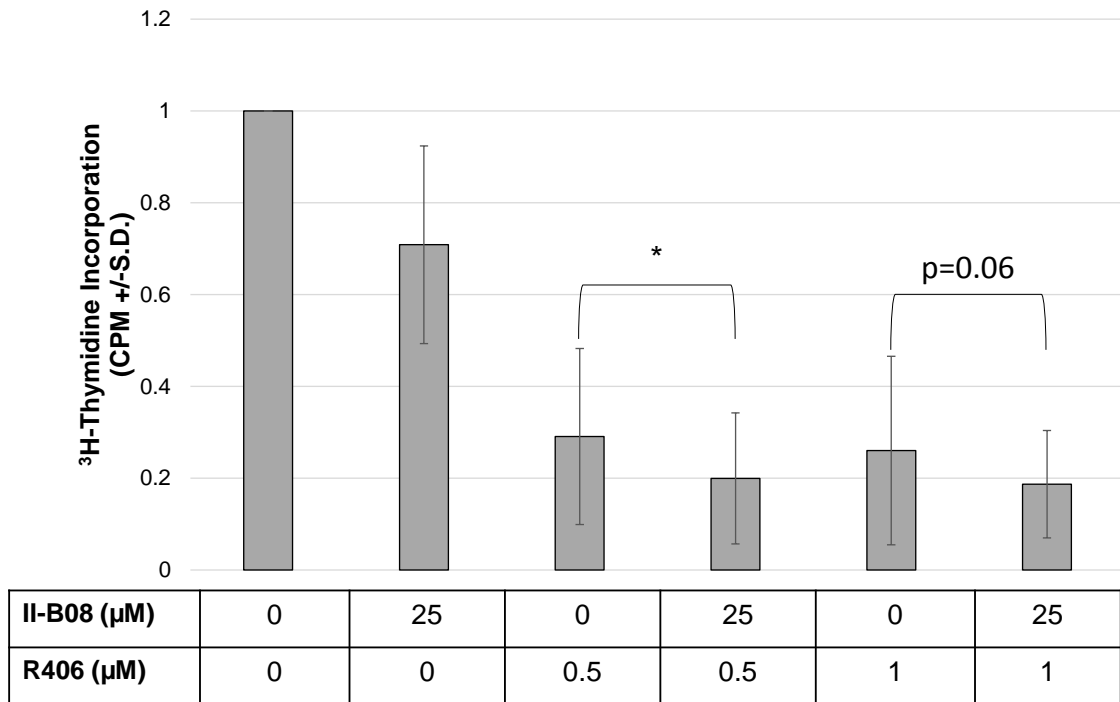


Figure 3.15. Shp2 inhibition and Syk inhibition work cooperatively to reduce the proliferation of AML patient samples.

All primary AML cells were cultured in FL (50 ng/mL) in the presence of Shp2 phosphatase inhibitor, II-B08, and/or Syk inhibitor, R406. Proliferation was measured via ^3H -thymidine incorporation assay. Data is represented as percent average proliferation in the absence of drug for each independent sample. * $p < 0.01$, $n = 13$ independent samples for R406 (0.5 μM) vs. R406 (0.5 μM) AND II-B08; $p = 0.06$, $n = 11$ independent samples for R406 (1.0 μM) vs. R406 (1.0 μM) AND II-B08, using paired, two-tailed student's t test.

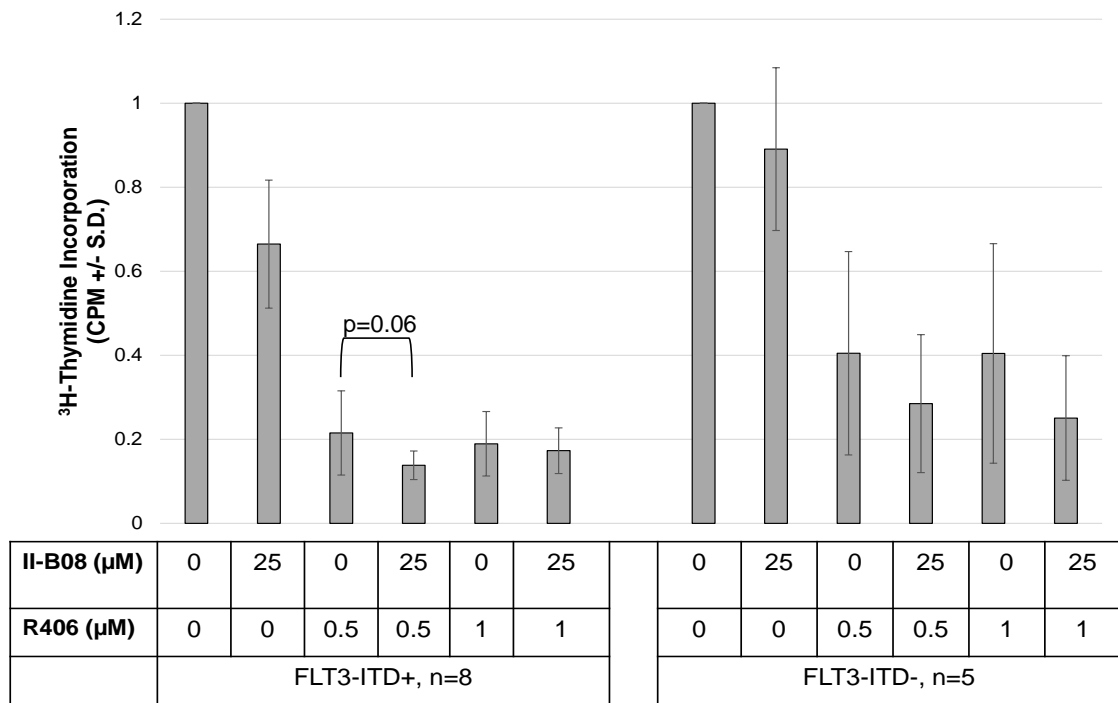


Figure 3.16. FLT3-ITD+ and FLT3-ITD- AML patient samples display cooperativity of Shp2 and Syk inhibition.

FLT3-ITD+ (right) and FLT3-ITD- (left) primary AML cells were cultured in FL (50 ng/mL) in the presence of Shp2 phosphatase inhibitor, II-B08, and/or Syk inhibitor, R406. Proliferation was measured via ³H-thymidine incorporation assay. Data is represented as percent average proliferation in the absence of drug for each independent sample. p=0.06 comparing n=8 independent samples for FLT3-ITD+ and n=4-5 independent samples, for FLT3-ITD- with R406 (0.5 μM) and II-B08 (25 μM) using unpaired, two-tailed student's *t* test.

We next wanted to examine the biochemical consequences of Shp2 and Syk inhibition in our 32D cells to determine if the reduction in hyperproliferation upon Shp2 and Syk inhibition corresponds to a reduction in STAT5 activation. For these studies, WT FLT3- and N51-FLT3-expressing cells were growth factor-deprived overnight in starvation media (0.2% BSA-IMDM), subjected to drug treatment for one hour in normal growth media (10% FBS, 2% Pen/Strep), and total cellular protein was collected. The drug treatment was as follows for both cell types: no drug (baseline), II-B08 alone (25 μ M), R406 alone (10 nM), or II-B08 (25 μ M) AND R406 (10 nM).

As shown in Figure 3.17, STAT5, Shp2, Akt, and Erk phosphorylation levels were all increased in the N51-FLT3-expressing cells compared to WT FLT3-expressing cells at baseline (compare lanes 5 and 1). II-B08, R406, or combination did not have a significant impact on any signaling protein in the WT FLT3-expressing cells (lanes 1-4). In the N51-FLT3-expressing cells, however, the combination treatment of R406 and II-B08 reduced the levels of STAT5, Shp2, Akt, and Erk activation (Figure 3.17 lane 8 and Figure 3.18). Interestingly, Syk inhibition reduced the levels of phospho-Shp2 in the N51-FLT3-expressing cells, suggesting a possible positive feedback loop from Shp2 to Syk, back to Shp2. We found that in the case of both phospho-Akt and phospho-Erk, II-B08 alone did not have an effect (lane 6). R406 alone was able to reduce the levels of active Akt and Erk (Figure 3.17 lane 7), but the combination of II-B08 and R406 had the greatest reduction on active Akt and Erk (lane 8). In multiple experiments, we found that R406 and II-B08 consistently and significantly reduced activation of STAT5 (Figure 3.18). These findings collectively indicate that Syk does regulate the signaling of PI3K/Shp2 at Tyr768.

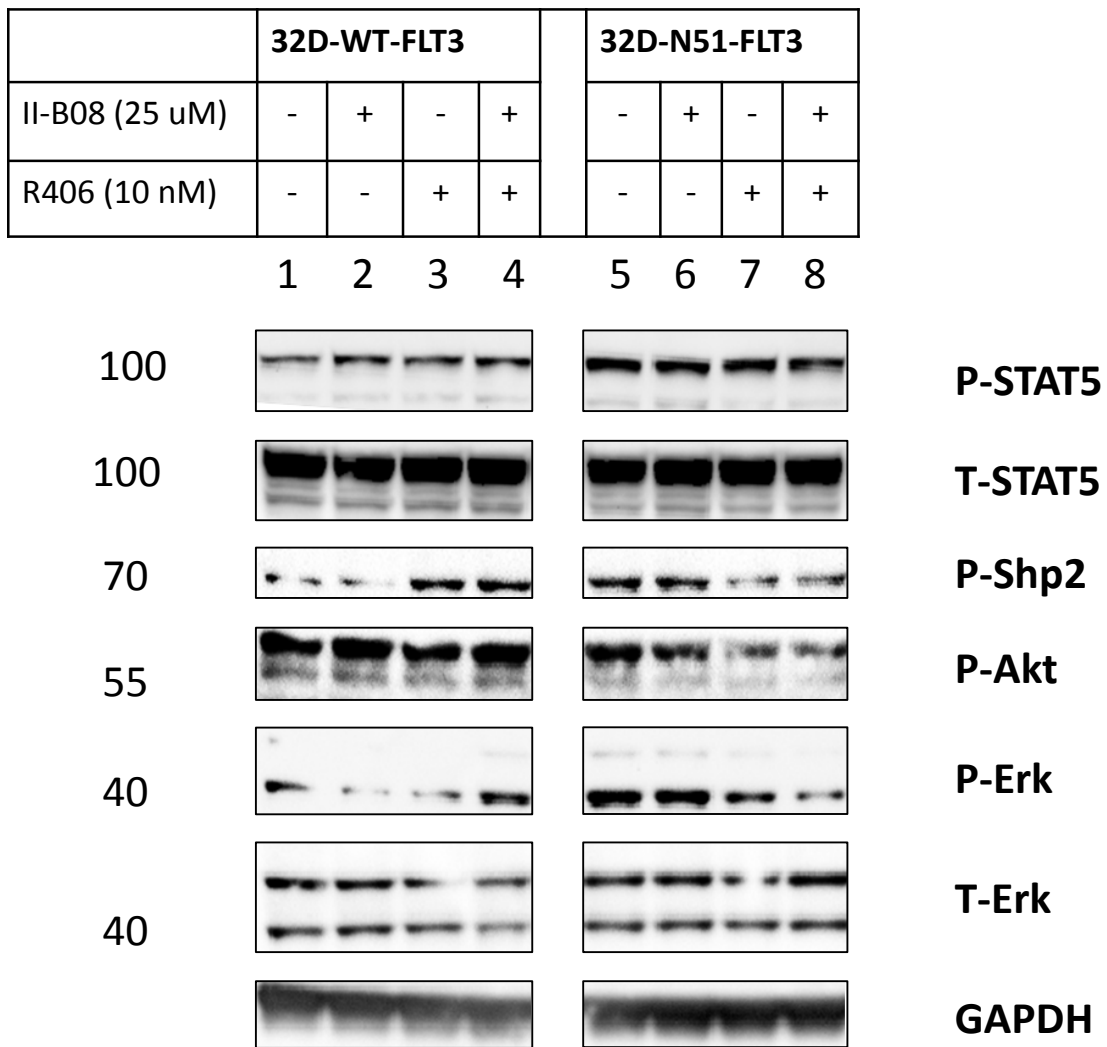


Figure 3.17. Inhibition of Shp2 and Syk results in lower levels of STAT5, Akt, and Erk phosphorylation in N51-, but not WT, FLT3 cells.

WT FLT3 and N51-FLT3 32D cells were starved overnight, and treated in media (10% FBS, 2% Pen/Strep) with drug (II-B08 alone, R406 alone, or the combination) for one hour. Total cellular lysates were collected, and samples were analyzed via western blot analysis. Representative of three independent experiments. Figure cropped to only show II-B08 +/- R406.

	N51-FLT3			
II-B08 (μM)	0	25	0	25
R406 (nM)	0	0	10	10

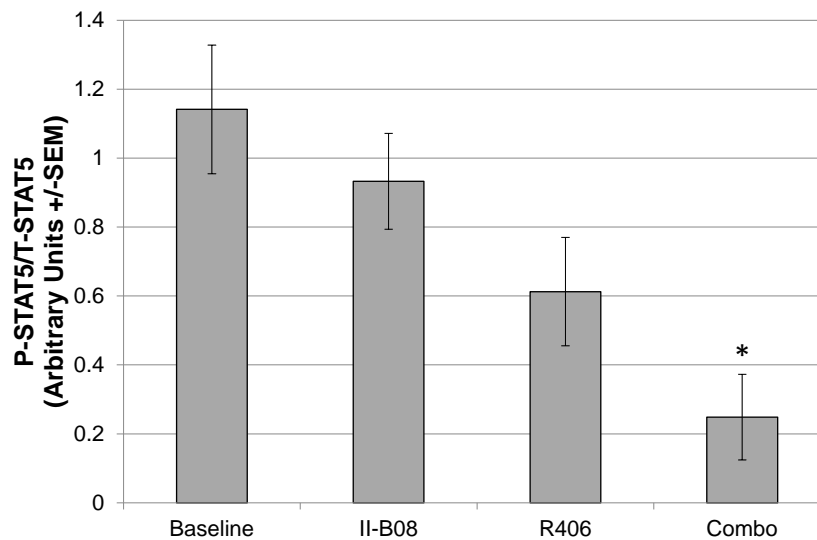
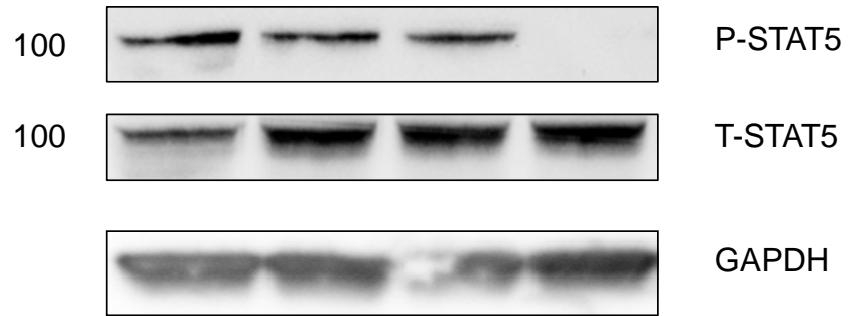


Figure 3.18. Inhibition of Shp2 and Syk lower the level of active STAT5 in N51-FLT3-expressing 32D cells.

N51-FLT3 32D cells were starved overnight, and treated in media (10% FBS, 2% Pen/Strep) with drug (II-B08 alone, R406 alone, or the combination) for one hour. Total cellular lysates were collected, and samples were analyzed via western blot analysis.

*n=4, $p < 0.05$ for baseline vs. combo, using unpaired, two-tailed student's *t* test.

We next focused on PI3K inhibition in combination with Shp2 inhibition. We hypothesized that in FLT3-ITD+ cells, PI3K and Shp2 work cooperatively at Tyr768 to activate Akt and Erk signaling, and therefore positively regulate proliferation. To determine if Shp2 and PI3K cooperate, we analyzed primary AML patient samples treated with II-B08 and/or GDC-0941, a PI3K inhibitor that targets the p110 α and p110 δ catalytic subunits. Samples were treated with increasing doses of GDC-0941, in the absence or presence of II-B08, and subjected to ³H-thymidine incorporation assays. GDC-0941 alone inhibited proliferation in a dose-dependent manner (Figure 3.19). Moreover, II-B08 and GDC-0941 exhibited cooperativity even at low doses of GDC-0941, such that the combination of the two resulted in lower proliferation levels than either drug alone. Of these AML samples, we next compared the response of known FLT3-ITD- and known FLT3-ITD+ patient samples to GDC-0941 and/or II-B08. FLT3-ITD+ cells appear to be more sensitive to GDC-0941 treatment alone or to II-B08 treatment alone (Figure 3.20). However, GDC-0941 and II-B08 have a cooperative effect on both the FLT3-ITD+ and FLT3-ITD- cells, as the addition of II-B08 to GDC-0941 significantly reduces proliferation in both (Figure 3.20). While not statistically significant, there was a trend that FLT3-ITD+ cells were more sensitive to the combination treatment compared to FLT3-ITD- (p=0.065); with an increased sample size the increase in sensitivity will be confirmed. Our data suggest that targeting both Shp2 and PI3K could hold therapeutic benefit for all AML patients, and in particular FLT3-ITD+ patients.

We next evaluated the cooperativity of Shp2 and PI3K inhibition on the activation of FLT3-ITD effectors in our 32D cells expressing either WT FLT3 or N51-FLT3. Cells

were starved overnight and treated with drug for one hour, followed by protein extraction. As expected, PI3K reduced levels of active Akt and Erk (Figure 3.21, lane 7). II-B08 alone had a slight effect of both Akt and Erk (lane 6), but the greatest reduction was seen with II-B08 and GDC-0941 (lane 8), suggesting that Shp2 and PI3K work cooperatively to activate Akt and Erk signaling. Interestingly, GDC-0941 also reduced levels of phospho-STAT5 and phospho-Shp2 (Figure 3.21), suggesting that PI3K may also play a role in the signaling occurring through Tyr599. It is also possible that PI3K has a positive feedback loop at Tyr768 to regulate Shp2.

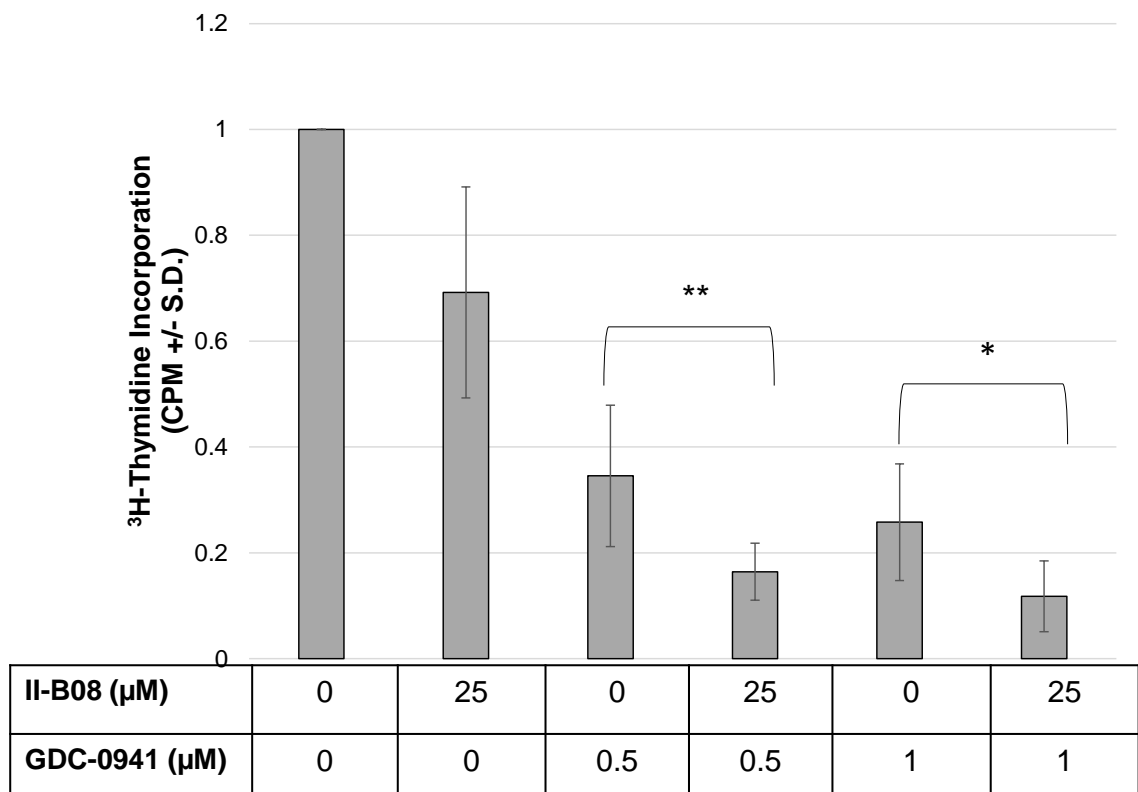


Figure 3.19. Primary AML patient samples are sensitive to the inhibition of PI3K and cooperate with Shp2 inhibition to reduce proliferation.

All primary AML cells were cultured in FL (50 ng/mL) in the presence of Shp2 phosphatase inhibitor, II-B08, and/or PI3K inhibitor, GDC-0941. Proliferation was measured via ^3H -thymidine incorporation assay. Data is represented as percent average proliferation in the absence of drug for each independent sample. *n=12 independent samples, $p < 0.005$ for GDC-0941 (0.5 μM) vs. GDC-0941 (0.5 μM) AND II-B08 (25 μM), **n=17 independent samples, $p < 0.001$ for GDC-0941 (1 μM) vs. GDC-0941 (1 μM) AND II-B08 (25 μM), using paired, two-tailed student's *t* test.

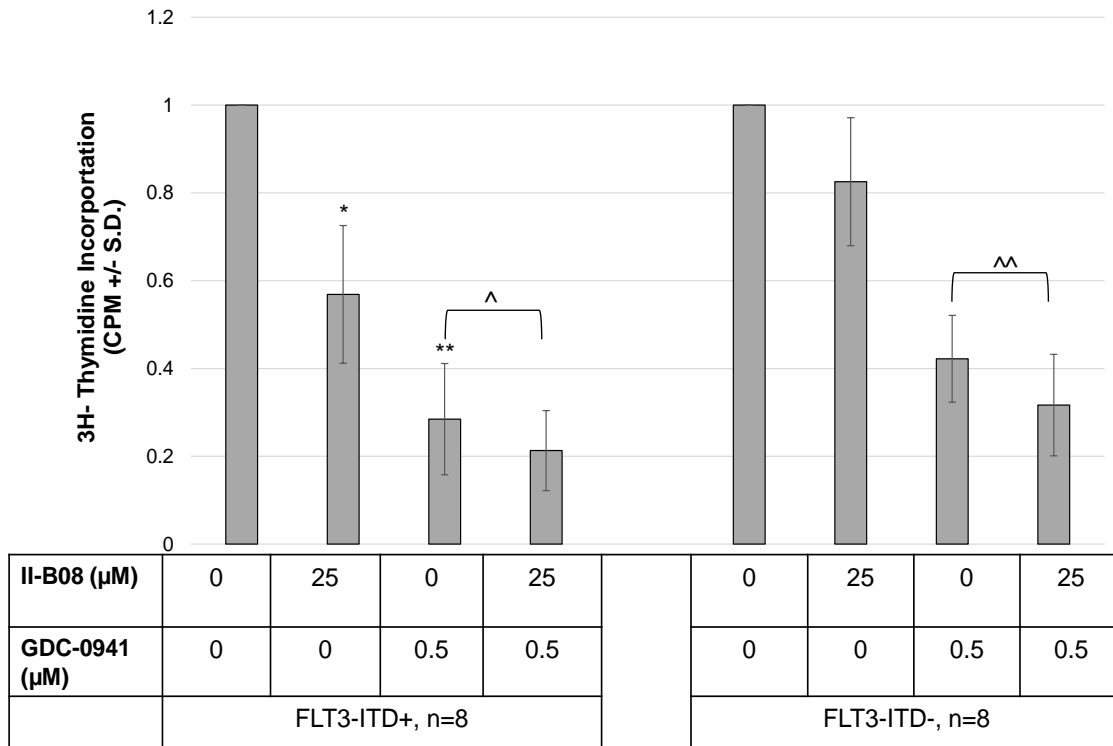


Figure 3.20. FLT3-ITD+ primary AML patient samples are more sensitive to Shp2 or PI3K inhibition alone compared to FLT3-ITD- primary AML patient samples.

FLT3-ITD+ (right) and FLT3-ITD- (left) primary AML cells were cultured in FL (50 ng/mL) in the presence of Shp2 phosphatase inhibitor, II-B08, and/or PI3K inhibitor, GDC-0941. Data represented as percent average proliferation in the absence of drug for each independent sample. * $p < 0.01$ comparing FLT3-ITD+ vs. FLT3-ITD- in the presence of II-B08 (25 μM); ** $p < 0.05$ comparing FLT3-ITD+ vs. FLT3-ITD- in the presence GDC-0941 (0.5 μM), using unpaired, two-tailed student's *t* test. ^ $p < 0.01$ comparing FLT3-ITD+ samples in the presence GDC-0941 (0.5 μM) vs. GDC-0941 (0.5 μM) and II-B08 (25 μM); ^^ $p < 0.05$ comparing FLT3-ITD- samples in the presence GDC-0941 (0.5 μM) vs. GDC-0941 (0.5 μM) and II-B08 (25 μM), using paired, two-tailed student's *t* test.

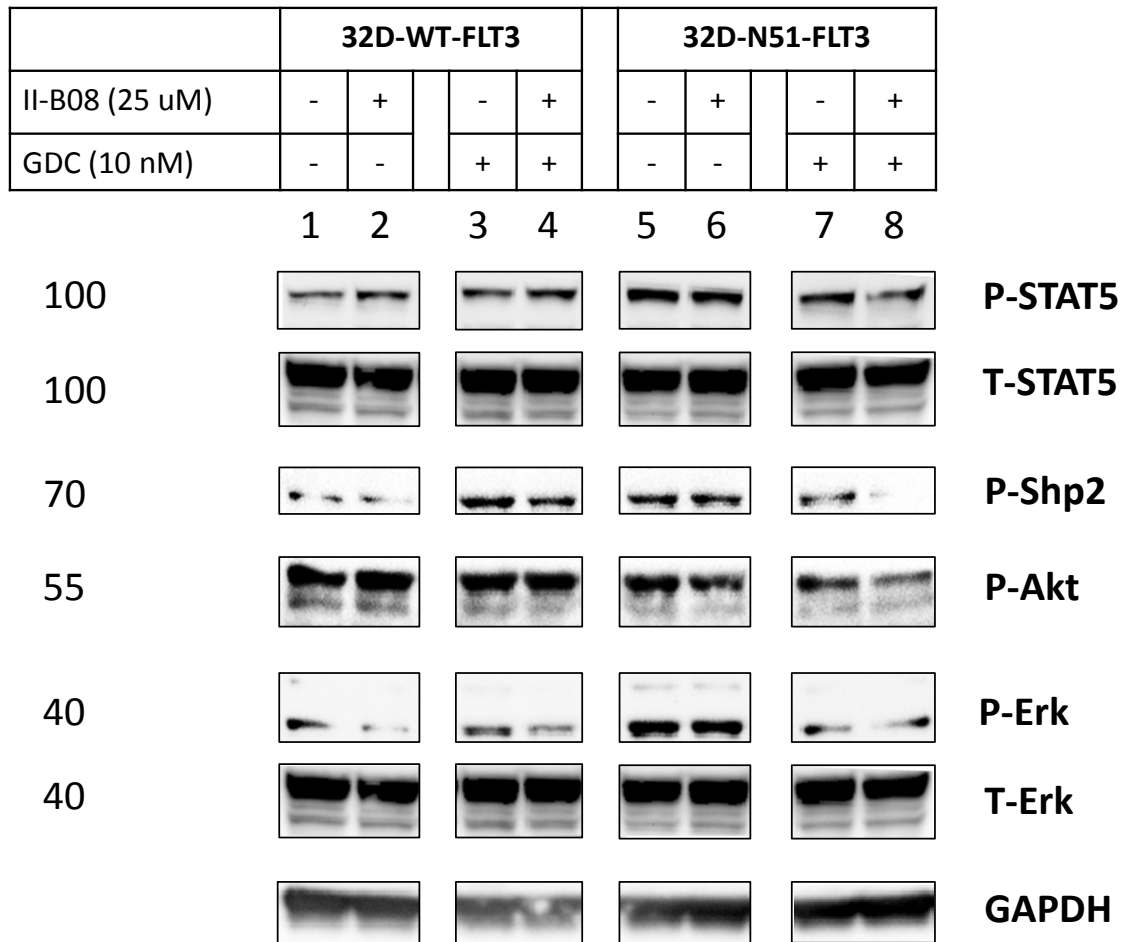


Figure 3.21. Inhibition of Shp2 and PI3K lower the levels of STAT5, Akt, and Erk phosphorylation in N51-, but not WT, FLT3 cells.

WT FLT3 and N51-FLT3 32D cells were starved overnight, and treated in media (10% FBS, 2% Pen/Strep) with drug (II-B08 alone, GDC-0941 alone, or the combination) for one hour. Total cellular lysates were collected, and samples were analyzed via western blot analysis. Representative of three independent experiments. Figure cropped to only show II-B08 +/- GDC-0941.

Finally, we examined FLT3-ITD+ and FLT3-ITD- primary AML patient samples for their response to Shp2 inhibition with II-B08 alone at varying doses. Cells were starved for three hours, counted, plated in a 96 well plate to equal numbers (3×10^4 cells/well) with increasing doses of II-B08, and subjected to a ^3H -thymidine incorporation assay. When comparing FLT3-ITD- patient samples to FLT3-ITD+ patient samples, it is clear that FLT3-ITD+ cells are uniquely sensitive to the loss of Shp2, such that there is a dose-dependent reduction in proliferation of FLT3-ITD+ AML patient samples, which is less pronounced in FLT3-ITD- patient samples (Figure 3.22). This is consistent with our findings that FLT3-ITD+ 32D cells are more sensitive to Shp2 inhibition than WT FLT3 cells.

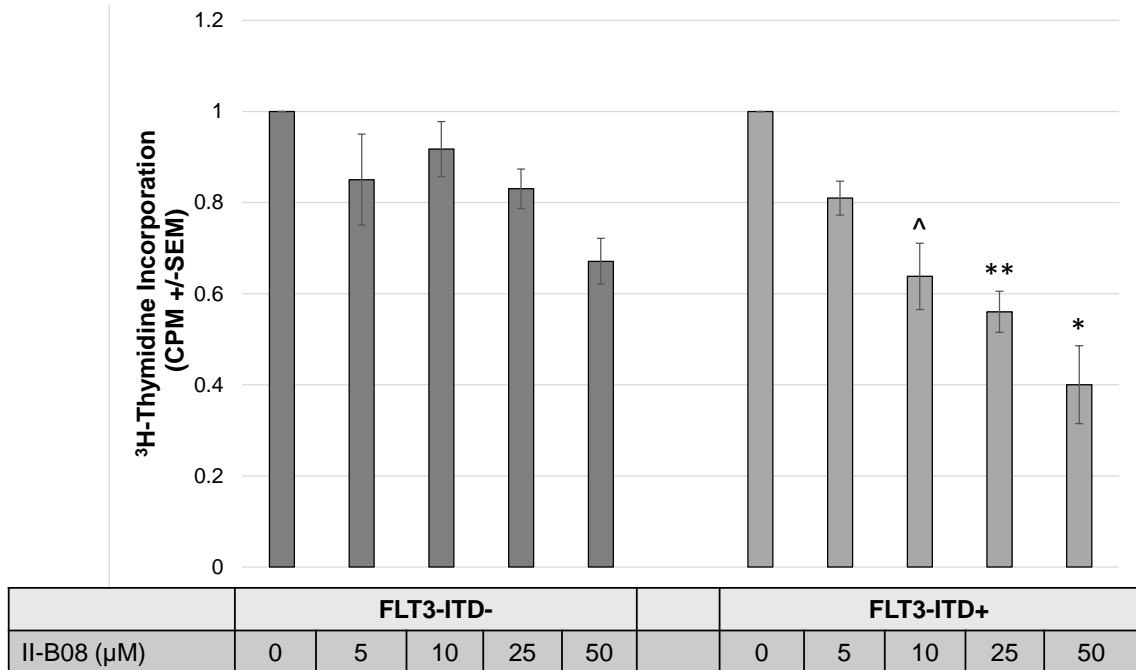


Figure 3.22. FLT3-ITD+ AML patient samples are uniquely sensitive to Shp2 inhibition by II-B08.

FLT3-ITD+ (right) and FLT3-ITD- (left) primary AML cells were cultured in FL (50 ng/mL) in the presence of increasing doses of the Shp2 phosphatase inhibitor, II-B08. Data represented as percent average proliferation in the absence of drug for each independent sample. [^]n=3 FLT3-ITD+ and 6 FLT3-ITD- AML samples, p<0.05 comparing FLT3-ITD+ to FLT3-ITD- at II-B08 10 μM; ^{**}n=10 FLT3-ITD+ and n=12 FLT3-ITD- AML samples, p<0.001 comparing FLT3-ITD+ to FLT3-ITD- at 25 μM II-B08; ^{*}n=7 FLT3-ITD+ and n=9 FLT3-ITD- AML samples, p<0.05 comparing FLT3-ITD+ to FLT3-ITD- at 50 μM, using unpaired, two-tailed student's *t* test.

In vivo analysis of the efficacy of Shp2 and PI3K inhibition on mitigating FLT3-ITD-induced myeloproliferative disease

Because of the promising results of II-B08 alone and in combination with GDC-0941 treatment on primary AML patient samples, we next wanted to see if these drugs would be effective *in vivo* in a syngeneic mouse model of N51-FLT3-induced myeloproliferative disease (MPD). In preliminary studies done in the Chan lab, treatment of a mouse exhibiting expansion of an eGFP positive (indicative of N51-FLT3 expression) clone of 32D cells with II-B08 treatment for one week was sufficient to diminish the expansion of this clone, and prevent recurrence for an extended period of time (Figure 3.23). Therefore, in our drug study, we hypothesized that treatment with II-B08 or GDC-0941 alone, and more so the dual blockade of Shp2 and PI3K activity would mitigate the development and progression of MPD in C3H/HeJ mice transplanted with N51-FLT3-ITD-expressing 32D cells.

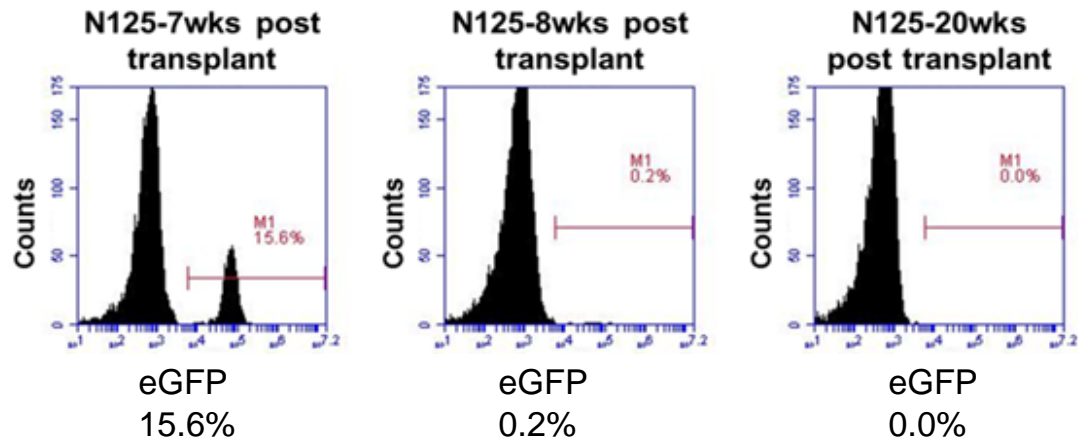
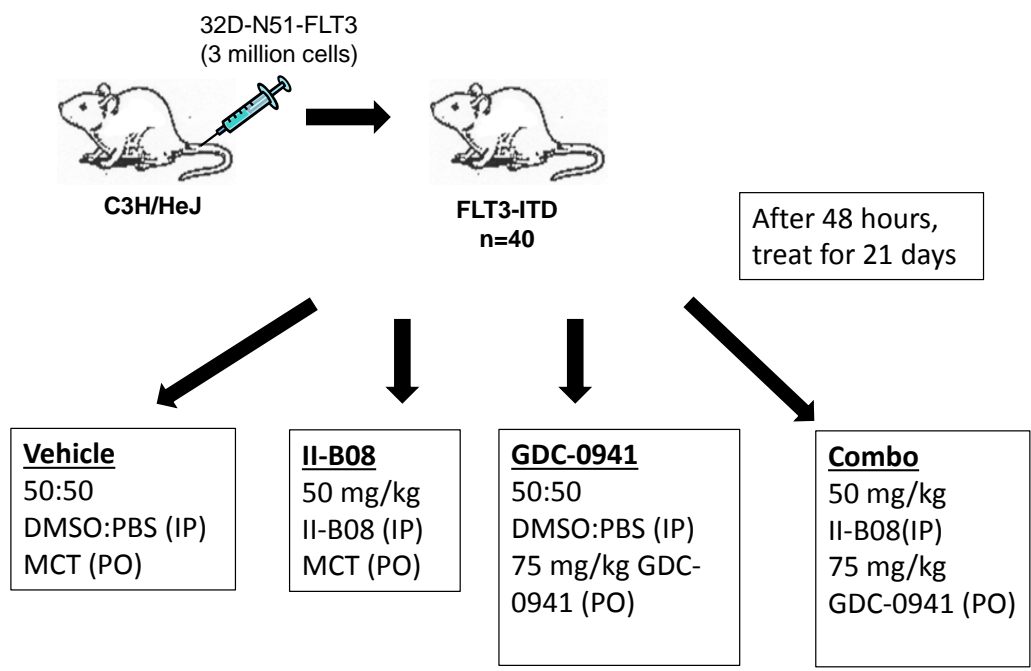


Figure 3.23. II-B08 markedly reduced the clonal expansion of N51-FLT3-ITD-expressing cells.

Peripheral blood of the same mouse at 7, 8, and 20 weeks post-transplant were analyzed for eGFP positivity (indicative of N51-FLT3-expressing donor cells) using flow cytometry.

For our study, C3H/HeJ mice were transplanted with 32D-N51-FLT3 cells (3×10^6) and treated 48 hours post-transplant with either: vehicle intraperitoneally (IP) and vehicle orally (PO), II-B08 IP and vehicle PO, vehicle IP and GDC-0941 PO, or II-B08 IP and GDC-0941 PO (Figure 3.24). Duration (21 days) and dosing of II-B08 (50 mg/kg) were determined based on pharmacokinetic studies performed and published by the Chan lab (Mali, Ma et al. 2012). Dosing (10 mg/kg) and delivery of GDC-0941 were determined based on previously published studies (Folkes, Ahmadi et al. 2008, Edgar, Wallin et al. 2010). Based on our experience using this syngeneic transplant model for oncogenic KIT-induced leukemia (Mali, Ma et al. 2012), we determined that we needed 10 animals per treatment group. Mice were analyzed four weeks after transplant for signs of eGFP expansion and elevated WBC counts in the peripheral blood. Survival was followed and upon necropsy, specimen samples were saved in formalin for histopathological diagnosis, as well as examination of the spleen size for an indication of splenomegaly.



MCT= 0.5% methylcellulose, 0.2% Tween 80

Figure 3.24. Schematic overview depicting the experimental procedure for analysis of II-B08 and/or GDC-0941 in preventing FLT3-ITD-induced leukemogenesis *in vivo*.

For our eGFP and WBC analysis, we hypothesized that II-B08 and GDC-0941 would have lower counts than vehicle, and that the combination of the two drugs would most effectively lower eGFP positivity and WBC counts in the peripheral blood. While there was a modest effect of either drug alone, the combination treatment group had the lowest eGFP positivity and WBC counts among the four groups (Figure 3.25 and Figure 3.26, respectively), consistent with our hypothesis that Shp2 and PI3K work cooperatively to promote leukemogenesis.

As seen in Figure 3.27, neither II-B08 alone, GDC-0941 alone, nor the combination of II-B08 and GDC-0941 were sufficient to prevent N51-FLT3-induced leukemia based on spleen size and pathology at the time of death (Figure 3.27). Furthermore, there was no statistically significant difference in overall survival among the four groups (Figure 3.28). However, mice receiving combination treatment did have a higher median survival compared to vehicle (51 days and 38 days, respectively, Figure 3.29), suggesting that the combination of both drugs do have an effect on the progression to leukemogenesis. Taken together, this suggests that Shp2 and PI3K work cooperatively to induce FLT3-ITD-induced leukemogenesis and that targeting Shp2 and PI3K may reduce the severity of the disease. However, dosing and/or duration may not have been optimized for this study. It may be that increased dosing of II-B08 or GDC-0941 could have further prevented MPD.

Since we observed that the combination of Syk and Shp2 was also able to reduce hyperproliferation of N51-FLT3-expressing 32D cells and primary AML patient samples *in vitro*, we would be interested in conducting an *in vivo* drug study with these compounds in the future. We would hypothesize that, similar to what is seen with GDC-

0941 and II-B08, combination treatment with R406 and II-B08 would most significantly alter MPD. Since the greatest effect on inhibition of leukemogenesis was mutation of the binding site of Syk (i.e. Tyr599), we would hypothesize that R406 and II-B08 may have a stronger effect *in vivo* than the GDC-0941 and II-B08 combination.

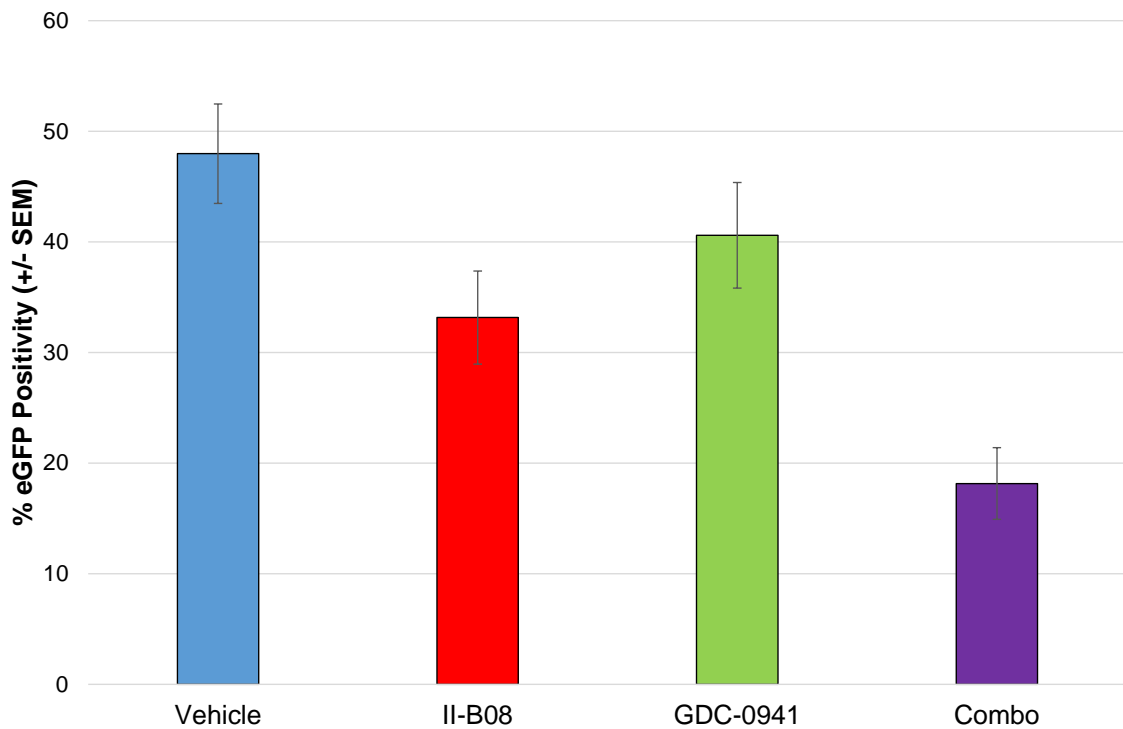


Figure 3.25. Combination treatment of II-B08 and GDC-0941 reduces the level of eGFP positive cells in the peripheral blood.

At 4 weeks post-transplant, peripheral blood was collected from each mouse. Samples underwent red blood cell lysis and cells were analyzed by flow cytometry. n=10 for vehicle, n=7 for II-B08, and n=8 for GDC-0941 and the combination treatment groups.

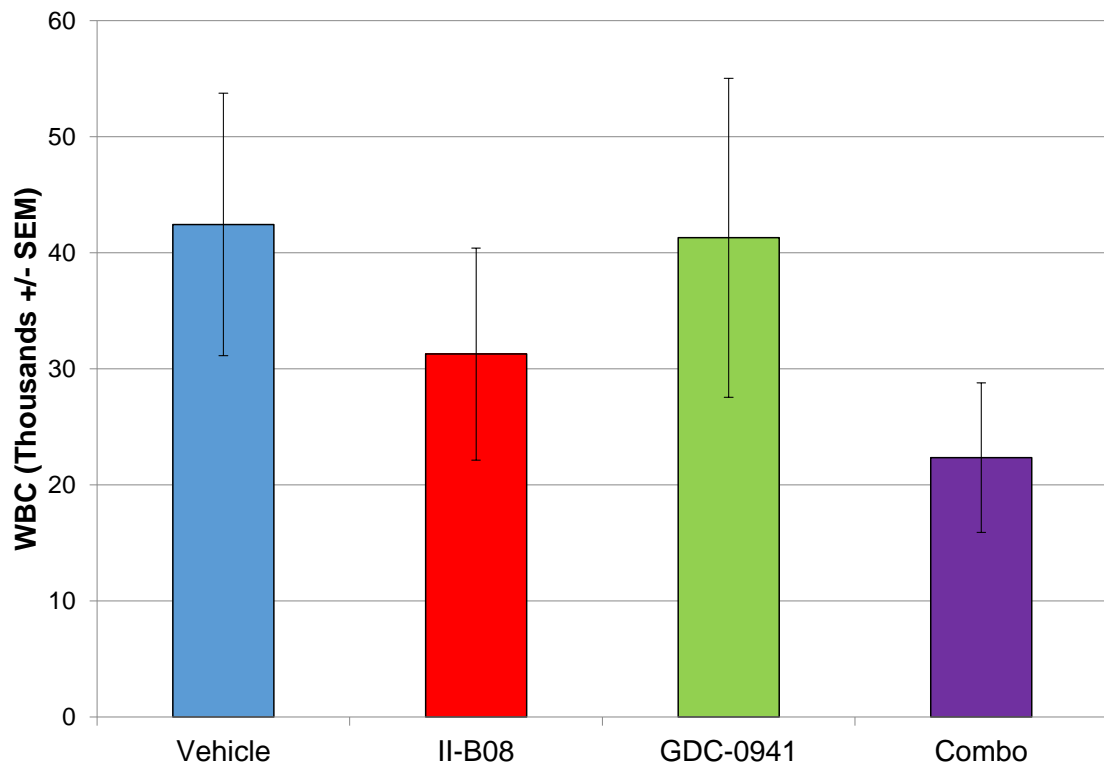


Figure 3.26. Combination treatment of II-B08 and GDC-0941 trends toward a reduction in elevated WBC counts in the peripheral blood.

At 4 weeks post-transplant, peripheral blood was collected from each mouse. Samples were analyzed for complete blood counts (CBCs) using a Hemavet. n=10 for vehicle, n=7 for II-B08, and n=8 for GDC-0941 and the combination treatment groups. p=0.13 comparing combo treatment with vehicle using unpaired, two-tailed student's *t* test.

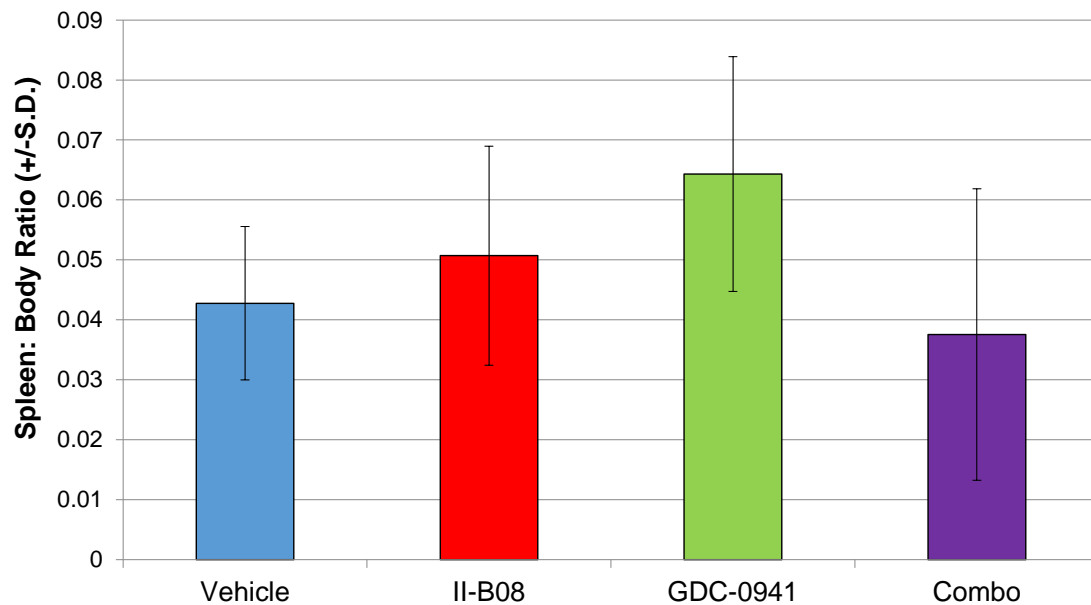


Figure 3.27. N51-FLT3-expressing mice treated with II-B08 and/or GDC-0941 all display splenomegaly upon morbidity.

Mice transplanted with N51-FLT3-expressing 32D cells were followed for survival after treatment with II-B08 and/or GDC-0941. Upon morbidity, mice were weighed and specimens were collected including the spleen, which was weighed as an indication of splenomegaly. n=4 (vehicle), n=7 (II-B08), n=2 (GDC-0941), and n= 4 (combo).

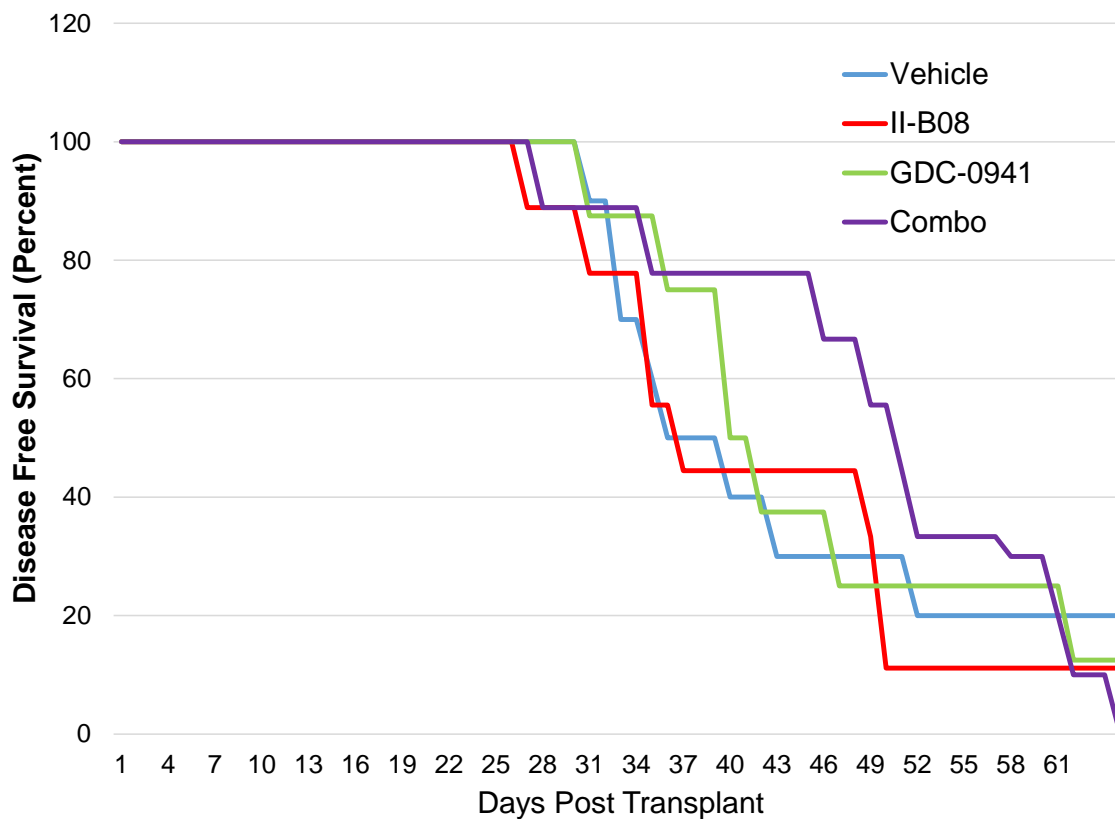


Figure 3.28. Shp2 inhibition and/or PI3K inhibition did not prevent progression to MPD in N51-FLT3-expressing mice.

C3H/HeJ mice were transplanted with N51-FLT3-expressing 32D cells (3×10^6). At 48 hours post-transplant, mice were treated with vehicle, II-B08 alone, GDC-0941 alone, or the combination treatment for 21 consecutive days. Mice were followed for overall survival. n=10 per treatment group.

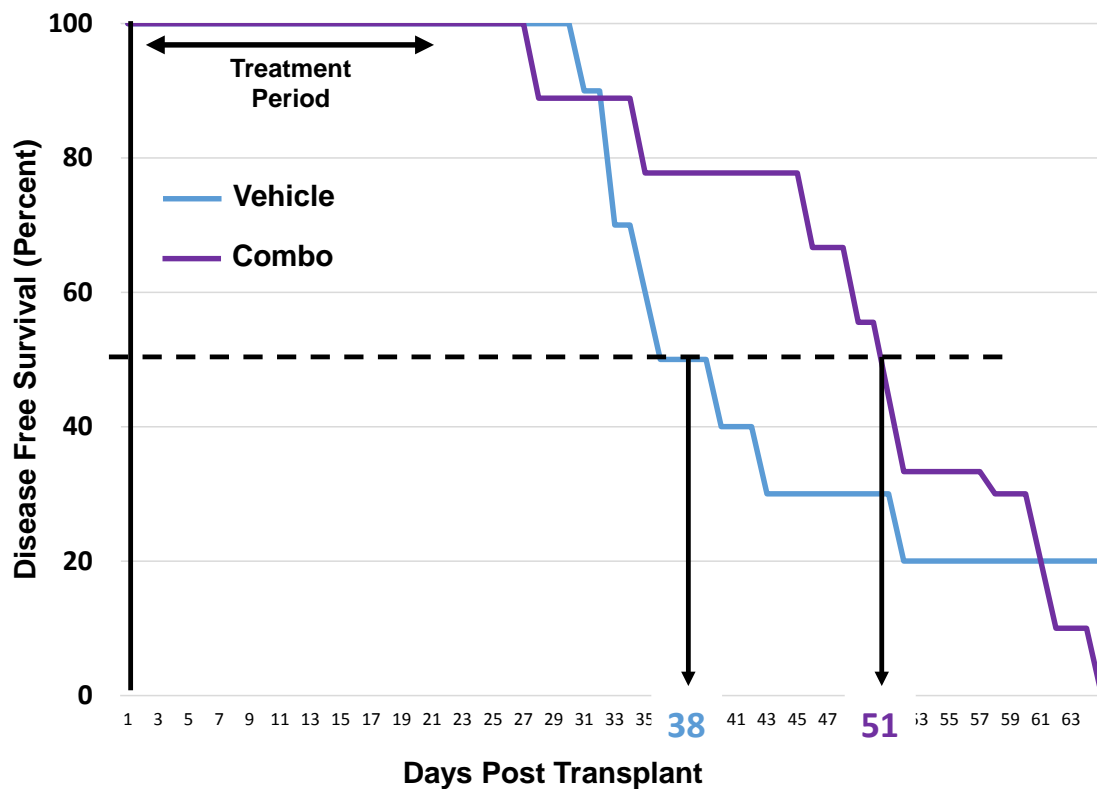


Figure 3.29. II-B08 and GDC-0941 treatment increases the median survival of N51-FLT3-expressing mice.

C3H/HeJ mice were transplanted with N51-FLT3-expressing 32D cells (3×10^6). At 48 hours post-transplant, mice were treated with vehicle, II-B08 alone, GDC-0941 alone, or the combination treatment for 21 consecutive days. Mice were followed for overall survival. n=10 per treatment group.

Discussion

While it is widely recognized that FLT3-ITD mutations aberrantly activate STAT5, the mechanism through which STAT5 becomes activated is still unclear. Additionally, there are some discrepancies in the field regarding the overall importance of STAT5 signaling to FLT3-ITD-induced leukemogenesis. We have previously shown that Shp2 phosphatase positively regulates FLT3-ITD-induced leukemogenesis, as deletion of Shp2 can result in increased overall survival of N51-FLT3-expressing mice (Nabinger, Li et al. 2013). However, how Shp2 functions at the FLT3-ITD receptor is still unknown. By mutating the Shp2 interaction sites on FLT3-ITD, we were able to study how Shp2 functions at the FLT3 receptor to signal downstream effectors and promote FLT3-ITD-induced leukemogenesis.

First, we sought to examine Shp2 signaling from FLT3-ITD receptor by mutating known binding sites on FLT3, Tyr599 and Tyr768, and creating 32D cell lines. This allowed us to examine the outcome of these mutations on FLT3-ITD signaling and leukemogenesis. We found that mutating either duplicated Tyr599 (Y599F1/2) or Tyr768 (Y768F) reduced Shp2 interaction with FLT3-ITD (Figure 3.6) and significantly reduced the hyperproliferation of N51-FLT3-ITD 32D cells *in vitro* (Figure 3.7). In total cellular lysates of these mutant cell lines, we observed lower levels of active STAT5 upon mutation of duplicated Tyr599, and lower levels of active Erk upon mutation of Tyr768, suggesting different signaling pathways emanating from the different tyrosine residues (Figure 3.11). To determine the importance of the differential signaling on the progression to FLT3-ITD-induced MPD *in vivo*, we employed a syngeneic mouse model in which our 32D cell lines can be transplanted into recipient C3H/HeJ, without any

environmental manipulation (i.e. irradiation). While Tyr768 mutation did not have an effect on progression to MPD, we did observe a delayed progression in the duplicated Tyr599 mutant cells (Y599F1/2), suggesting that the signaling from Tyr599 to STAT5, is more important to leukemogenesis than the signaling from Tyr768 to Erk (Figure 3.10).

Syk kinase has been linked to the development of hematologic malignancies, leading to our interest in its role in FLT3-ITD+ AML and potential cooperation with Shp2. Syk kinase is a hematopoietic specific kinase that binds to FLT3-ITD and is a critical factor for FLT3-ITD-induced leukemogenesis (Heiss, Masson et al. 2006). We hypothesized that Syk and Shp2 cooperate to promote STAT5 activation at FLT3-ITD Tyr599. As Syk has also been shown to phosphorylate Tyr768, we hypothesized that mutation of Tyr599 should also reduce the signaling from Tyr768, and that mutation of Tyr768 would phenocopy mutation of duplicated Tyr599. However, we did not observe a normalization of Erk or Akt upon mutation of duplicated Tyr599, and mutation of Tyr768 did not prolong survival. Syk has been shown to be recruited to Tyr589, Tyr591, and Tyr597 in addition to Tyr599 (Puissant, Fenouille et al. 2014). Therefore, mutation of one of the binding sites of Syk may not be sufficient to reduce Syk signaling downstream to the inter-kinase domain of FLT3. In addition, it is possible that redundancies in the signaling machinery could exist in FLT3-ITD.

We next tested the inhibition of Shp2 signaling using pharmacologic inhibitors. II-B08 is a Shp2 phosphatase inhibitor that has previously been shown to reduce FLT3-ITD+ AML proliferation (Nabinger, Li et al. 2013). Recently II-B08 has been shown to inhibit Ras/Erk signaling and suppress oncogenesis in a glioblastoma model (Bunda, Burrell et al. 2015). We combined Shp2 inhibition with Syk or PI3K inhibition to

determine if we could target pathways at multiple points to alter FLT3-ITD-mediated signaling and hyperproliferation further.

The Syk pharmacologic inhibitor R406 has been shown to act on both Syk and FLT3 (albeit, to a lesser extent) (Braselmann, Taylor et al. 2006), making it an attractive therapeutic target for FLT3-ITD+ AML patients. Syk inhibition using R406 has been shown to reduce leukemic burden *in vivo* (Hahn, Berchuck et al. 2009, Miller, Al-Shahrour et al. 2013). Therefore, we hypothesized that treatment of N51-FLT3-expressing 32D cells and primary AML patient samples with the combination of II-B08 and R406 would have a significant effect on proliferation and signaling. Indeed, we saw a cooperative effect on the hyperproliferation of these oncogenic cells (Figure 3.14 and Figure 3.15), but not on WT FLT3-expressing 32D cells (Figure 3.13). Additionally, we saw that total Syk inhibition, as opposed to just one binding site of Syk on FLT3-ITD, was able to reduce levels of active STAT5, Akt, and Erk (Figure 3.17), and that there was a cooperative effect of Shp2 and Syk inhibition on STAT5 phosphorylation (Figure 3.18).

We observed a similar effect in the case of PI3K inhibition (using GDC-0941) and Shp2 inhibition. GDC-0941 has demonstrated activity toward solid tumors in humans and is currently being used in Phase I clinical trials for chronic lymphoid leukemia (CLL) and non-Hodgkin's lymphoma (Folkes, Ahmadi et al. 2008, Sarker, Kristeleit et al. 2009, Wagner, Von Hoff et al. 2009). We saw the greatest reduction in proliferation of AML patient samples when using the combined drug treatment (Figure 3.19). Again, this reduction corresponded to reduced levels of active STAT5, Akt, and Erk (Figure 3.21). While we were able to detect a strong effect *in vitro*, the same could not be said for our *in vivo* studies. An encouraging trend emerged, resulting in increased

median survival of combination treatment with Shp2 and PI3L inhibition. However, we did not see that either drug alone or the combination treatment of Shp2 and PI3K inhibition to mitigated MPD *in vivo* (Figure 3.29 and Figure 3.28, respectively). Recently, a study was published showing that FLT3-ITD cells, because of the strong STAT5 hyperactivation, are unaffected by inhibition of the PI3K/Akt pathway and are protected from apoptosis (Nogami, Oshikawa et al. 2015). Therefore, targeting STAT5 activation through Syk/Shp2 at the juxtamembrane domain may be a better option, and warrants further studies.

When analyzing primary AML patient samples based on their FLT3-ITD-status, we saw that FLT3-ITD+ patient samples are more sensitive to Shp2 inhibition than FLT3-ITD- patient samples (Figure 3.22). This selectivity was also seen for low doses of GDC-0941 alone but was not observed in the combination of low doses of GDC-0941 with II-B08 (Figure 3.21). Given the similar response of both FLT3-ITD+ and FLT3-ITD- AML samples to the combination of II-B08 and GDC-0941, it might be that Shp2 inhibition cooperates with PI3K inhibition at the inter-kinase domain Tyr768, which participates in both WT FLT3 and FLT3-ITD signaling. As GDC-0941 is a more potent drug than II-B08, it may be that PI3K inhibition overtakes the preferential effect of Shp2 phosphatase inhibition of the FLT3-ITD+ samples over the FLT3-ITD- samples at the higher doses of GDC-0941.

When analyzing the same patient samples for preferential effect of II-B08 with R406, FLT3-ITD+ patients trended towards greater sensitivity to the combination treatment of II-B08 with low doses of R406 compared to FLT3-ITD- patient samples (Figure 3.16). However, more patient samples are needed to determine significance. In

a recently published paper, others have found that FLT3-ITD+ samples were more sensitive to Syk inhibition compared to FLT3-ITD- samples (Puissant, Fenouille et al. 2014). It would be of interest to treat N51-FLT3-expressing mice with II-B08 and/or R406 to determine if these two drugs, whose targets both work at the duplicated juxtamembrane domain, could significantly alter progression to MPD.

Consistent with our genetic studies, mutation of duplicated Tyr599 was able to phenocopy Syk inhibition, such that both normalized STAT5 activation and significantly reduced hyperproliferation. Since Tyr768 is a substrate of Syk kinase, we hypothesized that Tyr768 should also phenocopy Syk inhibition, but this was not seen. Syk has been shown to phosphorylate Tyr955 in addition to Tyr768 (Puissant, Fenouille et al. 2014). Furthermore, the protein complex of Gab2, Grb2, p85 α , and Shp2 have been shown to be recruited to Tyr955 as well as Tyr768 (Masson, Liu et al. 2009). Taken together, this may be the reason why we do not see an effect of Tyr768 mutation, as there are other compensatory signaling pathways occurring to dampen the effect. Therefore, a double mutant of Tyr768 AND Tyr955 may better phenocopy Syk inhibition. PI3K inhibition, however, did mimic Tyr768 mutation, once again suggesting that Tyr768 mainly signals through PI3K.

Collectively, our findings for the first time demonstrate that Shp2 phosphatase and Syk inhibition or PI3K inhibition cooperate to reduce the proliferation of AML samples, and that Shp2 phosphatase inhibition as a single agent preferentially inhibits the proliferation of FLT3-ITD+ compared to FLT3-ITD- AML cells. Moreover, it may be favorable to target these pathways at multiple points for the treatment of AML.

CHAPTER FOUR

REGULATION OF SENESCENCE IN FLT3-ITD-EXPRESSING MALIGNANCY-INITIATING CELLS BY SHP2

Introduction

Shp2 has been shown to be essential in the hematopoietic stem and progenitor cell compartment for normal hematopoiesis (Chan, Li et al. 2006). Additionally, we have previously shown that Shp2 positively regulates FLT3-ITD-induced proliferation *in vitro* (Nabinger, Li et al. 2013). Therefore, we examined the hypothesis that deletion of Shp2 in FLT3-ITD-expressing cells would prolong the progression to myeloproliferative disease (MPD) *in vivo*. To study this, low density mononuclear cells (LDMNCs) were isolated from Shp2^{flox/flox}; Mx1-Cre⁺ mice and subjected to lineage depletion in order to enrich for a more primitive HSPC population (called Lin⁻). Lin⁻ cells were transduced with pMSCV-N51-FLT3 (which co-express eGFP) and sorted based on eGFP positivity. N51-FLT3 (1 x 10⁶) cells, along with supporting splenocytes (1.5 x 10⁵), were transplanted into lethally irradiated (1100 cGy) F1 (C57/BoyJ) recipient mice in an adoptive transfer model. In an adoptive transfer, donor cells are not stressed by having to compete with wild-type “competitor” cells. After cells had sufficient time to engraft and repopulate the bone marrow (approximately 4 weeks), polyI:C treatment was given to half of the mice in order to delete Shp2, while the other half received PBS as a control. Mice were followed long term for chimerism and overall survival. While deletion of Shp2 reduced N51-FLT3-induced malignancy and prolonged time to malignancy-induced mortality, there was a subset of polyI:C treated mice that rapidly died approximately two

weeks after polyI:C treatment due to bone marrow failure (Figure 4.1A). Histology sections showed increased adipose cells and decreased myeloid cells in the marrow of polyI:C treated mice (Figure 4.1B). Additionally, in the spleen, polyI:C treated mice display extramedullary hematopoiesis, another indication of bone marrow failure (Figure 4.1B). These findings suggest that FLT3-ITD-expressing cells are particularly dependent on Shp2 for normal function.

As Shp2 is known to play a critical role in normal hematopoiesis (Chan, Li et al. 2006), one thought is that any transplanted mouse, regardless of FLT3-ITD status, would exhibit bone marrow failure upon the loss of Shp2. To determine if the bone marrow failure phenotype was specific to FLT3-ITD status, a similar experiment was done including WT FLT3-expressing donor cells. Interestingly, despite have similar chimerism levels before treatment (baseline, Figure 4.2A), loss of Shp2 in mice transplanted with FLT3-ITD-expressing cells reduced chimerism to a greater extent compared to mice transplanted with WT FLT3-expressing cells (Figure 4.2B, compare purple and green lines). This finding suggests that FLT3-ITD-expressing cells are more sensitive to the loss of Shp2 compared to WT FLT3-expressing cells, and that FLT3-ITD cells have an increased dependence on Shp2. This corresponds to what is seen in primary AML patient samples, that FLT3-ITD+ patient peripheral blood samples have a more profound response to Shp2 inhibition using II-B08 compared to those that are FLT3-ITD- (Figure 3.22).

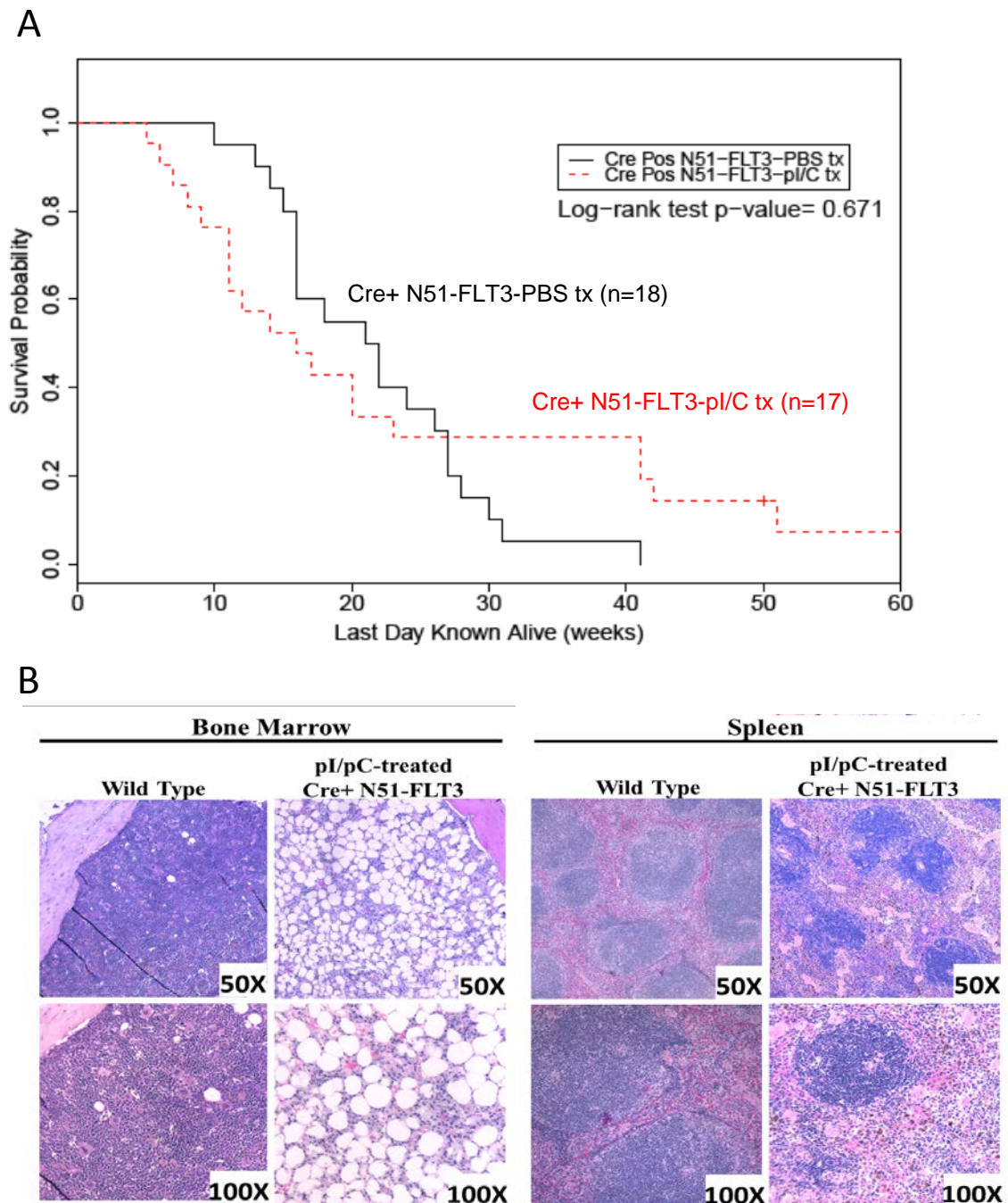


Figure 4.1. Deletion of Shp2 in FLT3-ITD-expressing mice leads to bone marrow failure.

(A) Kaplan-Meier analysis of overall survival for mice transplanted with N51-FLT3-ITD transduced Lin⁻ cells treated with polyI:C to delete Shp2 (n=17) compared to PBS-treated control animals (n=18). $p=0.671$ using a log-rank test; (B) Histology sections of the

bone marrow and spleen of mice transplanted with N51-FLT3-transduced Lin⁻ cells and treated with polyI:C compared to a WT control mouse.

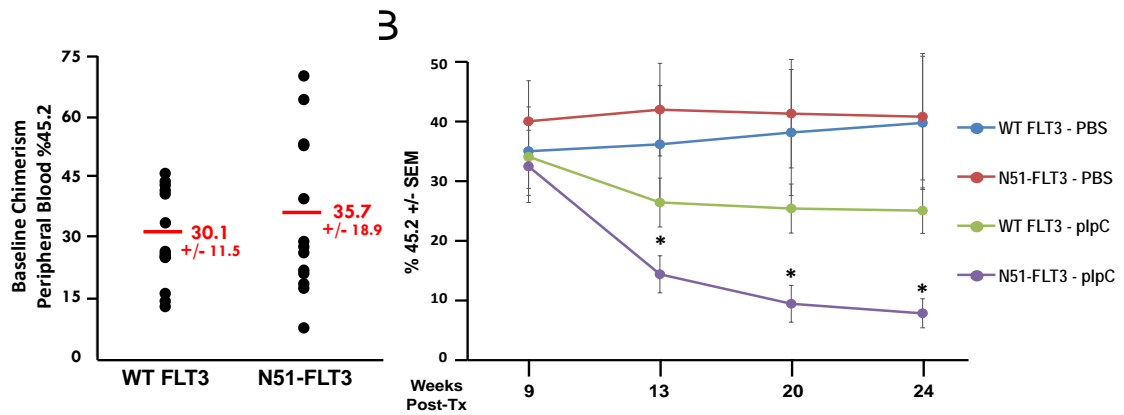


Figure 4.2. Mice transplanted with FLT3-ITD-transduced cells uniquely display lower chimerism upon Shp2 deletion.

(A) Peripheral blood chimerism of mice that were transplanted with either WT FLT3 or N51-FLT3 Lin⁻ cells before treatment (baseline); **(B)** Animals were treated with either PBS or polyI:C. Chimerism expressed as percentage of donor cells. n=6-7 transplanted mice per group, *p<0.03 comparing N51-FLT3-polyI:C treated mice to WT FLT3-polyI:C treated mice using unpaired, two-tailed student's *t* test.

As we are interested in Shp2 as a possible therapeutic target for FLT3-ITD+ AML, we next determined a mechanism by which Shp2 deletion could lead to bone marrow failure in FLT3-ITD-expressing cells. One potential candidate that could play a role in bone marrow integrity was B-cell-specific Maloney murine leukemia virus integration site 1 (Bmi1) protein. Bmi1 is a polycomb group protein in the PRC1 complex that represses transcription through chromatin modification (Sparmann and van Lohuizen 2006). Bmi1 is a known regulator of p16^{Ink4a}/p19^{Arf} (Jacobs, Kieboom et al. 1999) and knockdown of Bmi1 by an RNAi approach leads to increased p16^{Ink4a}/p19^{Arf} (Rizo, Olthof et al. 2009).

Bmi1 has been shown to be indispensable for both normal and leukemic stem cell function. Bmi1 was shown to be required for the maintenance of adult HSCs, as deletion of Bmi1 lead to reduced HSC frequency and ability to reconstitute all lineages (Park, Qian et al. 2003). Bmi1 knockout mice showed proliferative arrest, impaired differentiation, and transplant failure, suggesting an essential role in leukemic stem and progenitor cells (Lessard and Sauvageau 2003). In the context of neural stem cells, conditional deletion of Shp2 reduced the self-renewal capacity as evidenced by early postnatal lethality. Additionally, deletion of Shp2 resulted in decreased levels of c-Myc and Bmi1. Ectopic expression of Bmi1 in Shp2 deficient cells rescued the phenotype and increased the proliferation of the neural progenitor cells (Ke, Zhang et al. 2007). Finally, Bmi1 was linked to AML in the finding that showed Bmi1 expression could be used as a potential prognostic marker for AML. Patients with lower Bmi1 positivity had longer survival compared to those patients with higher Bmi1 positivity. Moreover, 27% of patients with high Bmi1 levels were FLT3-ITD+, whereas only 6% of patients with

low Bmi1 levels were FLT3-ITD+ (Chowdhury, Mihara et al. 2007), suggesting that Bmi1 level and FLT3 status are correlated. Therefore, we hypothesized that upon the loss of Shp2, FLT3-ITD-expressing HSPCs are sensitized to either apoptosis and/or senescence, possibly through downregulation of Bmi1 and compensatory upregulation of p16/p19. Whereas apoptosis is defined by cell death, senescence is defined by the growth arrest of cells in response to aging or a stressor. Senescence is regulated by pathways including p16/pRB and p53/p21 (Campisi 2013). Either apoptosis or senescence could result in bone marrow failure in mice.

Results

Determination of the role of Shp2 on apoptosis and senescence

To determine if apoptosis or senescence was the primary cause of the bone marrow failure phenotype displayed upon the loss of Shp2, we first did *in vitro* assays using transduced LDMNCs. Shp2^{flox/flox}; Mx1-Cre⁺ mice were treated with polyI:C to delete Shp2. Five weeks after treatment and upon confirmation of Shp2 deletion, LDMNCs were isolated and transduced with either pMSCV-WT FLT3 or pMSCV-N51-FLT3 and sorted for eGFP positive cells. Cells were cultured in various conditions and stained with Annexin V (indicator of early apoptosis) and propidium iodide (PI, indicator of late apoptosis or necrosis). We observed that levels of apoptosis in FLT3-ITD cells were lower compared to WT FLT3 cells (Figure 4.3), suggesting that enhanced apoptosis in the N51-FLT3-transduced cells does not account for the observed bone marrow failure. To confirm this finding, and to determine if HSPCs expressing N51-FLT3 display an

increased apoptosis *in vivo*, bone marrow from WT FLT3- and N51-FLT3-ITD-transplanted mice was isolated two weeks after Shp2 deletion with polyI:C, the time point that we commonly observe the bone marrow failure phenotype in the N51-FLT3-transplanted mice. Isolated bone marrow LDMNCs were stained for lineage markers as well as Annexin V to specifically examine apoptosis in a population enriched for HSPCs (Figure 4.4A). Again, we did not observe a significant difference in apoptosis levels in Lin- cells. Finally, we stained the bone marrow of the transplant mice for Caspase 3, a marker of apoptosis, and analyzed them with the assistance of Dr. George Sandusky, Department of Pathology at IUSM. There was no qualitative difference in Caspase 3 staining when comparing the WT FLT3 or N51-FLT3-ITD bone marrow sections (Figure 4.4B). Taken together, we concluded that apoptosis was not the primary mechanism through which a bone marrow failure phenotype was achieved in the N51-FLT3-transplanted mice.

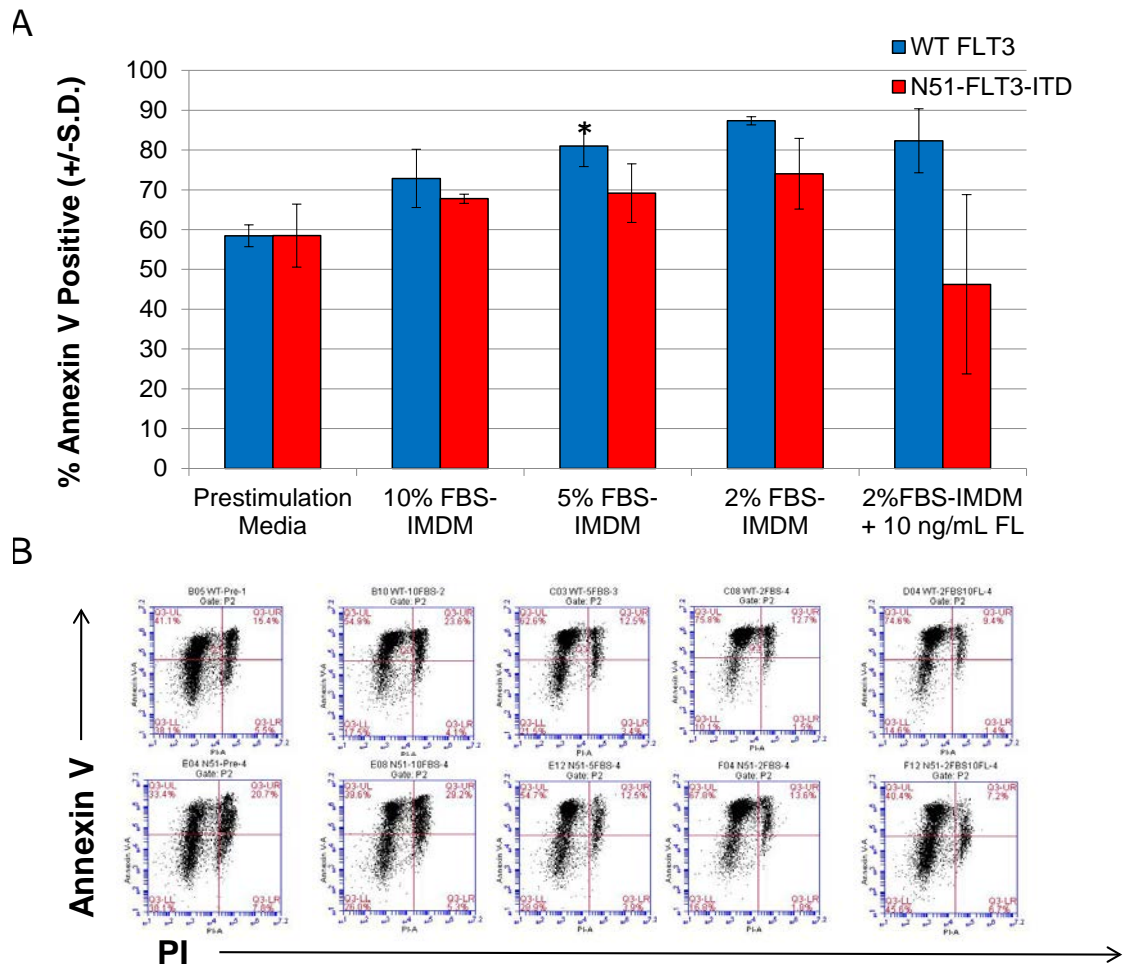


Figure 4.3. Deletion of Shp2 in FLT3-ITD-expressing cells does not result in increased apoptosis.

(A) LDMNCs isolated from polyI:C treated $Shp2^{flx/flx}$; $Mx1Cre^{+}$ mice were transduced with WT FLT3 or N51-FLT3 followed by culture for 48 hours in different media conditions and assayed for apoptosis using Annexin V and PI staining. $n=4$, $*p<0.05$ comparing N51-FLT3 to WT FLT3 using unpaired, two-tailed student's t test. (B) Representative flow charts are shown for each media condition,

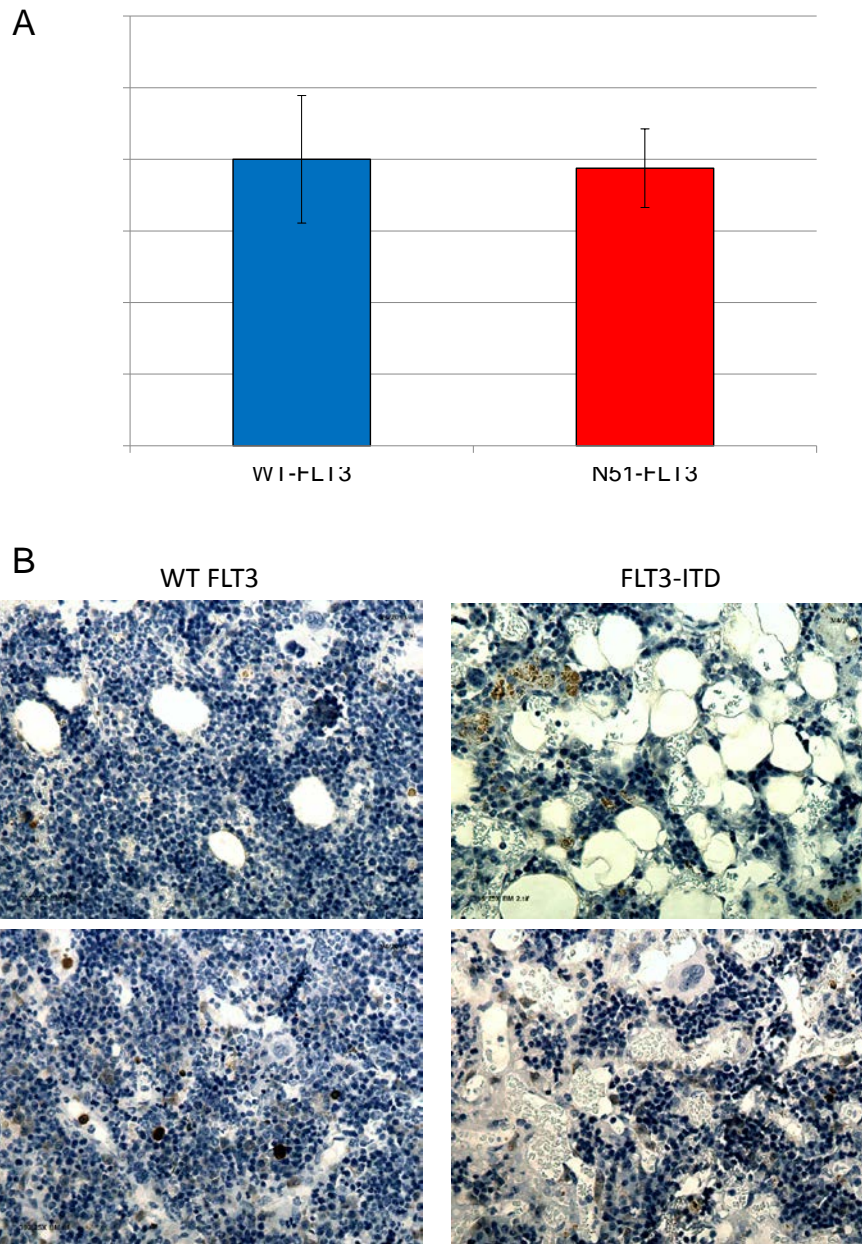


Figure 4.4. Mice transplanted with WT FLT3 or FLT3-ITD do not display increased apoptosis upon the loss of Shp2.

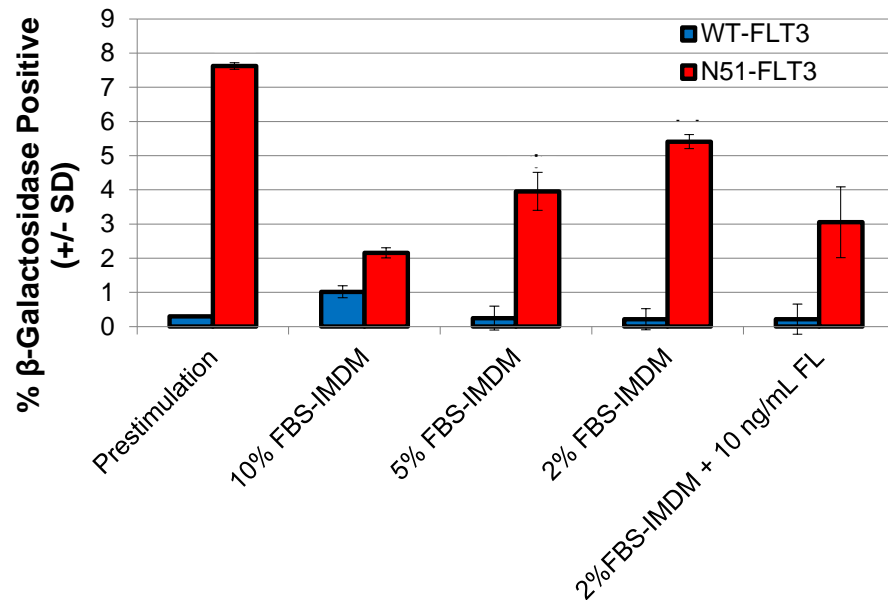
(A) Lineage negative cells taken from WT FLT3- and FLT3-ITD-transplanted mice two weeks post-polyI:C were analyzed for apoptosis via Annexin V staining, and measured by flow cytometry, n=5 for WT FLT3 and n=2 for N51-FLT3; (B) WT FLT3 and FLT3-ITD mice were euthanized two weeks post-polyI:C treatment and sections of bone marrow were sent for Hematoxylin and eosin (H&E) staining, along with staining for apoptotic marker Caspase 3. Two representative mice from each group shown.

Because of the link between Shp2 and Bmi1 in neural stem cells (Ke, Zhang et al. 2007), and because of the established importance of Bmi1 on senescence (Jacobs, Kieboom et al. 1999), we next examined if senescence is increased in FLT3-ITD-expressing cells upon the loss of Shp2. We first examined senescence using the senescence-associated (SA) β -galactosidase staining assay *in vitro*. When cells undergo senescence, they have elevated levels of lysosomal β -galactosidase, which can cleave X-gal to emit a blue color that can be detected under a microscope. Therefore, by quantifying the number of blue cells, one can determine the percentage of cells undergoing senescence. Similar to the apoptosis assay, a pilot study was done in which LDMNCs from Shp2^{flox/flox}; Mx1-Cre⁺ polyI:C treated mice were isolated and transduced with either pMSCV-WT FLT3 or pMSCV-N51-FLT3 and sorted for eGFP positive cells by FACS. Cells (1×10^4) were plated on poly-L-lysine coated 4-well chamber slides in various media conditions to induce stress in the cells. Approximately 24 hours post-plating, cells were fixed and stained for β -galactosidase activity by incubating overnight in the presence of X-gal (pH 6.0). In all conditions, there was a significantly higher level of senescence in cells expressing FLT3-ITD compared to WT FLT3 (Figure 4.5). This suggests that loss of Shp2 uniquely triggers senescence in FLT3-ITD-expressing cells, and may account for the observed bone marrow failure of mice transplanted with N51-FLT3-expressing cells lacking Shp2.

Again, to determine if senescence is occurring in the more primitive HSPC compartment, lineage depletion was done on Shp2^{flox/flox}; Mx1-Cre⁺ (referred to as Lin-Cre⁺) and on Shp2^{flox/flox}; Mx1-Cre⁻ (Lin-Cre⁻) cells post-polyI:C treatment. Cells were transduced with WT or N51-FLT3 and senescence was measured by SA- β -galactosidase

staining. Consistent with what is observed in LDMNCs, Lin⁻ cells transduced with N51-FLT3 in which Shp2 was deleted by Mx1-Cre also had elevated levels of β -galactosidase (Figure 4.6). These findings suggest that Shp2 functions in the primitive HSPC compartment to protect N51-FLT3-expressing cells from senescence.

A



B

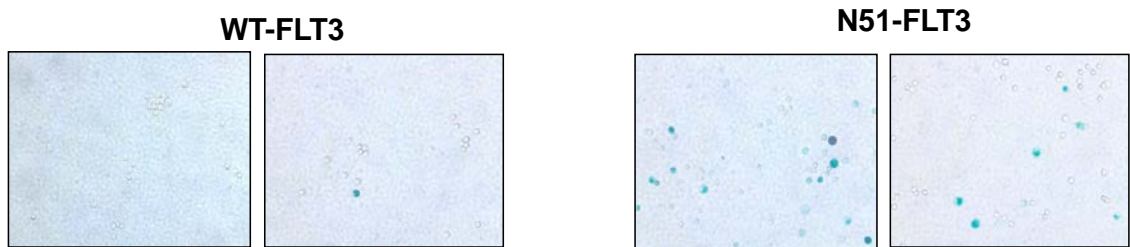


Figure 4.5. FLT3-ITD-transduced cells display increased senescence compared to WT FLT3-transduced cells.

(A) LDMNCs isolated from polyI:C treated $Shp2^{flox/flox}$; $Mx1Cre+$ mice were transduced with WT FLT3 or N51-FLT3 followed by culture for 48 hours in different media conditions and assayed for senescence using SA- β -galactosidase staining. $n=3$. (B) Representative pictures of senescent cells in WT FLT3 and N51-FLT3 cells.

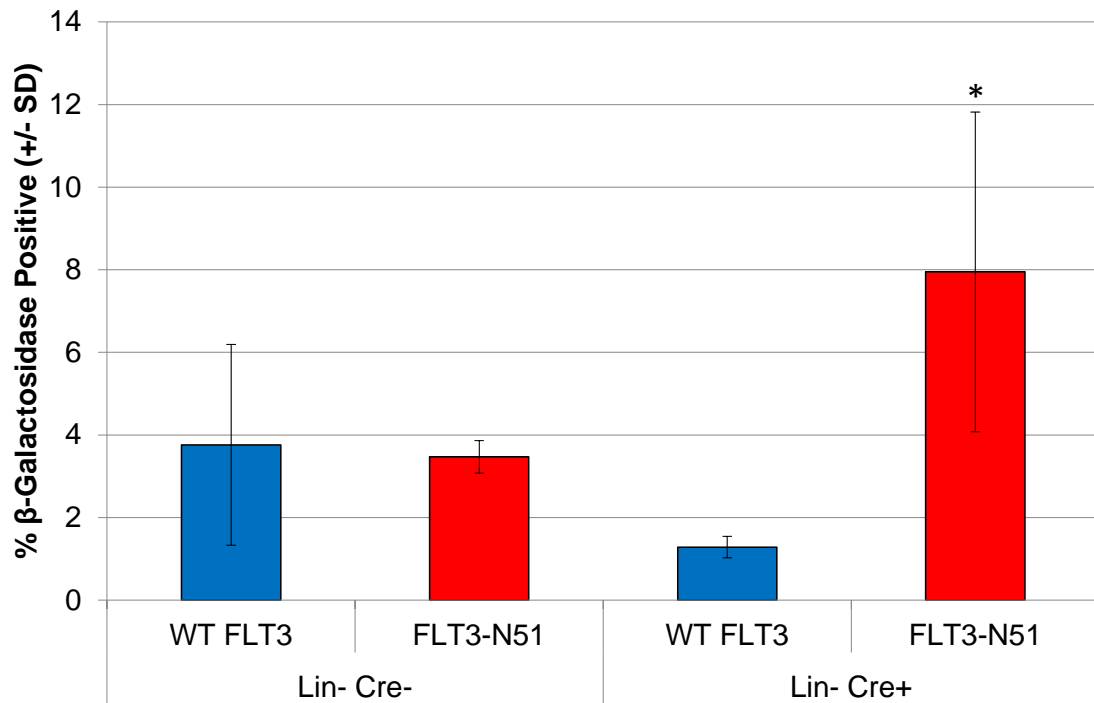


Figure 4.6. Lineage depleted FLT3-ITD-expressing cells display increased senescence upon the loss of Shp2.

Lin- bone marrow cells from polyI:C treated $Shp2^{flx/flx}$; Mx1-Cre- and $Shp2^{flx/flx}$; Mx1-Cre+ mice were isolated, transduced with either WT FLT3 or N51-FLT3, and cultured in 2% FBS-IMDM. Senescence was measured using SA- β -galactosidase staining, n=3, *p<0.02 comparing N51-FLT3 to WT FLT3 in Lin- Cre+ cells using unpaired, two-tailed student's *t* test. Representative of four independent experiments.

Because of the strong senescent phenotype, we next wanted to determine a molecular mechanism by which loss of Shp2 results in increased senescence in the context of FLT3-ITD; therefore, we examined Bmi1 expression in Lin- bone marrow cells isolated from mice transplanted with WT FLT3 and N51-FLT3-transduced cells two or four weeks after deletion of Shp2. Total cellular RNA was isolated, and Bmi1 expression levels were examined using quantitative Real Time PCR (RT-PCR). At two weeks post-polyI:C treatment to delete Shp2, there was lower Bmi1 expression in the FLT3-ITD-expressing cells compared to WT FLT3. However, by four weeks post-treatment, both WT FLT3 and N51-FLT3 cells had similarly low levels of Bmi1 levels (Figure 4.7). This indicates that the N51-FLT3 cells are more sensitive to the loss of Shp2, accounting for the faster response and rapid decrease in Bmi1, whereas WT FLT3 cells are not as dependent on Shp2 function, indicated by the slower response.

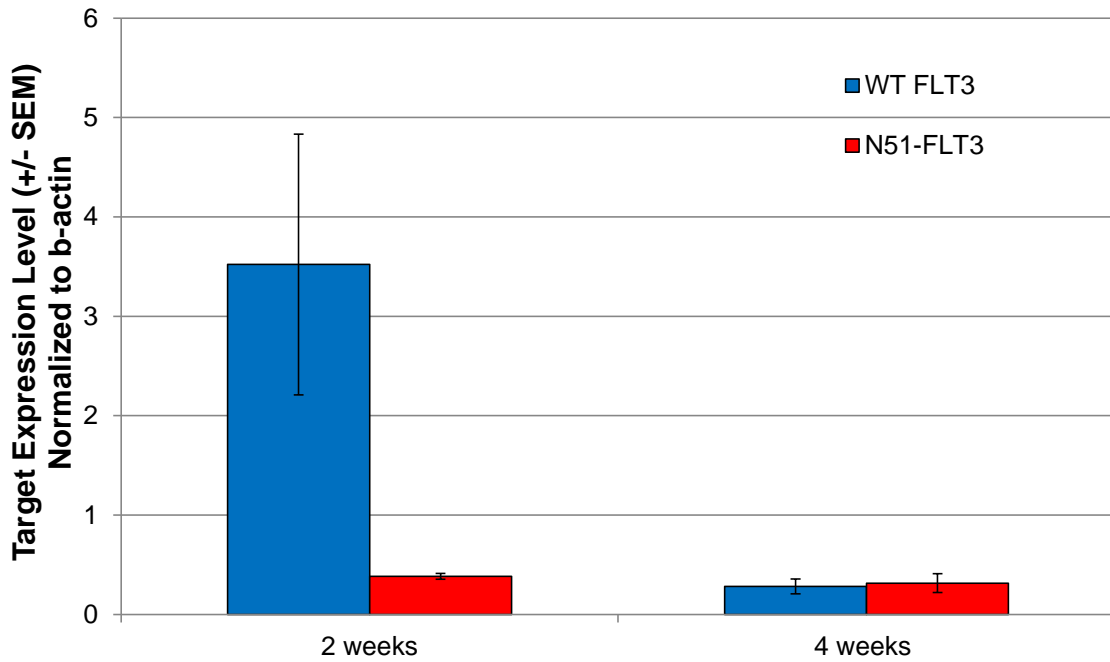


Figure 4.7. FLT3-ITD-expressing cells rapidly reduce Bmi1 expression levels upon the loss of Shp2 compared to WT FLT3-expressing cells.

Total cellular RNA was isolated from Lin- bone marrow of mice transplanted with either WT FLT3 or N51-FLT3 2 or 4 weeks post-polyI:C treatment to delete Shp2. Fold change in Bmi1 mRNA levels was determined using quantitative RT-PCR and normalized to a b-actin control.

Examination of Shp2 heterozygosity on senescence in FLT3-ITD-expressing cells

To study the regulation of senescence in FLT3-ITD cells in a more physiologic model, we used a knock-in model of FLT3-ITD created by Gary Gilliland (Lee, Tothova et al. 2007). In this model, N51-FLT3-ITD expression is regulated by the endogenous FLT3 promoter, and no drug treatment required to induce expression. We crossed the FLT3-ITD^{+/-} mouse model with our Shp2^{flox/flox}; Mx1-Cre mouse model to create mice in which Shp2 can be deleted in the presence of FLT3-ITD (Figure 4.8). This creates a better clinical representation, as manipulation of cells through transduction is no longer needed.

For the following studies, we used a combination of the following mouse genotypes: **WT** (WT FLT3; Shp2^{flox/+}; Mx1-Cre⁻), **Shp2 +/-** (WT FLT3; Shp2^{flox/+}; Mx1-Cre⁺), **ITD** (FLT3-ITD; Shp2^{flox/+}; Mx1-Cre⁻), and **ITD; Shp2 +/-** (FLT3-ITD; Shp2^{flox/+}; Mx1-Cre⁺) (Figure 4.8). Upon polyI:C treatment, one allele of Shp2 was deleted in mice expressing Cre, resulting in Shp2 heterozygosity in the presence or absence of FLT3-ITD. We then used bone marrow LDMNCs from these mice to analyze proliferation, senescence, and stem cell function (Figure 4.8B). Genotypes were confirmed before and after polyI:C treatment by PCR (Figure 4.9).

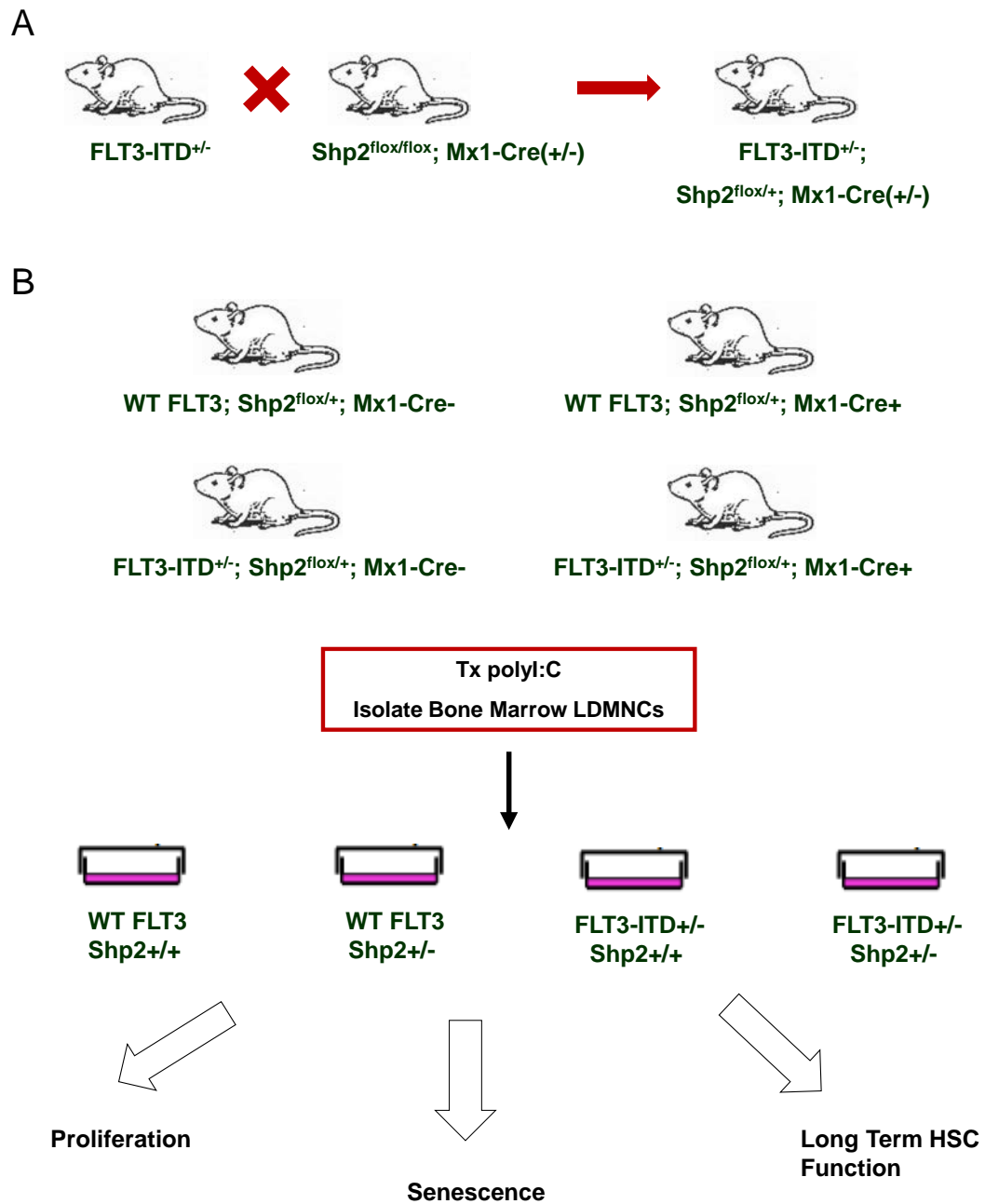


Figure 4.8. Schematic of the FLT3-ITD mouse model used to study the function of Shp2 on senescence and HSC function.

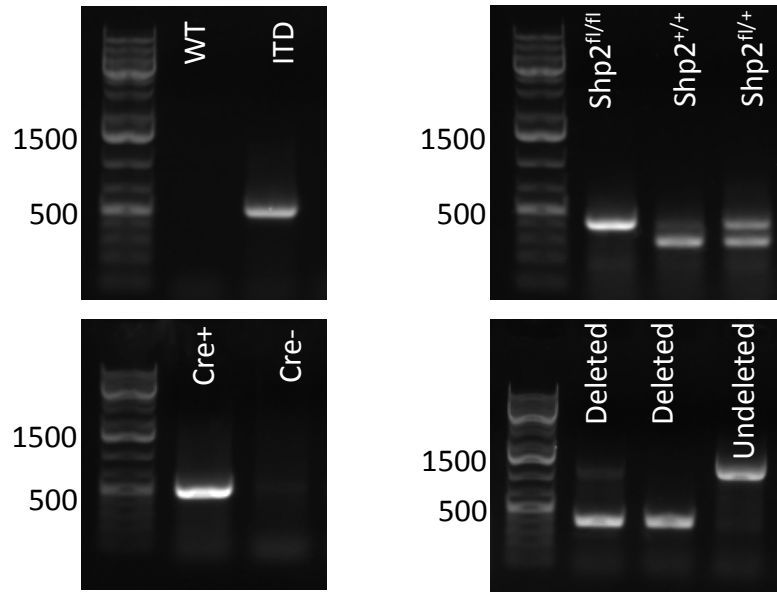


Figure 4.9. Examples of PCR reactions used to determine the genotypes of experimental mice.

ITD status, identification of floxed *Ptpn11* alleles, and Cre status were analyzed for each mouse prior to polyI:C treatment and before experimentation. Additionally, after polyI:C treatment, evidence of recombined *Ptpn11* allele was determined by PCR. Expected band sizes are as follows: ITD 500 bp, Shp2^{fl^{ox}} 400 bp, Shp2⁺ 300 bp, Cre 450 bp, Shp2 deleted 400 bp, Shp2 undeleted 1100 bp.

In our studies described above, we clearly demonstrate that Shp2 functions in the regulation of senescence FLT3-ITD-expressing HSCs, and suggest that FLT3-ITD-expressing HSCs are sensitive to loss of Shp2. However, transduced cells may not accurately recapitulate typical stem cell function. Furthermore, based on the observed embryonic lethality of Shp2 homozygous knockout mice (Saxton, Henkemeyer et al. 1997), complete inhibition of Shp2 would likely be too toxic for therapeutic application. However, murine models heterozygous for Shp2 demonstrate normal peripheral hematopoietic cell counts, yet clearly demonstrate reduced hematopoietic stem cell function due to reduced self-renewal (Chan, Li et al. 2006). We first asked the question if we could see a similar senescent phenotype with deletion of only one Shp2 allele, rather than homozygous depletion. This would make a stronger case for targeting Shp2 pharmacologically in patients with FLT3-ITD+ AML, as partial deletion may be strong enough to elicit a reduction of the oncogenic phenotype. FLT3-ITD^{+/-}; Shp2^{flox/+}; Mx1-Cre mice were treated with polyI:C to create Shp2 heterozygous mice. As we have shown previously that homozygous depletion of Shp2 reduces the hyperproliferation of FLT3-ITD-transduced cells (Nabinger, Li et al. 2013), we first examined proliferation of the FLT3-ITD; Shp2^{flox/+}; Mx1-Cre⁺ and FLT3-ITD; Shp2^{flox/+}; Mx1-Cre⁻ controls by conducting ³H-thymidine incorporation assays. Five weeks post-polyI:C treatment, mice were euthanized and bone marrow LDMNCs were isolated and cultured in prestimulation media (IMDM supplemented with FBS, Pen/Strep, TPO, SCF, and G-CSF) for approximately 24 hours. Cells were then starved, plated to equal numbers (3 x 10⁴ cells/well) and subjected to ³H-incorporation the following day in the presence and absence of FLT3 ligand (FL, 50 ng/mL). Deletion of one allele of Shp2 was indeed

sufficient to significantly reduce the proliferation at both baseline and upon stimulation with FL (Figure 4.10).

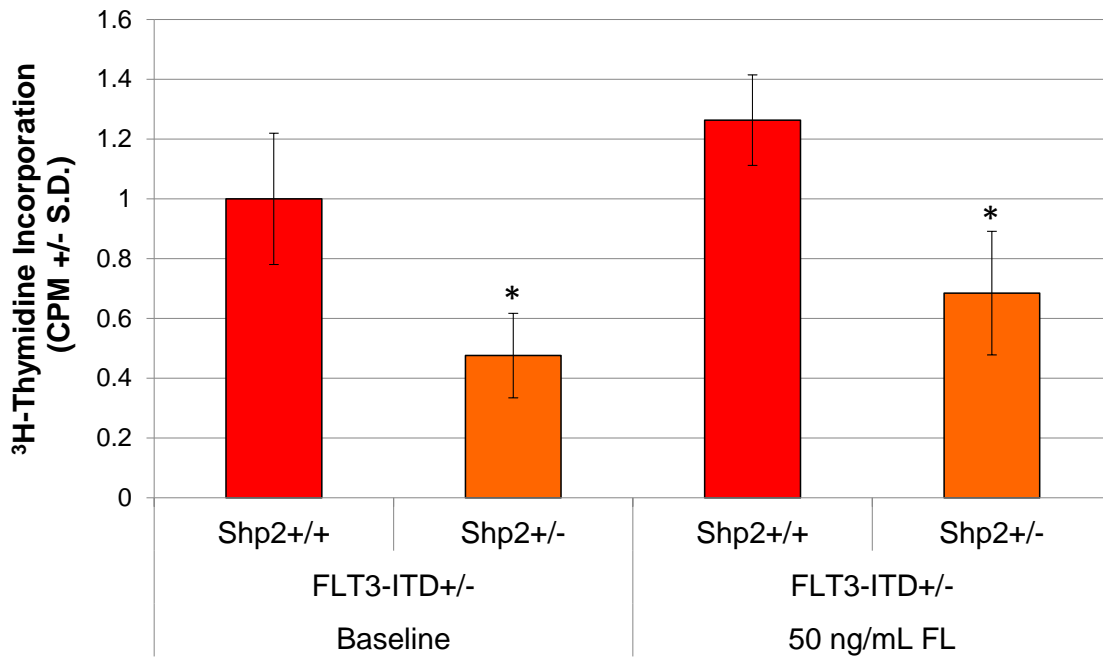


Figure 4.10. Shp2 heterozygosity in FLT3-ITD-expressing LDMNCs leads to a reduction in proliferation.

³H-thymidine incorporation assay was used to measure proliferation of FLT3-ITD; Shp2^{+/+} and FLT3-ITD; Shp2^{+/-} cells. Compiled from 3 independent experiments, *p<0.05 using unpaired, two-tailed student's *t* test.

Since an increase in senescence in N51-FLT3-transduced cells was observed, we next determined to what extent heterozygous deletion of Shp2 would also lead to an increase in senescence. We first looked at senescence phenotypically by using SA- β -galactosidase staining. Five weeks after polyI:C treatment, Shp2 heterozygosity was confirmed and mice were euthanized. LDMNCs from the bone marrow were isolated and cultured for 3 days in prestimulation media, followed by 24, 48, or 96 hours in 2% FBS-IMDM. Cells (2 or 4×10^4) were plated in 4-well chamber slides and stained with SA- β -galactosidase staining solution. At each time point, there was an elevation of senescence in FLT3-ITD^{+/-}; Shp2^{+/-} LDMNCs compared to FLT3-ITD^{+/-}; Shp2^{+/+} controls (Figure 4.11), suggesting that Shp2 heterozygosity is sufficient to cause an increase in senescence in FLT3-ITD-expressing cells.

Additionally, we compared the loss of Shp2 in the context of WT FLT3 in addition to FLT3-ITD in a more primitive stem cell compartment, by enriching for lineage negative cells. Mice were treated with polyI:C to create mice that were WT (Shp2^{fllox/+}; Mx1-Cre⁻; ITD^{+/-}), Shp2^{+/-} (Shp2^{fllox/+}; Mx1-Cre⁺; ITD^{+/-}), ITD (Shp2^{fllox/+}; Mx1-Cre⁻; ITD^{+/-}) and ITD; Shp2^{+/-} (Shp2^{fllox/+}; Mx1-Cre⁺; ITD^{+/-}). Lineage depletion was done on isolated LDMNCS and subjected to SA- β -galactosidase staining assay 24 hours after incubation in 2% FBS-IMDM. In a WT FLT3 background, deletion of Shp2 did not significantly increase senescence (Figure 4.12). However, in the context of oncogenic FLT3-ITD, there was a drastic increase in senescence upon the deletion of Shp2. Consistent with our findings in transduced cells, these data suggest that FLT3-ITD-expressing HSPCs are sensitive to the loss of Shp2, and that Shp2 is regulating senescence in cells enriched for HSPCs.

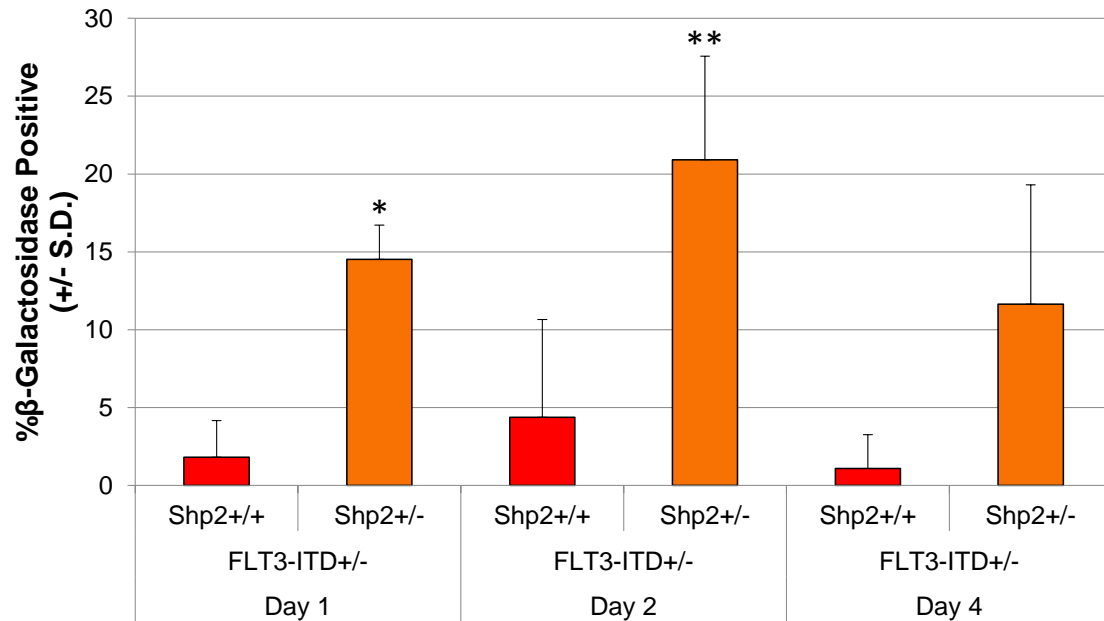


Figure 4.11. Shp2 heterozygosity leads to elevated senescence in FLT3-ITD-expressing cells.

LDMNCs were isolated from FLT3-ITD; Shp2^{+/+} and FLT3-ITD; Shp2^{+/-} mice and cultured for 72 hours in prestimulation media, followed by 2% FBS overnight. Senescence was measured using β -galactosidase, n=4, *p<0.0005 for Shp2^{+/+} vs. Shp2^{+/-} at Day 1; **p<0.05 for Shp2^{+/+} vs. Shp2^{+/-} at Day 2 using unpaired, two-tailed student's *t* test.

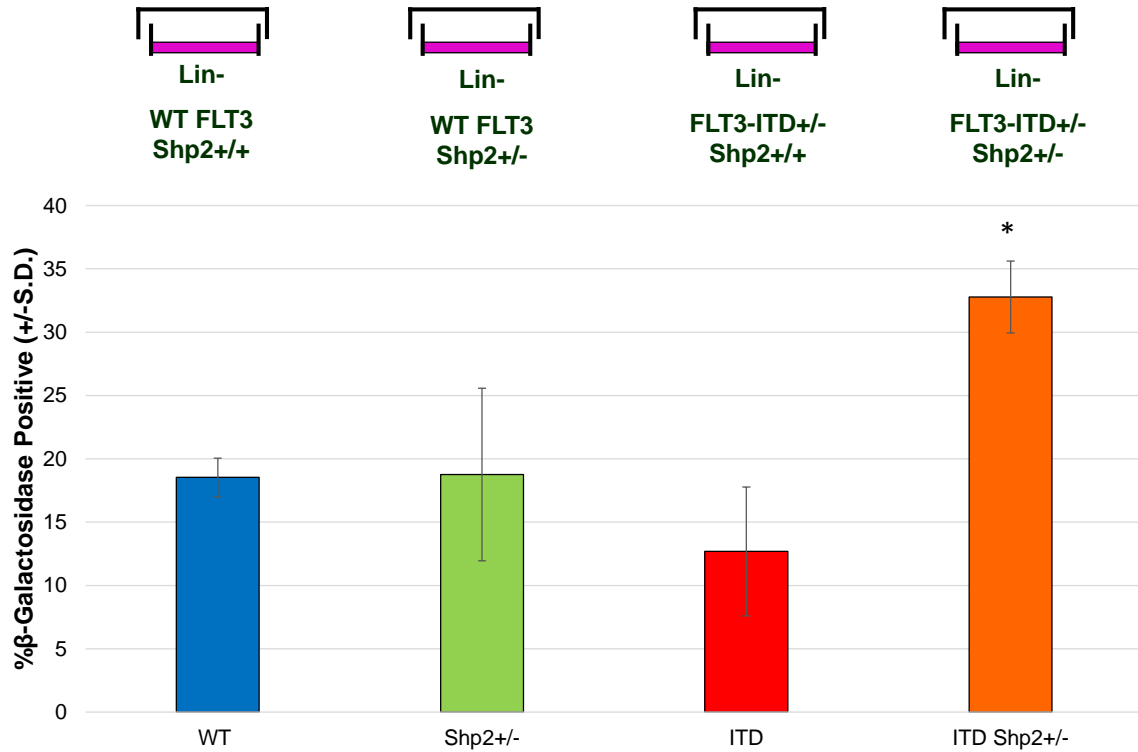


Figure 4.12. Shp2 heterozygosity in Lin- bone marrow cells result in increased senescence in FLT3-ITD-expressing cells only.

Lineage cells were depleted from LDMNCs derived from WT, Shp2^{+/-}, ITD, and ITD; Shp2^{+/-} to provide a population of cells enriched for HSPCs. Lin- cells were cultured in prestimulation media for 72 hours, followed by 2% FBS-IMDM overnight. n=4, *p<0.0005 for ITD; Shp2^{+/-} vs. WT, Shp2^{+/-}, and ITD using unpaired, two-tailed student's *t* test.

Because of the elevated senescence in FLT3-ITD cells upon loss of one allele of Shp2, we began to examine a signaling transduction pathway through which Shp2 can regulate senescence. As we saw Bmi1 expression change as a result of loss of Shp2 in murine LDMNCs, we wanted to examine Bmi1 signaling in depth, looking at effectors both upstream and downstream of Bmi1. Since Bmi1 is a known inhibitor of p16 activity (Jacobs, Kieboom et al. 1999), we first wanted to test if there was an upregulation of p16 upon the loss of Shp2, as a result from decreased Bmi1 expression. Total cellular RNA was isolated from mice treated with polyI:C to delete one allele of Shp2 in the presence of FLT3-ITD, and coding DNA (cDNA) was used to measure mRNA expression levels by RT-PCR. With lower Shp2 expression levels, we saw concordant decrease in Bmi1 and increase in p16 levels (Figure 4.13). However, these differences were not statistically significant.

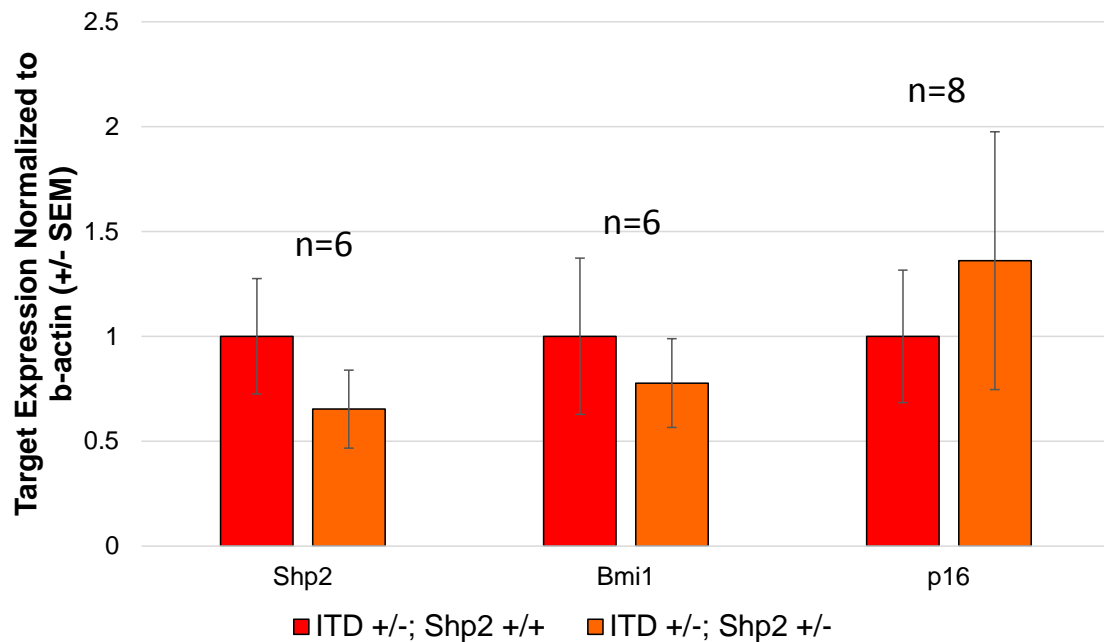


Figure 4.13. Shp2 heterozygosity corresponds to slightly reduced Bmi1 levels and elevated p16 mRNA levels.

Total cellular RNA was isolated from LDMNCs of FLT3-ITD; Shp2^{+/+} and FLT3-ITD; Shp2^{+/-} mice after polyI:C treatment. Fold change in target mRNA levels was determined using quantitative RT-PCR and normalized to a β -actin control.

As the reduction in Bmi1 was only modest, and seemingly not enough to cause the drastic senescent phenotype observed in the staining assays, we examined other possible regulators of senescence. This led us to examine the transcription factor, Homeobox A9 (Hoxa9). Hoxa9 is a member of the HOX gene set of conserved homeodomain transcription factors. HoxA7-11 transcription factors are important in myeloid progenitors, and expression level decreases as cells transition from CD34+ to CD34- as they become more mature (Sauvageau, Lansdorp et al. 1994). However, Hox gene expression levels have been shown to be maintained in leukemia, suggesting their importance for disease progression (Kawagoe, Humphries et al. 1999). Additionally, it has been shown that Hoxa9, along with Hoxa7, is elevated in cells expressing FLT3-ITD compared to WT FLT3 cells (Greenblatt, Li et al. 2012). In a study looking at MLL fusion proteins, Smith et al. found that both Bmi1 and Hoxa9 can act independently to regulate p16 and, therefore, senescence (Smith, Yeung et al. 2011).

Interestingly, Shp2 has been linked to Hoxa9 in MLL1-oncogenic leukemogenesis, such that inhibiting Shp2 (using the pharmacologic inhibitor SSG) in AML patient samples lowered expression of Hoxa9 mRNA levels (Bei, Shah et al. 2014). Additionally, these investigators found that AML patient samples displaying high Shp2 phosphatase activity also had high Hox levels. Taken together, we hypothesized that loss of Shp2 may result in reduced Hoxa7 and Hoxa9 expression in FLT3-ITD-expressing cells. In RT-PCR analysis, we did not observe a reduction in Hoxa7 expression, but Hoxa9 was substantially reduced (Figure 4.14). This suggests that, similar to what is seen in MLL-fusion-induced leukemogenesis, in FLT3-ITD-expressing

cells, both Bmi1 and Hoxa9 regulate p16 activity, and that Shp2 may be upstream of Bmi1 and Hoxa9.

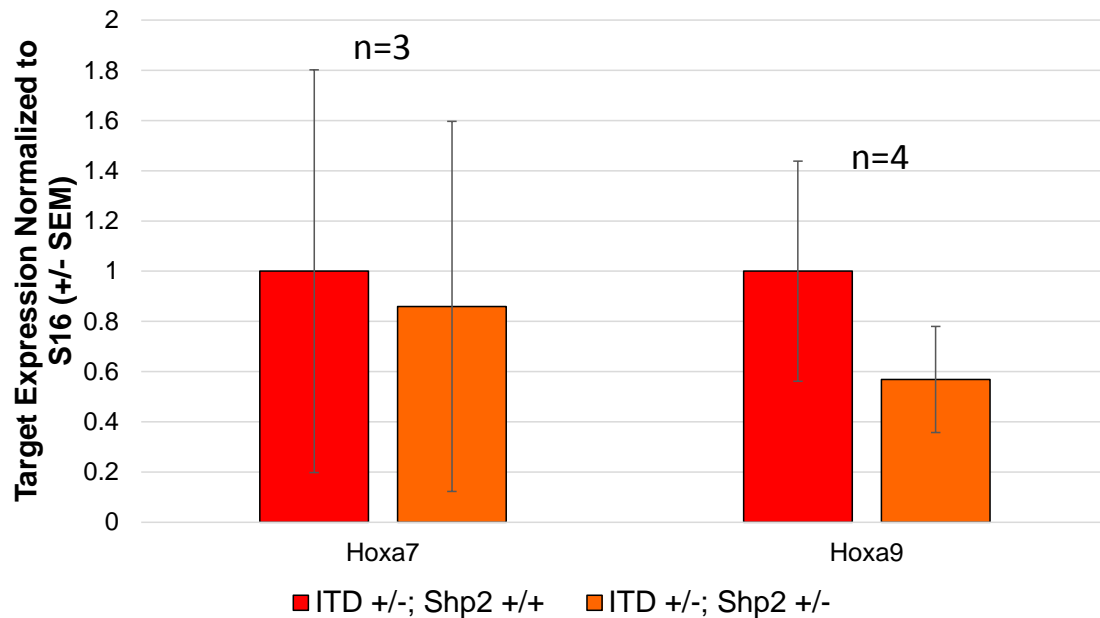


Figure 4.14. Shp2 heterozygosity does not affect Hoxa7 but lowers Hoxa9 mRNA levels.

Total cellular RNA was isolated from LDMNCs of FLT3-ITD; Shp2^{+/+} and FLT3-ITD; Shp2^{+/-} mice after polyI:C treatment. Fold change in target mRNA levels was determined using quantitative RT-PCR and normalized to a S16 control.

As we believe Shp2 is regulating senescence through Bmi1 and/or Hoxa9, we next examined potential intermediates through which Shp2 phosphatase may be leading to the activation of Bmi1 and/or Hoxa9. For the following studies, we focused on Bmi1. One intermediate we investigated was c-Myc, a known regulator of Bmi1 (Guney, Wu et al. 2006). As mentioned earlier, in the study of neural stem cells, Ke et al. found that deletion of Shp2 led to reduction in both active c-Myc and Bmi1 (Ke, Zhang et al. 2007). On the *BMI1* promoter, there is a Myc consensus sequence (CACGTG) approximately 180 bp upstream of the transcription start site (TSS) (Figure 4.15). Therefore, we hypothesized that there would be increased Myc bound to the *BMI1* promoter in FLT3-ITD+ cells. Using the FLT3-ITD- HL60 and the FLT3-ITD+ MV411 cell lines, we performed chromatin immunoprecipitation (ChIP) analysis. After crosslinking the bound protein to DNA, samples were incubated with anti-Myc or anti-IgG control, immunoprecipitation was conducted, and fragments around the Myc consensus sequence were amplified. We observed elevated levels of Myc bound to the promoter of *BMI1* in the presence of FLT3-ITD (Figure 4.16). However, when looking at total Myc mRNA levels in our mouse model system, Shp2 deletion did not have an effect on the level of Myc expression (data not shown), suggesting that Myc alone may not be the key regulatory intermediate between Shp2 and Bmi1 in the context of FLT3-ITD.

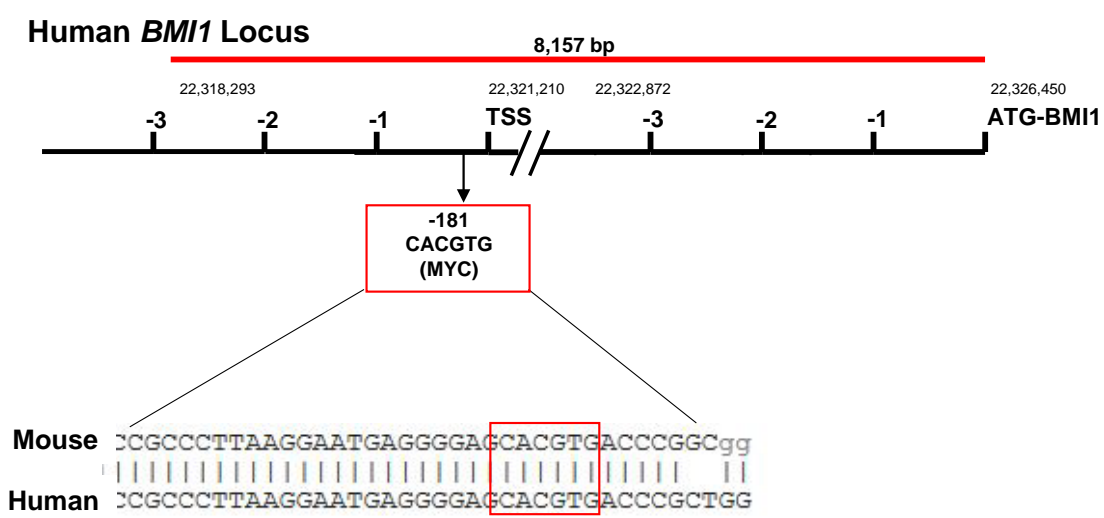


Figure 4.15. The murine and human *BMI1* locus have a conserved MYC consensus sequence 181 bp upstream of the transcription start site.

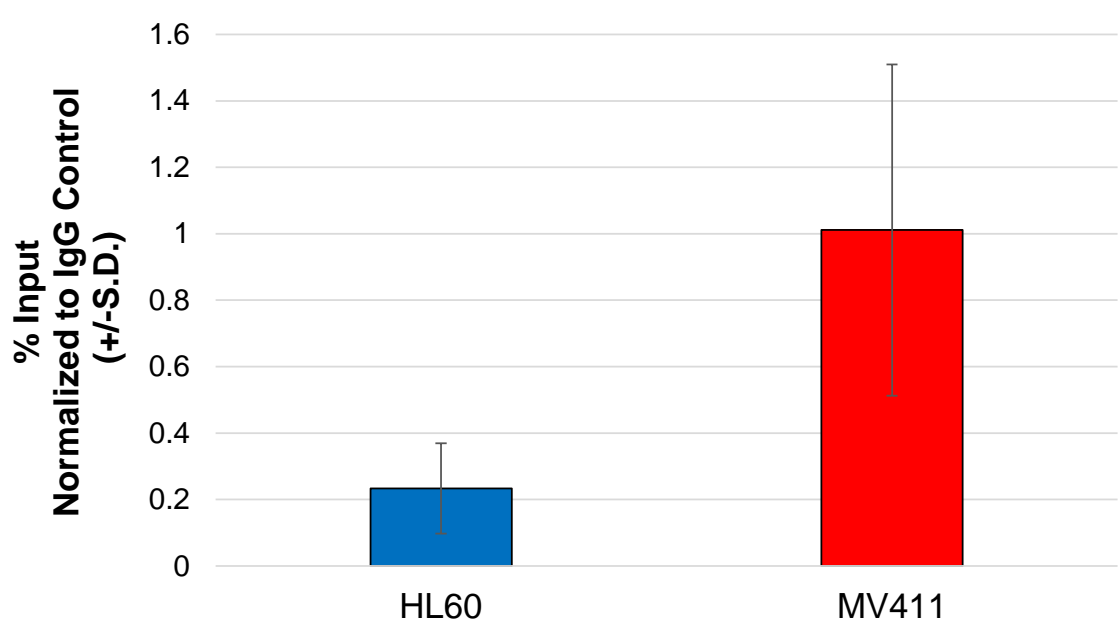


Figure 4.16. MYC binding to the *BMI1* promoter is increased in the presence of FLT3-ITD.

HL60 cells (FLT3-ITD-) and MV411 cells (FLT3-ITD+) were subjected to ChIP analysis using an antibody against Myc. PCR was done to amplify fragments around the Myc consensus sequence on the *BMI1* promoter. Data compiled from two independent experiments.

We next investigated STAT5 as a potential intermediate, as we have shown previously that Shp2 positively regulates FLT3-ITD-induced leukemogenesis through increased STAT5 activation. When Shp2 phosphatase is inhibited using the pharmacologic inhibitor II-B08, there is a reduction of activated (phosphorylated) STAT5 in FLT3-ITD-expressing cells (Nabinger, Li et al. 2013). Additionally, we found four potential STAT5 consensus sequences near the transcription start site of the *BMII* promoter that are highly conserved between human and mouse (Figure 4.17).

We again conducted ChIP experiments to look at the level of STAT5 bound to each consensus site in the *BMII* promoter in MV411 cells (FLT3-ITD+) and HL60 cells (FLT3-ITD-). In three of the four sites, we did not find an elevation of STAT5 interaction with the *BMII* promoter in the presence of FLT3-ITD, suggesting that these sites are not the main regulatory sites through which Bmi1 expression is regulated by STAT5 in FLT3-ITD cells. In the fourth site, however, there was an elevation of STAT5 bound to the *BMII* promoter (Figure 4.18), suggesting that STAT5 may contribute to upregulation of Bmi1 expression in FLT3-ITD-expressing cells by interacting with the *Bmi1* locus approximately 1600 bp upstream of the ATG start site (Figure 4.18).

Taken together, our findings suggest that in the context of FLT3-ITD, Shp2 suppresses senescence by positively regulating Bmi1 and Hoxa9 (Figure 4.19). Bmi1 and Hoxa9 have been shown to be suppressors of p16, a cell cycle regulator that promotes senescence. Consistently, upon deletion of one allele of Shp2, we see lower levels of Bmi1 and Hoxa9, while observing a compensatory upregulation of p16. We believe that Shp2 might regulate Bmi1 primarily through STAT5, and to a lesser extent, Myc. Additionally, our findings suggest that Shp2 might regulate Hoxa9 through

STAT5 as well. However, more studies need to be performed to confirm this mechanism.

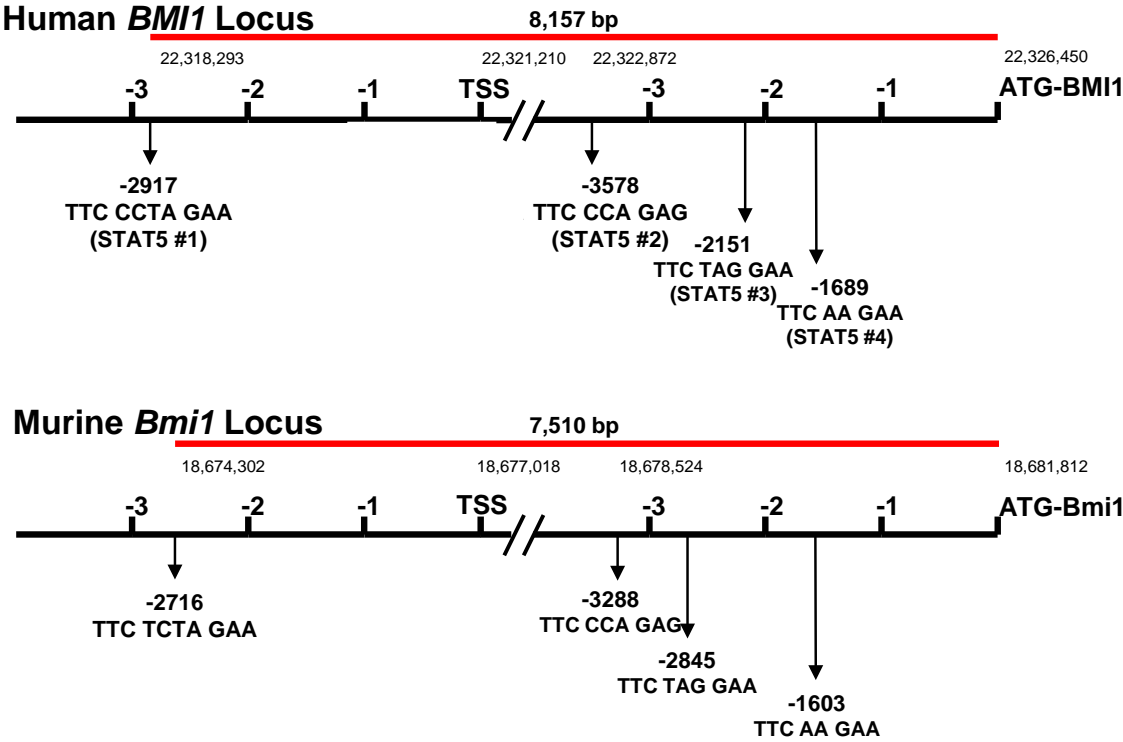


Figure 4.17. The human *BMI1* locus contains four STAT5 consensus sequences that are conserved in the murine *Bmi1* locus.

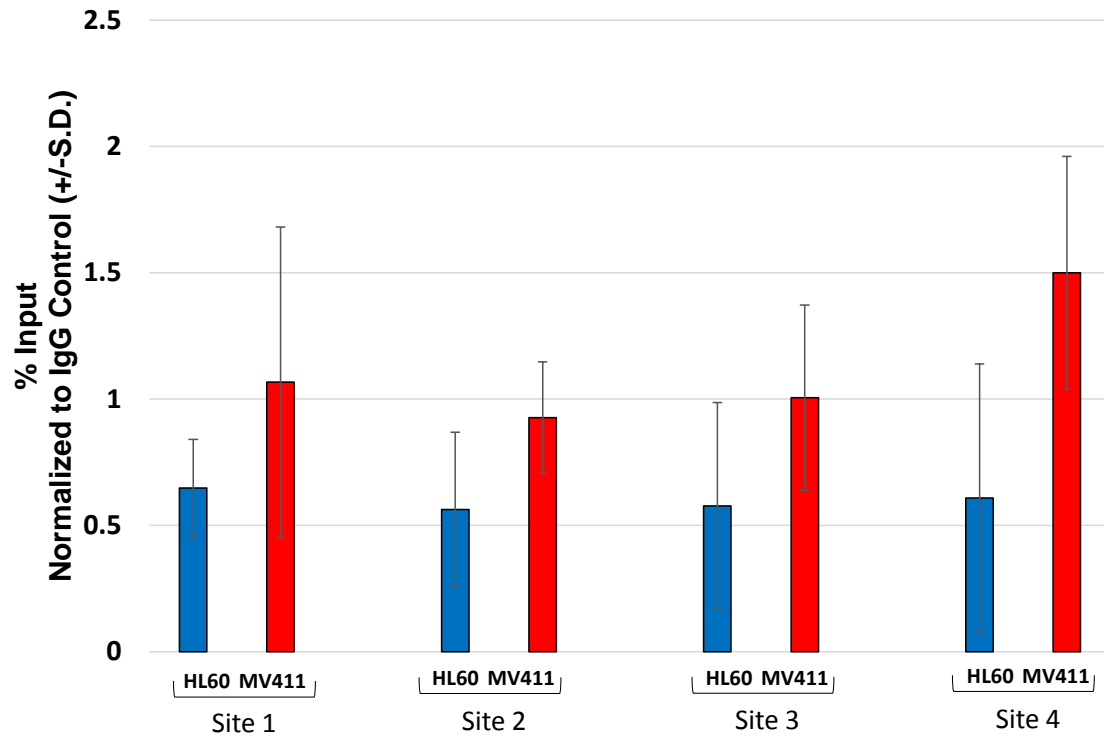


Figure 4.18. STAT5 binding to the *BMI1* locus is slightly elevated in FLT3-ITD-expressing MV411 cells.

HL60 cells (FLT3-ITD-) and MV411 cells (FLT3-ITD+) were subjected to ChIP assay using an antibody against STAT5. PCR was done to amplify fragments around each of the four STAT5 consensus sequence on the *BMI1* promoter. Data are compiled from three independent experiments.

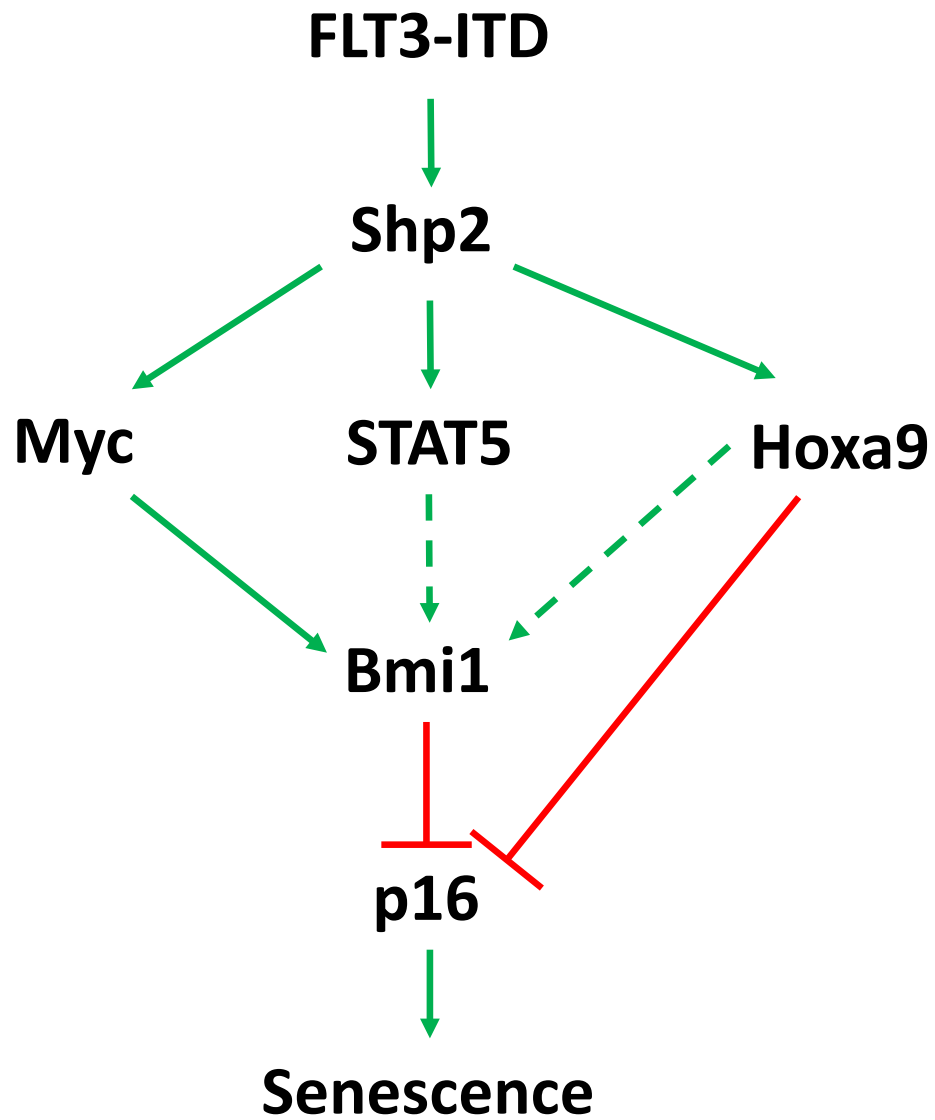


Figure 4.19. Schematic overview of the Shp2 phosphatase-mediated mechanism that regulates senescence in FLT3-ITD-expressing cells.

Examination of Shp2 heterozygosity on FLT3-ITD+ stem cell function

Because we found that genetic deletion of Shp2 led to an increase in senescence of the primitive HSPC compartment (Figure 4.6), we hypothesized that Shp2 is regulating the malignancy-initiating FLT3-ITD-expressing hematopoietic stem and progenitor cell (HSPC) function. The most accurate way to investigate stem cell function is a competitive transplant model. In a competitive transplant, experimental cells are transplanted along with normal competitor cells. If the experimental cells outcompete the competitor, the stem cells have a competitive advantage and demonstrate enhanced function, resulting in increased chimerism in recipient mice. If the experimental cells fail to compete with the competitor, the stem cells are at a disadvantage and demonstrate reduced stem cell function, as shown through decreased chimerism.

We sought to determine if Shp2 heterozygosity impairs engraftment and stem cell function in FLT3-ITD-expressing cells in a competitive transplant model. To do so, we first began by polyI:C treating FLT3-ITD; Shp2^{fl^{ox}/+}; Mx1-Cre⁺ and FLT3-ITD; Shp2^{fl^{ox}/+}; Mx1-Cre- C57/Bl6 mice (expressing cell surface marker CD45.2) to selectively delete one allele of Shp2 in a subset of mice. Five weeks post-treatment, genotypes were confirmed and LDMNCs were isolated from the mice. Cells were transplanted in a 1:1 or 1:2 ratio with competitor BoyJ cells (expressing cell surface marker CD45.1) (1-2 x 10⁶ experimental to 2 x 10⁶ competitor cells) into lethally irradiated BoyJ recipient mice (Figure 4.20). Engraftment and stem cell function was followed over time by routine blood draws every four weeks and chimerism was analyzed by staining peripheral blood for CD45.1 and CD45.2.

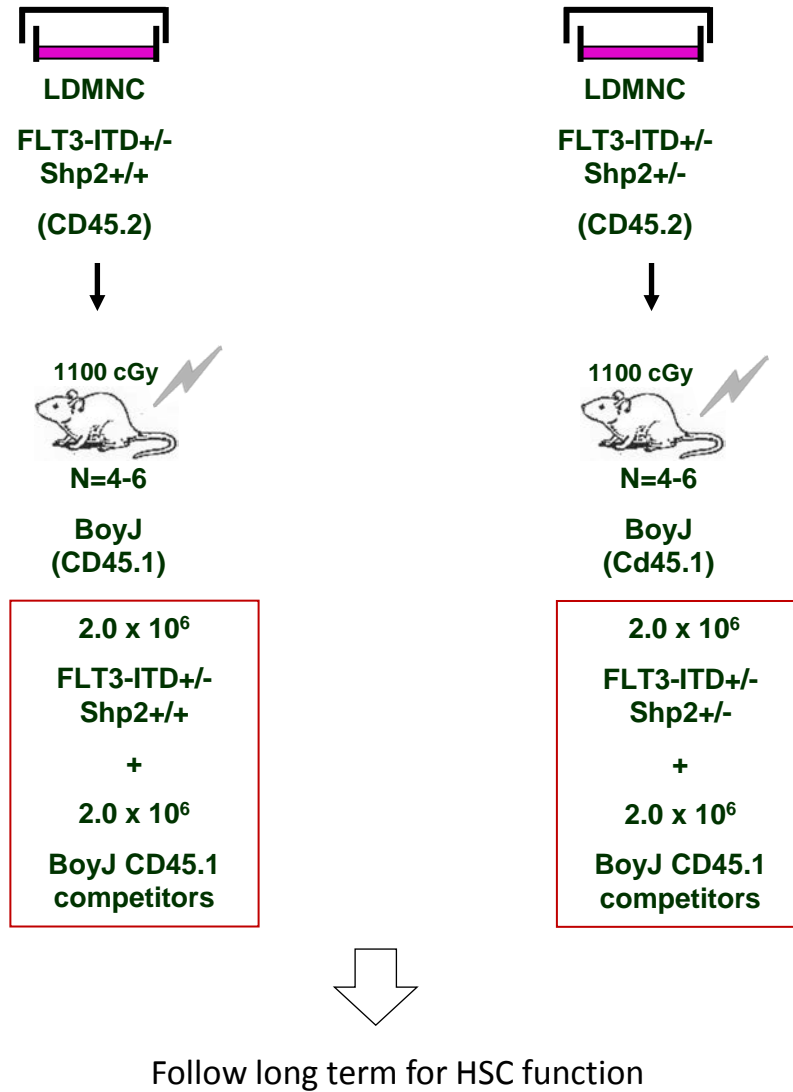


Figure 4.20. Experimental method for competitive transplants to examine the effect of Shp2 heterozygosity on FLT3-ITD+ HSC engraftment.

Again, in a competitive transplant in which the experimental cells function the same as the competitor, one would expect to see equal composition of CD45.1 and CD45.2 in the peripheral blood. Interestingly, Chu et al. showed that FLT3-ITD-expressing cells have reduced quiescence and decreased repopulating ability as evidenced by lower chimerism compared to WT control (Chu, Heiser et al. 2012). Therefore, we did not expect an equal repopulation of our experimental FLT3-ITD-expressing cells at baseline. Given our hypothesis that Shp2 plays a critical role in FLT3-ITD+ HPSCs, we hypothesized that ITD; Shp2^{+/-} mice would have lower chimerism than ITD; Shp2^{+/+} mice. As seen in Figure 4.21, FLT3-ITD-expressing cells with both alleles of Shp2 didn't have normal chimerism as expected, but did steadily increase over time, suggesting an altered stem cell function, but still capable of repopulating the bone marrow. However, the deletion of only one allele of Shp2 in FLT3-ITD-expressing cells was sufficient to further significantly reduce the repopulating ability of the FLT3-ITD-expressing stem cells. With only one allele of Shp2 in the context of FLT3-ITD, there was little to no engraftment at 4 weeks, and these cells were never able to increase over time to repopulate the bone marrow (Figure 4.21).

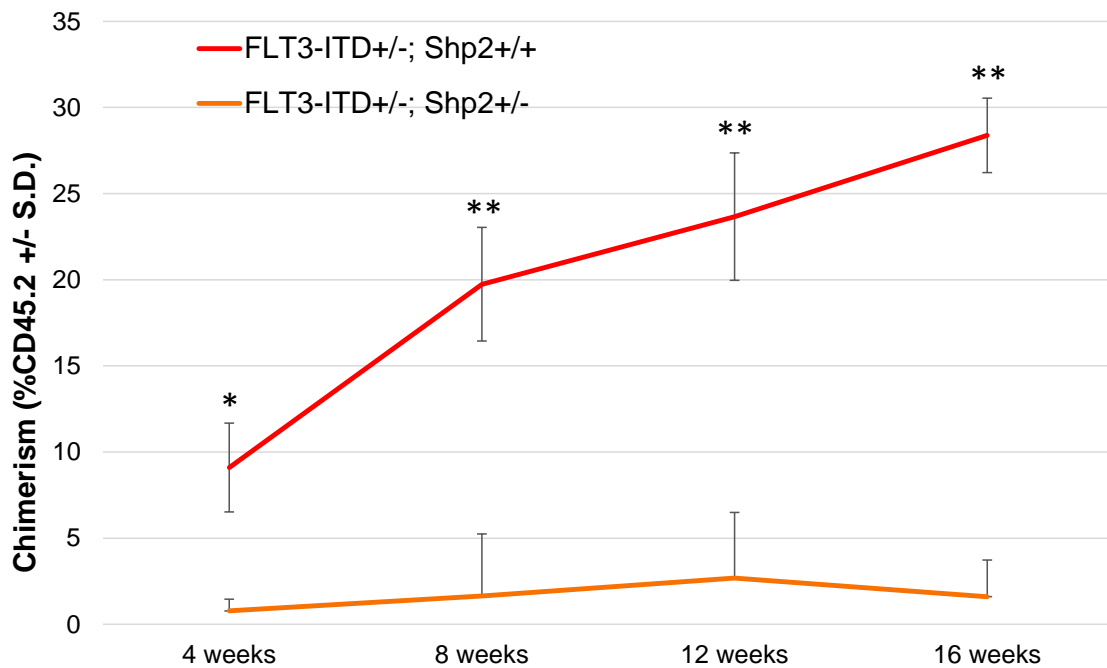


Figure 4.21. Shp2 heterozygosity severely reduces engraftment potential of FLT3-ITD-expressing cells in a competitive transplant model.

Lethally irradiated BoyJ mice were transplanted with FLT3-ITD; Shp2+/+ or FLT3-ITD; Shp2+/- experimental LDMNCs (CD45.2, 2×10^6) along with competitor BoyJ cells (CD45.1, 2×10^6). Peripheral blood chimerism was analyzed as percent CD45.2 in the peripheral blood over time. $n=5$, * $p<0.005$ and ** $p<0.0005$ for FLT3-ITD; Shp2+/+ vs. FLT3-ITD; Shp2+/- at all time points using unpaired, two-tailed student's *t* test.

Additionally, we saw no difference between mice that were transplanted with cells in a 1:1 ratio or a 1:2 ratio (data not shown), so for simplicity, only mice with a 1:1 ratio are displayed in Figure 4.21, as that is the ratio used for subsequent experiments. For a secondary transplant, which is a test to measure stem cell self-renewal, bone marrow LDMNCs from the primary recipient mice (1×10^6) were transplanted into lethally irradiated BoyJ secondary recipients. As expected, no CD45.2+ chimerism emerged in mice transplanted with cells from the ITD; Shp2^{+/-} mice (Figure 4.22). Whereas chimerism was relatively high in FLT3-ITD mice at the time of euthanasia (approximately 30%), transplantation of these cells into new recipient mice resulted in lower initial engraftment (down to 10%), again supporting the idea that FLT3-ITD-expressing HSPC have lower stem cell activity and lack robust self-renewal capacity. Taken together, these data suggest that Shp2 is crucial for the stem cell function of FLT3-ITD HSPCs. The reduction of Shp2 expression was sufficient to cause altered stem cell function, most likely through an enhanced reduction in quiescence, consistent with what is seen in Shp2 heterozygous HSPCs (Chan, Li et al. 2006) and FLT3-ITD HSPCs (Chu, Heiser et al. 2012), and could ultimately result in bone marrow failure in the absence of normal competitors.

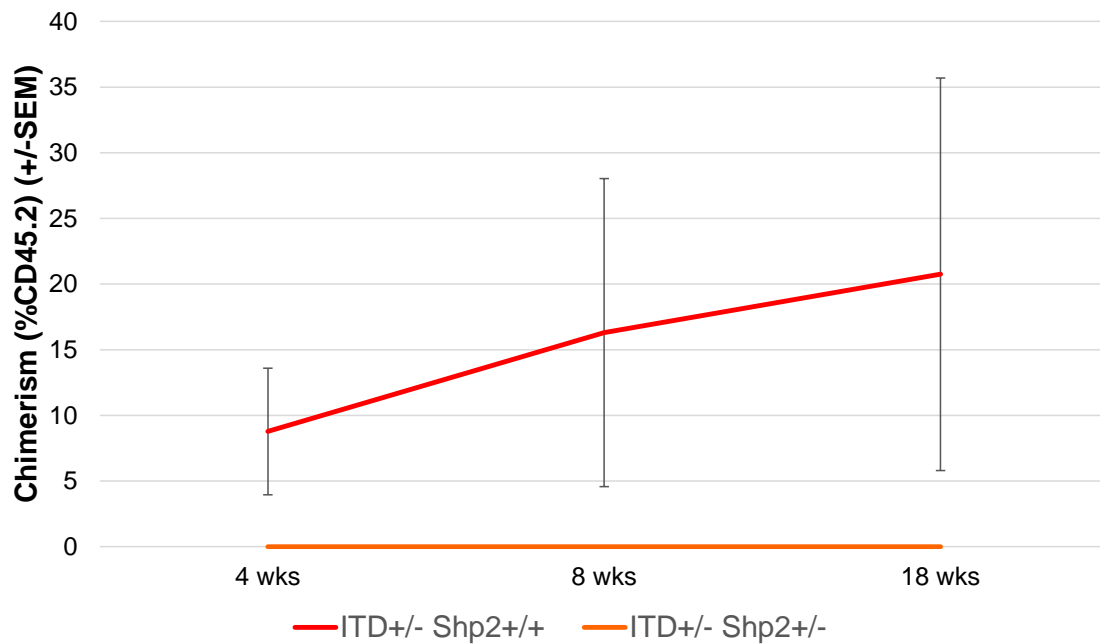


Figure 4.22. Shp2 heterozygosity continues to reduce engraftment potential of FLT3-ITD-expressing cells in a secondary transplant model.

LDMNCs (1×10^6) from primary transplant mice (Figure 4.20) were transplanted into lethally irradiated secondary recipient BoyJ mice. Chimerism was analyzed as percent CD45.2 in the peripheral blood over time. $n = 5$ per group.

While it has been shown previously that Shp2 heterozygosity can lower stem cell function (Chan, Li et al. 2006), and ITD can lower stem cell function (Chu, Heiser et al. 2012), we wanted to compare the HSPC function of our FLT3-ITD; Shp2^{+/-} mice to WT, Shp2^{+/-} alone, and ITD alone mice. We hypothesized that while Shp2 heterozygosity can affect stem cell function in both the context of WT FLT3 and FLT3-ITD, there would be increased sensitivity of loss of Shp2 in the FLT3-ITD-expressing mice and that FLT3-ITD; Shp2^{+/-} mice would have the lowest overall engraftment of all cell types. Therefore, we repeated the competitive transplant to include the two new genotypes. Mice expressed the following genotypes: WT FLT3; Shp2^{fllox/+}; Mx1-Cre⁻, WT FLT3 Shp2^{fllox/+}; Mx1-Cre⁺, FLT3-ITD; Shp2^{fllox/+}; Mx1-Cre⁻, and FLT3-ITD; Shp2^{fllox/+}; Mx1-Cre⁺, and were treated with polyI:C to delete one allele of Shp2 to produce WT, Shp2^{+/-}, ITD, and ITD; Shp2^{+/-} mice, respectively. Again, 5 weeks after treatment, genotypes were confirmed and mice were euthanized in order to isolate LDMNCs. A 1:1 experimental: competitor ratio was given to all mice (Figure 4.23) and chimerism was analyzed using peripheral blood samples every four weeks for stem cell function.

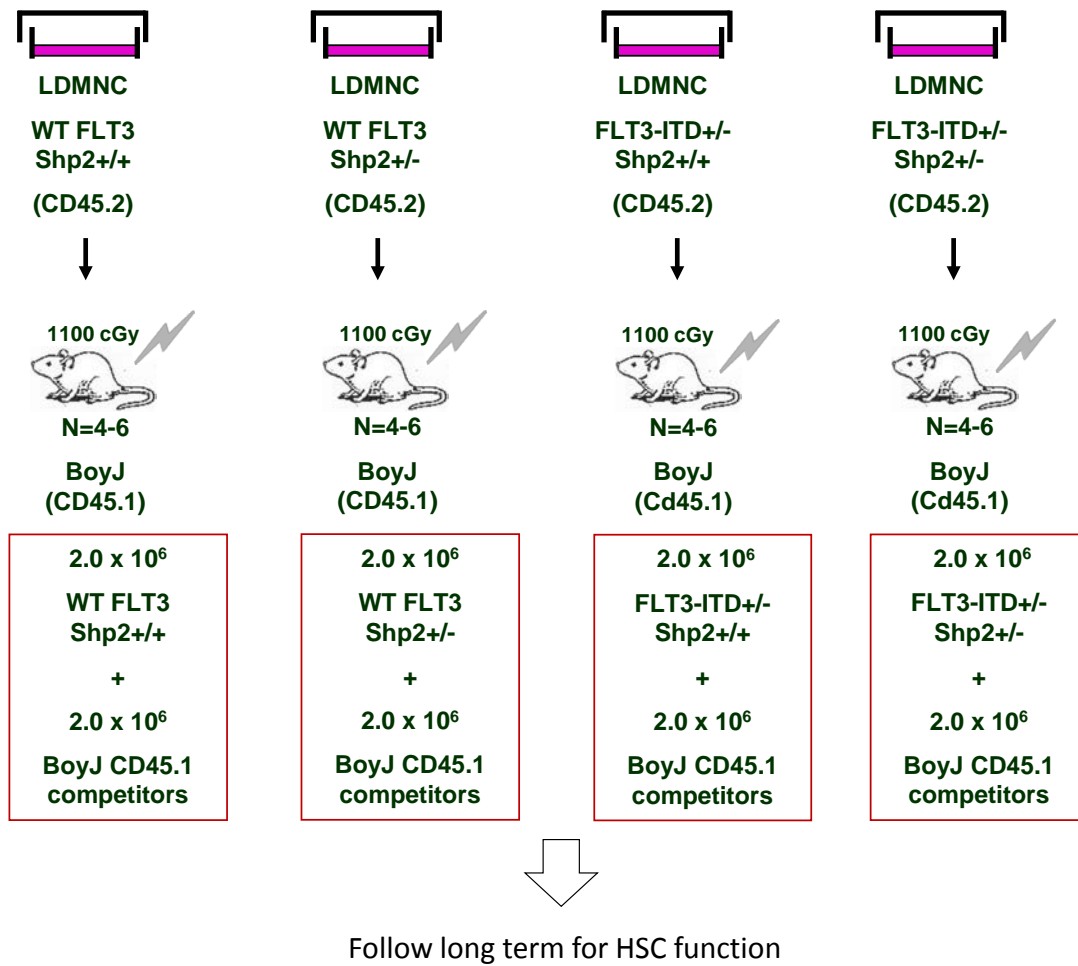


Figure 4.23. Experimental method for competitive transplants to examine the effect of Shp2 heterozygosity on FLT3-ITD+ HSC engraftment in comparison to WT, Shp2 heterozygosity alone, and ITD alone.

As expected, WT mice had the highest level of chimerism, reaching 50% by 16 weeks post-transplant (Figure 4.24). Shp2 heterozygous (Shp2^{+/-}) and ITD mice displayed lower chimerism, consistent with findings that both alterations led to decreased repopulating ability of stem cells (Chan, Li et al. 2006, Chu, Heiser et al. 2012). Shp2 heterozygous mice had higher chimerism than ITD, suggesting that ITD alone may have a stronger effect on stem cell function compared to Shp2 heterozygosity in WT FLT3 cells. Both Shp2^{+/-} and ITD were able to increase the chimerism over time, again indicating stem cell function was altered, but not lost. Consistent with our previous transplants, FLT3-ITD; Shp2^{+/-} mice had the lowest chimerism, again, close to 0% CD45.2, which did not significantly increase over time (Figure 4.24), suggesting a loss of stem cell function, which would ultimately lead to bone marrow failure if CD45.1 competitor cells were not present. Furthermore, although both the WT FLT3- and FLT3-ITD-expressing cells have reduced stem cell activity upon loss of one allele of Shp2, the WT FLT3 cells were reduced by 1.5-fold at 16 weeks post-transplant while the N51-FLT3 cells had a 3.2-fold reduction in chimerism upon loss of one allele of Shp2. These findings are consistent with our previous results, suggesting that FLT3-ITD⁺ cells are more sensitive to the loss of Shp2, and therefore, more dependent on Shp2 function.

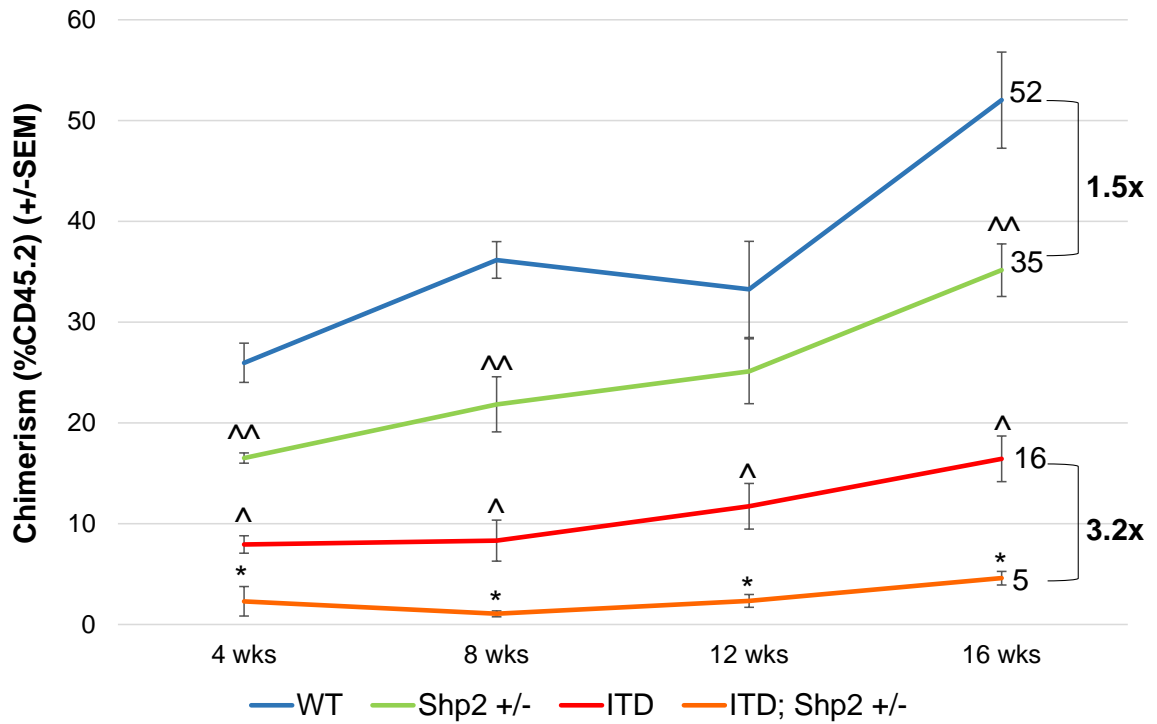


Figure 4.24. FLT3-ITD; Shp2^{+/-} mice display the lowest level of chimerism in a competitive transplant model.

Mice were transplanted with WT FLT3; Shp2^{+/+}, WT FLT3; Shp2^{+/-}, FLT3-ITD; Shp2^{+/+} or FLT3-ITD; Shp2^{+/-} experimental LDMNCs (CD45.2, 2×10^6) along with competitor BoyJ cells (CD45.1, 2×10^6) into lethally irradiated (1100 cGy) recipient BoyJ mice. Chimerism was analyzed as percent CD45.2 in the peripheral blood over time. n=9-10, ^^p<0.005 for WT vs Shp2^{+/-}; ^p<0.005 for WT vs ITD; *p<0.005 for ITD vs. ITD; Shp2^{+/-} using unpaired, two-tailed student's *t* test.

Because of the altered chimerism of FLT3-ITD; Shp2^{+/-} cells, we wanted to examine the bone marrow to determine if the chimerism in the bone marrow matched the altered chimerism observed in the peripheral blood. Additionally, we wanted to examine the lineage composition of the bone marrow and peripheral blood of our animals at the end of the study. For these studies, we isolated peripheral blood from the tail vein prior to euthanasia and performed a red blood cells lysis on these samples. Additionally, bone marrow cells and splenocytes (data not shown) were harvested from each mouse. Samples were stained for flow cytometry analysis using fluorescently conjugated antibodies in order to analyze the myeloid compartment (Mac-1⁺/Gr-1⁺), the B cell compartment (CD19⁺), as well as chimerism (CD45.2⁺). When examining the peripheral blood chimerism at the end of analysis, we observed the same trend as in our periodic blood draw. Both Shp2 heterozygosity and the presence of FLT3-ITD alone lowered the chimerism in the peripheral blood. Again, we saw that mice transplanted with ITD; Shp2^{+/-} cells displayed drastically low levels of chimerism in the peripheral blood (Figure 4.25A, left set of bars). When looking at the chimerism in the bone marrow, however, mice transplanted with ITD; Shp2^{+/-} did not display the same level of reduced chimerism that was observed in the peripheral blood. In fact, the level of chimerism was the same as Shp2^{+/-} alone and ITD alone (Figure 4.25B, left set of bars), suggesting that there is another factor at play contributing to the overall low levels of chimerism in the peripheral blood. Therefore, we next wanted to examine the lineage composition in the peripheral blood and bone marrow of the recipient mice. We found that in mice transplanted with ITD; Shp2^{+/-} LDMNCs, there was an elevation of circulating myeloid cells in the peripheral blood and spleen, with a corresponding

reduction in the level of circulating B cells (Figure 4.25A, middle and right sets of bars, and data not shown). This drastic reduction in B cell levels was also observed in the bone marrow of the mice transplanted with ITD; Shp^{+/-} LDMNCs (Figure 4.25B, set of bars). This suggests that Shp2 heterozygosity in the context of FLT3-ITD not only affects stem cell function, but also the differentiation into mature B cells, explaining the robust drop in peripheral blood chimerism in the recipient mice transplanted with ITD; Shp2^{+/-} LDMNCs. Because of the differences in myeloid and B cell lineage composition, we believe that Shp2 is functioning in FLT3-ITD expressing cells to maintain a balance of myeloid and B cells. Therefore, upon the loss of Shp2, this balance is skewed. Interestingly, this phenomenon only seems to be apparent in FLT3-ITD-expressing cells, as Shp2 heterozygosity alone does not result in a block of B cell differentiation.

Because of these surprising findings in our recipient mice, we wanted to determine the cellular composition phenotype of the donor cells before transplant. Consistent with our competitive transplants, mice were treated with polyI:C and 5 weeks after treatment, peripheral blood via the tail vein was collected prior to euthanasia. Peripheral blood and LDMNCs were stained for chimerism (CD45.2), the myeloid compartment (Mac-1/Gr-1), and the B cell compartment (CD19), and a marker for immature myeloid blasts (c-Kit/Mac-1). Consistent with the recipient transplant mice, we saw a reduction of B cells and an increase in myeloid cells in the bone marrow and peripheral blood of ITD; Shp2^{+/-} mice (Figure 4.26A). As we saw an increase in circulating myeloid cells, we wanted to determine if these myeloid cells were terminally differentiated, or if there was an expansion of immature myeloid cells, consistent with the

disease phenotype. Cells positive for both c-Kit and Mac-1 represent myeloid blast cells in mouse models, and expansion of this cell population is indicative of MPD. Therefore, we hypothesized that the expanded population was mature myeloid cells as opposed to immature blasts. When examining c-Kit/Mac-1 positive cells, we did not see an expansion in the double positive population (Figure 4.26B). Additionally, the intensity of the Mac-1 stain can be indicative of myeloid maturity. Cells staining dim for Mac-1 are immature myeloid cells, while the Mac-1 bright cells are the terminally differentiated myeloid cells. As seen in Figure 4.26B, the expansion of Mac-1 positive myeloid cells is of the mature myeloid cell population. Collectively, this suggests that Shp2 heterozygosity in FLT3-ITD-expressing cells skews lineage commitment to promote myeloid maturation while blocking the B cell differentiation. However, it remains to be determined at which stage in the B cell differentiation pathway does this block occur. Also, it is of interest if the same block is seen in T cell differentiation. Interestingly, it has been shown previously that FLT3-ITD mice show a reduction in pro-B cells and an expansion of pre-pro-B cells, suggesting that FLT3-ITD alters the differentiation at this stage (Mead, Kharazi et al. 2013). Therefore, it is likely that Shp2 heterozygosity in FLT3-ITD-expressing cells promotes this lineage block even further.

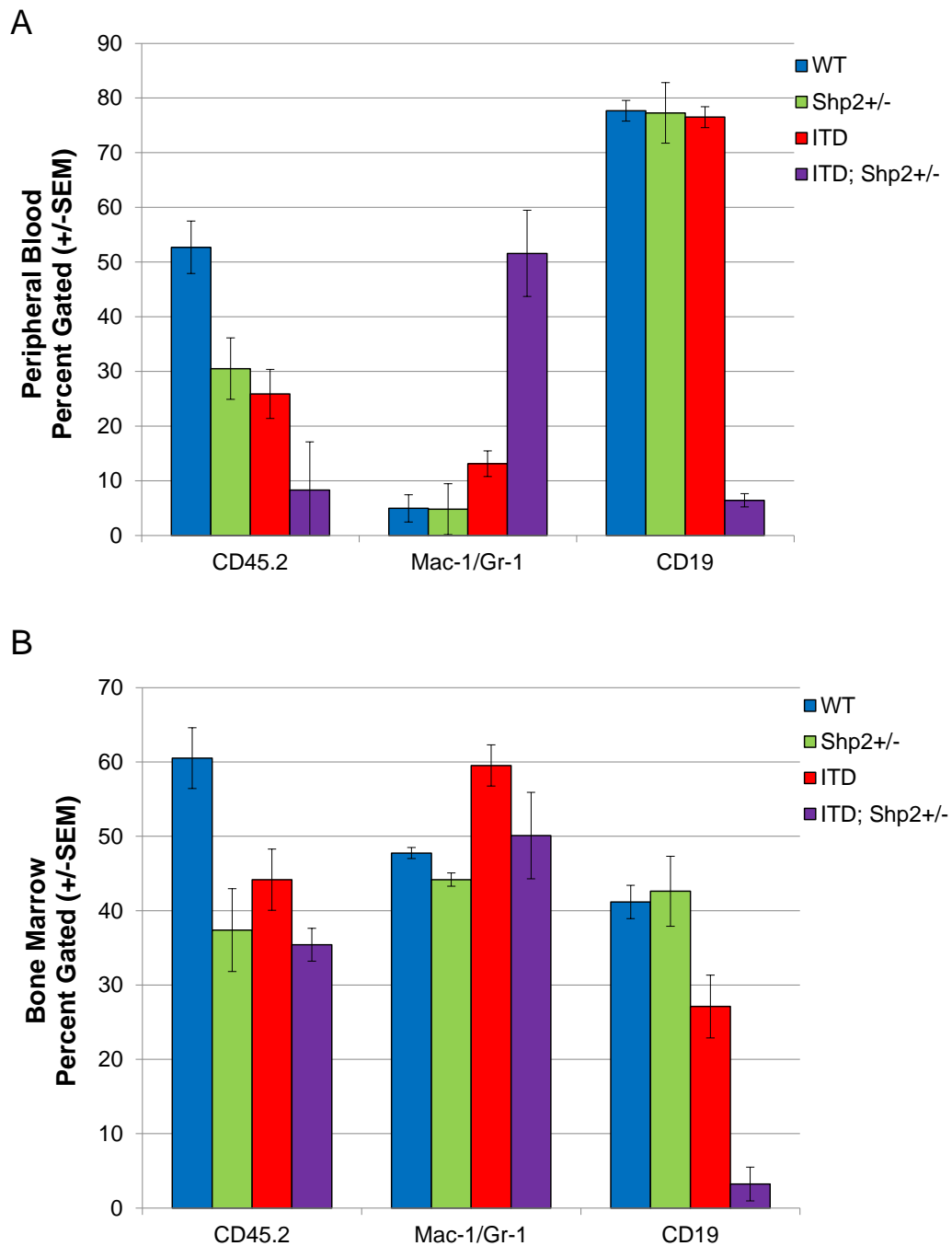
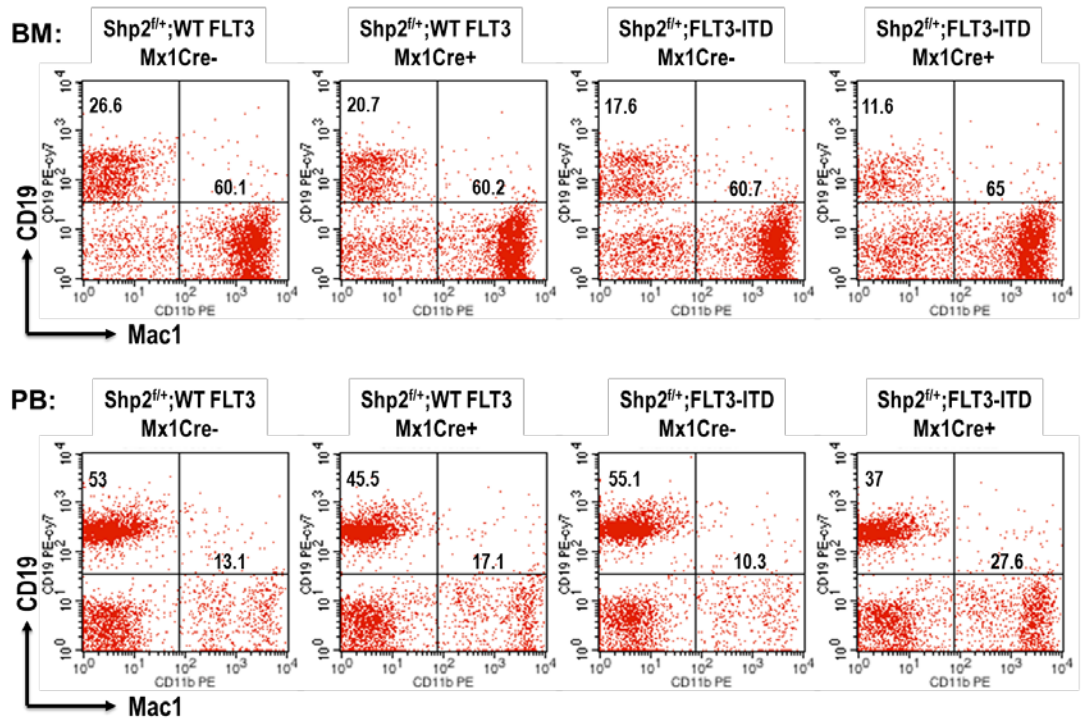


Figure 4.25. Deletion of one allele of Shp2 significantly alters differentiation of FLT3-ITD-expressing cells, but not WT FLT3-expressing cells.

Peripheral blood and bone marrow were collected from recipient mice 24 weeks post-transplant. Cells were stained to look at chimerism (CD45.2), myeloid cells (Mac-1/Gr-1), and B cells (CD19) via flow cytometry. n= 6 for WT, n= 8 for Shp2+/-, n= 15 for ITD, and n= 16 for ITD; Shp2+/- in the bone marrow, and n= 5 for WT, n= 12 for Shp2+/-, n= 19 for ITD, and n= 20 for ITD; Shp2+/- in the bone marrow.

A



B

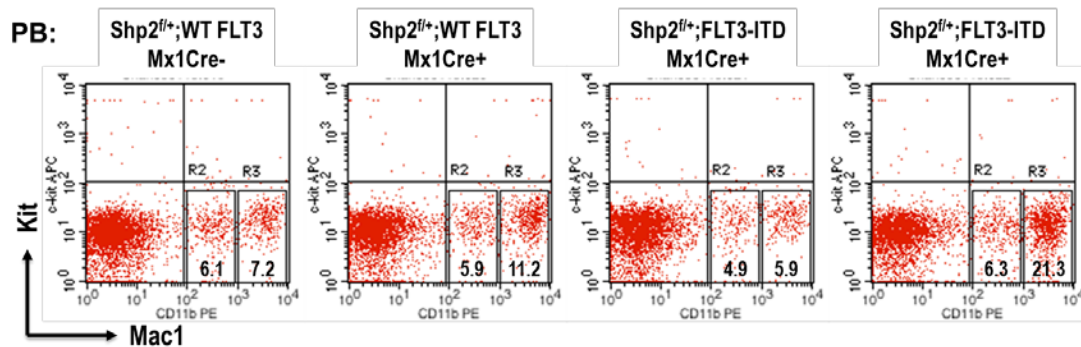


Figure 4.26. Shp2 heterozygosity in FLT3-ITD donor cells have an expanded mature myeloid and reduced B cell population.

Peripheral blood and bone marrow were collected from donor mice 5 weeks post polyI:C treatment. Cells were stained to look at the mature myeloid cell (Mac-1), immature myeloid cell (Mac-1/c-Kit), and B cell (CD19) compartments via flow cytometry. Flow plots are representative of 4 mice per group.

Discussion

Due to the positive role of Shp2 in FLT3-ITD-induced leukemogenesis, we hypothesized that genetic deletion of *Ptpn11*, the gene encoding for Shp2, would increase latency to disease. While we did observe reduced malignancy-induced mortality, we also found several mice that, upon deletion of Shp2, succumbed to bone marrow failure. This phenotype occurred approximately two weeks after polyI:C treatment to delete Shp2, and was not seen in mice that expressed WT FLT3. This suggests that while Shp2 plays a role in the active signaling pathways in bulk FLT3-ITD+ tumor cells, the malignancy-initiating stem cells may also have an increased dependence on Shp2. We therefore sought to identify a mechanism by which Shp2 deletion can cause bone marrow failure, and to examine the importance of Shp2 in the malignancy-initiating FLT3-ITD+ stem cell.

We hypothesized that the most likely causes of bone marrow failure were apoptosis and/or senescence. We first examined apoptosis in mice approximately two weeks after Shp2 deletion (consistent with the time point when mice succumbed to bone marrow failure in previous experiments). Using Annexin V staining on WT FLT3- and N51-FLT3-expressing LDMNCs and a more primitive lineage-negative population, we did not observe increased apoptosis in the FLT3-ITD-expressing cells upon the loss of Shp2 (Figure 4.3 and Figure 4.4). Moreover, we examined apoptosis by staining femur sections for Caspase 3, an indicator of apoptosis. Again, there was no significant staining in either WT or N51-FLT3 expressing bone sections, all together suggesting that apoptosis is not the main driver of bone marrow failure after Shp2 deletion.

We next turned to senescence, a cellular process in which cells stop dividing induced by aging or stressors. When examining WT and N51-FLT3 LDMNCs and Lin-cells for SA- β -galactosidase after Shp2 deletion, we did observe a strong senescent phenotype in the N51-FLT3-expressing Shp2 negative cells compared to the WT FLT3-expressing Shp2 negative cells (Figures 4.5 and 4.6). This suggests that senescence is the driver of bone marrow failure upon deletion of Shp2 and occurs in a FLT3-ITD-dependent manner.

As Shp2 is a ubiquitously expressed protein and is essential for normal hematopoiesis, we wanted to determine if we could observe the same phenotype upon partial deletion of Shp2, thereby only deleting one allele of Shp2 instead of two as in previous experiments. Additionally, we wanted to use a more physiologic approach to examining senescence and stem cell function, so we employed a new mouse model. We crossed a FLT3-ITD knock-in mouse (Lee, Tothova et al. 2007) with our Shp2^{flox/flox}; Mx1-Cre mice to create a mouse model that endogenously expresses WT FLT3 or FLT3-ITD, and can be induced to be heterozygous at the *Ptpn11* locus (FLT3-ITD; Shp2^{flox/+}; Mx1-Cre) (Figure 4.8). We used this model to examine senescence by SA- β -galactosidase staining as well as molecular markers for senescence. Indeed, we once again observed a strong senescent phenotype in N51-FLT3-expressing cells upon deletion of one allele of Shp2 (Figure 4.11). This implies that FLT3-ITD cells are more sensitive to the loss of Shp2, that even Shp2 heterozygosity is sufficient to alter the cellular function.

We next initiated studies to look for a molecular mechanism of senescence in the context of FLT3-ITD. Using RT-PCR, we examined mRNA expression levels in FLT3-

ITD; Shp2 heterozygous cells. Upon deletion of one allele of Shp2, we saw a resultant decrease in Bmi1 and Hoxa9 mRNA levels, and an increase in p16 mRNA levels (Figure 4.13 and Figure 4.14). The cell cycle regulator, p16, has been shown to be inhibited by both Bmi1 and Hoxa9 in the context of MLL-AF9 induced leukemogenesis (Smith, Yeung et al. 2011). Consistent with these findings, we believe that Shp2 positively regulates both Bmi1 and Hoxa9 to inhibit senescence in FLT3-ITD+ cells. Therefore, upon the loss of Shp2, expression of Bmi1 and Hoxa9 decrease, allowing for higher levels of p16, and ultimately, senescence. Future experiments are carrying this forward by looking at the gene profiles of Lin- cells in the ITD; Shp2+/- cells compared to WT, Shp2+/-, and ITD alone using RNA-seq analysis. Additionally, a recent study emerged that linked Shp2 to senescence in mammary gland tumors. In their model, Lan et al. saw that Shp2 inhibits senescence through p27 and p53 by regulating *Skp2*, *Aurka*, and *Dll1* (Lan, Holland et al. 2015). It would be of interest to us to examine these same effectors in our FLT3-ITD system.

To begin to delineate how Shp2 is regulating Bmi1, we looked at the transcription factors Myc and STAT5 as potential intermediates. Myc is a known regulator of Bmi1 transcription, and there is a known Myc-binding consensus sequence approximately 180 bp upstream of the transcription start site on the *BMII* promoter. Additionally, STAT5 has four putative binding sites on the *BMII* promoter, both upstream and downstream of the transcription start site. Using ChIP, interaction of Myc and STAT5 (at one binding site) with the *BMII* promoter increased in the presence of FLT3-ITD (Figure 4.16 and Figure 4.18, respectively), suggesting that Shp2 may be regulating Bmi1 expression

through both Myc and/or STAT5. Further experiments will be conducted by the Chan laboratory to study this mechanism in detail.

As mentioned previously, deletion of Shp2 in an adoptive transfer model resulted in reduced chimerism in mice transplanted with FLT3-ITD-expressing cells compared to mice transplanted with WT FLT3-expressing cells. We therefore hypothesized that Shp2 plays a role in the FLT3-ITD⁺ stem cell compartment. In an adoptive transfer model, experimental cells were transplanted with supporting splenocytes and given time to engraft before Shp2 deletion. While these studies can give an implication of stem cell function, a competitive transplant must be done to examine stem cell function most accurately. In a competitive transplant, experimental cells are given along with competitor cells to determine if the altered experimental cells have enhanced or reduced stem cell function. As we saw bone marrow failure in our adoptive transfer model, we hypothesized that mice transplanted with ITD; Shp2^{+/-} cells would have reduced stem cell function, as evidenced by low chimerism. Indeed, we saw a drastic reduction in chimerism in both primary and secondary competitive transplants in ITD; Shp2^{+/-} mice compared to WT, Shp2^{+/-} or ITD alone (Figures 4.21, 4.22, and 4.24). This suggests again that FLT3-ITD-expressing HSPCs are sensitive to the loss of Shp2, and are dependent on Shp2 signaling for normal function.

Unlike the adoptive transfer studies, in which cells were given time to engraft prior to deletion of Shp2, our competitive transplant donor cells were manipulated to recombine the *Ptpn11* allele prior to transplant, leaving open the possibility that the reduced chimerism of the ITD; Shp2^{+/-} cells may be due to reduced homing. While we have not formally examined homing with the ITD; Shp2^{+/-} cells, we do know that in the

context of FLT3-ITD alone, homing studies demonstrated that the ITD status does not affect homing (Chu, Heiser et al. 2012). Additionally, homing was examined in a competitive transplant of Shp2 heterozygous cells, and Shp2 heterozygosity also didn't affect homing (Chan, Li et al. 2006). Therefore, while we will formally test homing in the future in our model, we do not predict that altered homing does not account for the reduced chimerism of the ITD; Shp2^{+/-} cells in competitive transplants.

One limitation of our competitive transplant model is the use of the Mx-1 Cre transgene to induce genetic recombination of the *Ptpn11* allele. Mx-1 relies on an interferon response (induced by polyI:C treatment) to activate Cre recombinase. Shp2 is an inhibitor of IFN- α and IFN- γ signaling, such that deletion of Shp2 enhances cytotoxicity as a result of IFN-induced growth inhibitory and apoptotic pathways (You, Yu et al. 1999). Therefore, in the future, we would like to move away from our Mx-1 Cre model to different Cre systems, such as Vav1- or LysM-mediated Cre expression. Neither the Vav1 nor the LysM promoter requires treatment to mediate expression of Cre. Instead, they are turned on naturally during development, avoiding the risk of toxicity. Additionally, both Vav1 and LysM mediate Cre expression in a more defined and narrower hematopoietic population, making both attractive models for our studies.

Because of the drastic reduction in chimerism seen in the peripheral blood of recipient mice transplanted with ITD; Shp2^{+/-} cells, we wanted to see if this drop was also seen in the bone marrow of the recipient mice. Upon analysis of the bone marrow, we saw lower chimerism in the ITD; Shp2^{+/-} mice, but unlike in the peripheral blood, the ITD; Shp2^{+/-} chimerism was not more reduced than the Shp2^{+/-} or ITD chimerism. This finding indicates that another factor in addition to reduced stem cell activity is

contributing to the reduction of peripheral blood chimerism of mice transplanted with ITD; Shp2^{+/-} cells. Upon analysis of the lineage compartments in the bone marrow and spleen, we saw that there was a reduction in mature B cells and an increase in differentiated myeloid cells (Figure 4.25). Upon further examination, we saw that the expansion of myeloid cells was of mature, terminally differentiated cells as opposed to immature myeloid blasts (Figure 4.26). The mechanism resulting in altered B cell and myeloid differentiation of the ITD; Shp2^{+/-} cells continues to be under investigation. FLT3-ITD expression alone has been shown to affect B cell differentiation (Mead, Kharazi et al. 2013). In this study, Mead et al. found that the transcription factor Pu.1 expression was increased in FLT3-ITD-expressing cells. Pu.1 is a known regulator of differentiation based on its expression level. When Pu.1 is elevated, cells are skewed to myeloid commitment and decreased B cell differentiation. It may be that Shp2 is further affecting Pu.1 expression in our ITD; Shp2^{+/-} model. Additionally, Hoxa9 and FLT3 regulate lymphopoiesis, such that double knockouts have severe deficiencies in B cells (Gwin, Shapiro et al. 2013). As we saw that Shp2 heterozygosity in FLT3-ITD-expressing LDMNCs resulted in lower Hoxa9 mRNA levels (Figure 4.14), it may be that Hoxa9 reduction as a result of Shp2 heterozygosity leads to a block in B cell differentiation in our FLT3-ITD model. Finally, Syk is also a regulator of lymphopoiesis (Turner, Mee et al. 1995). Therefore, as we have shown cooperativity of Shp2 and Syk in the context of FLT3-ITD, it may be that Shp2 heterozygosity lowers Syk activation, lowering the B cell differentiation capability.

FLT3-ITD is typically thought of a secondary mutation in the development of leukemia. This is evidenced by the fact that mice expressing FLT3-ITD as its only

mutation do not develop full blown leukemia, but rather myeloproliferative disorder (MPD) (Kelly, Liu et al. 2001). Another hit, usually an epigenetic hit known as a driver mutation, occurs first and, in combination with a second hit (i.e. FLT3-ITD), can develop into frank leukemia. Given our findings of the reduced stem cell function and alteration of lineage composition, we hypothesize that Shp2 heterozygosity would also affect the function of true leukemia stem cells (LSCs) as it does the malignancy-initiating HSCs.

To address this hypothesis, we are currently collaborating with the laboratory of Dr. Reuben Kapur to examine the effect of Shp2 heterozygosity on FLT3-ITD-expressing cells also lacking one copy of the epigenetic regulator, Tet2. Preliminary results demonstrate that FLT3-ITD; Tet2^{+/-}; Shp2^{+/-} also resulted in reduced chimerism, suggesting that Shp2 is also regulating classic leukemic stem cells.

CHAPTER FIVE

OVERALL CONCLUSIONS AND IMPLICATIONS

Although there have been great advancements in both technology and our understanding of AML, the general therapeutic strategy has remained largely the same for the past 30 years. FLT3-ITD is the most common mutation in AML and, consequently, an attractive therapeutic target. However, little success has been achieved when using FLT3 inhibitors as a monotherapy (Döhner, Weisdorf et al. 2015). Therefore, new therapeutic targets are needed. Due to the high rates of relapse in documented cases of AML, the current hypothesis is that we are not properly targeting all the necessary targets or cell populations required to eradicate the leukemia. While frank leukemia has been shown to bear approximately five mutations in the expanded clone, seemingly normal HSCs, with a single driver mutation, have been shown to have pre-leukemic properties. These cells are not targeted by conventional treatment regimens, and may give rise to the new clone that emerges upon leukemia relapse (Majeti 2014).

We previously demonstrated that the protein tyrosine phosphatase, Shp2, physically associates with FLT3-ITD at Tyr599 to positively regulate leukemogenesis. We also demonstrated that genetic disruption of *Ptpn11*, the gene encoding Shp2, increased malignancy-specific survival of animals transplanted with FLT3-ITD-transduced cells, suggesting that Shp2 may regulate the function of the malignancy-initiating cell. Taken together, we hypothesized that inhibiting Shp2 can target both FLT3-ITD+ bulk tumor cells as well as FLT3-ITD-expressing hematopoietic stem cells.

We investigated downstream targets of FLT3-ITD in order to develop new treatment strategies, and show that Shp2 inhibition can target both the bulk tumor cells as well as the malignancy-initiating cells.

We hypothesized that in bulk FLT3-ITD+ tumor cells, Shp2 is recruited to Tyr768 in addition to duplicated Tyr599, and that mutation of either would reduce hyperproliferation, activated signaling, and FLT3-ITD-induced leukemogenesis. To examine the importance of the signaling from each tyrosine, we employed both genetic studies and pharmacologic studies using FLT3-ITD-mutant 32D cell lines and primary AML patient samples. We saw that mutation of Tyr599 successfully reduced cellular hyperproliferation and STAT5 activation compared to FLT3-ITD cells, and significantly prolonged progression to MPD *in vivo*. This suggests that the signaling from Tyr599 to STAT5 partially accounts for the aggressiveness of the FLT3-ITD mutation.

As Syk kinase has been shown to be recruited to the juxtamembrane domain at Tyr599, as well as Tyr589, Tyr591, and Tyr597, and lead to the phosphorylation of Tyr768 on the inter-kinase domain of FLT3 (Puissant, Fenouille et al. 2014), we hypothesized that when Syk is recruited to FLT3-ITD at Tyr599, Shp2 cooperates with Syk, promoting Syk activation of STAT5, as well as promoting phosphorylation of Tyr768 and activation of PI3K. Using the pharmacologic inhibitor of Syk, R406, we saw that Syk inhibition led to decreased phosphorylation levels of STAT5, Akt, and Erk, consistent with our hypothesis. Moreover, Syk inhibition cooperated with Shp2 inhibition in N51-FLT3-expressing 32D cells and in primary AML patient samples to reduce proliferation. In N51-FLT3-expressing 32D cells, the combination of Shp2 and Syk inhibition resulted in the lowest levels of active STAT5, Akt, and Erk. Conversely,

Shp2 and/or Syk inhibition did not have a strong effect of activation levels of FLT3-effectors or proliferation in WT FLT3 expressing 32D cells. As our genetic disruption of Tyr599 phenocopies Syk inhibition, this suggests that the signaling from Syk at Tyr599 that acts both on the aberrant activation of STAT5 as well as downstream to other pathways.

When examining the FLT3-ITD signaling effectors in our mutant Tyr768 cell line, we saw that there was no effect on STAT5 activation, but we were able to detect a reduction in Erk activation. Unlike Tyr599 mutation, mutation of Tyr768 did not prolong the progression to MPD *in vivo*, suggesting that signaling to STAT5 may be more crucial for leukemogenesis than Erk/Akt signaling. While we believe Syk signals to Tyr768, Tyr768 mutation did not phenocopy Syk inhibition, suggesting that other signaling may compensate for the loss of signaling from Tyr768. One explanation is that Syk has also been shown to phosphorylate Tyr955 on FLT3-ITD (Puissant, Fenouille et al. 2014) and Gab2/Grb2/Shp2/PI3K have also been shown to be recruited to Tyr955 (Masson, Liu et al. 2009). Therefore, a double mutant of Tyr768 and Tyr599 may best phenocopy Syk inhibition in this case.

Additionally, we hypothesized that PI3K and Shp2 can work cooperatively at Tyr768 to further promote FLT3-ITD-induced leukemogenesis. We saw that PI3K and Shp2 inhibition, as with Syk and Shp2 inhibition, lowered the activation of STAT5, Akt, and Erk. Moreover, PI3K and Shp2 inhibition increased the median survival of N51-FLT3-expressing mice. As expected, in primary AML patient samples, PI3K and Shp2 inhibition worked cooperatively to lower the proliferation of these cells to the greatest degree. Interestingly, when examining primary patient samples based on their FLT3-

ITD status, we saw that patients that were FLT3-ITD+ were more sensitive to Shp2 inhibition alone than those patients that were FLT3-ITD-, suggesting again that FLT3-ITD+ cells are more dependent on Shp2 signaling. When examining this phenomenon with Syk or PI3K inhibition, FLT3-ITD status did not dictate sensitivity to any significant degree. Therefore, we believe that targeting Shp2 may hold therapeutic benefit for FLT3-ITD+ AML patients, and targeting Shp2 in combination with Syk or PI3K could hold therapeutic benefit for AML patients in general.

In the more primitive hematopoietic compartment, Shp2 has been shown to be an important modulator of stem cell activity in HSCs. Reduction of Shp2 expression through genetic manipulation lowers the repopulating ability of these cells, as a result of reduced quiescence (Chan, Li et al. 2006). Interestingly, FLT3-ITD expression results in a similar phenotype. FLT3-ITD knock-in mice display reduced quiescence and stem cell function (Chu, Heiser et al. 2012). Because of the increased dependence on Shp2 in FLT3-ITD bulk tumor cells, we hypothesized that Shp2 also plays a role in the malignancy-initiating HSC. When Shp2 knockout bone marrow cells are transplanted into recipient mice in an adoptive transfer model, cells that expressed FLT3-ITD as opposed to WT FLT3 fared much worse and some mice died from bone marrow failure, suggesting that FLT3-ITD HSCs are more dependent on Shp2. To more accurately examine the HSC function of the FLT3-ITD malignancy-initiating cell, we conducted several competitive transplants in which one allele of Shp2 was knocked out, resulting in Shp2 heterozygosity either in the context of WT FLT3 or FLT3-ITD. We saw that Shp2 heterozygosity severely reduced the peripheral blood chimerism of the FLT3-ITD expressing cells. Additionally, we saw that ITD; Shp2^{+/-} BM cells displayed a

reduction in mature B cells and an increase in mature myeloid cells. Therefore, the reduced peripheral blood chimerism is likely due to a combination of reduced stem cell function and reduced terminal B cell differentiation. This suggests that Shp2 inhibition can target the more primitive FLT3-ITD+ HSC compartment in addition to the bulk tumor cells.

Finally, we wanted to determine a mechanism through which Shp2 is regulating these malignancy-initiating cells, such that when Shp2 is deleted, the resulting phenotype is bone marrow failure. We did not observe an effect on apoptosis, but we did see that deletion of Shp2 resulted in increased senescence. While Shp2 has been linked to senescence in neural stem cells (Ke, Zhang et al. 2007) and in mammary gland tumors (Lan, Holland et al. 2015), it has never before been linked to senescence in the hematopoietic system. We have shown that Shp2 regulates senescence both in bulk tumor cells as well as in the more primitive Lin- population. We provide evidence that Shp2 may be regulating senescence through p16, with Hoxa9, Bmi1, and Myc as possible intermediates.

Collectively, we believe that Shp2 is essential for FLT3-ITD-induced leukemogenesis by function in both the bulk tumor cellular compartment as well as the malignancy-initiating cellular compartment. We believe that targeting Shp2 can significantly alter the function and progression of disease, and could hold therapeutic benefit for AML patients. Shp2 inhibition can work in combination with Syk or PI3K inhibition to significantly reduce activity of the bulk tumor cells. Since Shp2 is important in both compartments, inhibition of Shp2 may lower relapse rates in patients after conventional chemotherapy. Importantly, we show that partial reduction of Shp2

activity is sufficient to cause a profound phenotype. This becomes clinically relevant and widens the therapeutic window, as complete reduction of the ubiquitously expressed Shp2 would not be feasible due to normal tissue toxicity. Finally, our data strongly indicates that FLT3-ITD+ cells are uniquely dependent on Shp2. Therefore, targeting Shp2 should have a stronger effect on the malignant cells, and leave the normal hematopoietic cells and other normal tissues and cells largely unaffected.

REFERENCES

- Bei, L., C. Shah, H. Wang, W. Huang, L. C. Platanius and E. A. Eklund (2014). "Regulation of CDX4 gene transcription by HoxA9, HoxA10, the Mll-Ell oncogene and Shp2 during leukemogenesis." Oncogenesis **3**: e135.
- Blau, O., R. Berenstein, A. Sindran and I. Blau (2013). "Molecular analysis of different FLT3-ITD mutations in acute myeloid leukemia." Leukemia & Lymphoma **54**(1): 145-152.
- Bohmer, R., B. Neuhaus, S. Buhren, D. Zhang, M. Stehling, B. Bock and F. Kiefer (2010). "Regulation of developmental lymphangiogenesis by Syk(+) leukocytes." Dev Cell **18**(3): 437-449.
- Bowman, T., R. Garcia, J. Turkson and R. Jove (2000). "STATs in oncogenesis." Oncogene **19**: 2474-2488.
- Brasemann, S., V. Taylor, H. Zhao, S. Wang, C. Sylvain, M. Baluom, K. Qu, E. Herlaar, A. Lau, C. Young, B. R. Wong, S. Lovell, T. Sun, G. Park, A. Argade, S. Jurcevic, P. Pine, R. Singh, E. B. Grossbard, D. G. Payan and E. S. Masuda (2006). "R406, an orally available spleen tyrosine kinase inhibitor blocks fc receptor signaling and reduces immune complex-mediated inflammation." J Pharmacol Exp Ther **319**(3): 998-1008.
- Bunda, S., K. Burrell, P. Heir, L. Zeng, A. Alamsahebpor, Y. Kano, B. Raught, Z. Y. Zhang, G. Zadeh and M. Ohh (2015). "Inhibition of SHP2-mediated dephosphorylation of Ras suppresses oncogenesis." Nat Commun **6**: 8859.
- Campisi, J. (2013). "Aging, cellular senescence, and cancer." Annu Rev Physiol **75**: 685-705.
- Cancer Genome Atlas Research, N. (2013). "Genomic and epigenomic landscapes of adult de novo acute myeloid leukemia." N Engl J Med **368**(22): 2059-2074.
- Chan, G., L. S. Cheung, W. Yang, M. Milyavsky, A. D. Sanders, S. Gu, W. X. Hong, A. X. Liu, X. Wang, M. Barbara, T. Sharma, J. Gavin, J. L. Kutok, N. N. Iscove, K. M. Shannon, J. E. Dick, B. G. Neel and B. S. Braun (2011). "Essential role for Ptpn11 in survival of hematopoietic stem and progenitor cells." Blood **117**(16): 4253-4261.
- Chan, R. J. and G. Feng (2007). "*PTPN11* is the first identified proto-oncogene that encodes a tyrosine phosphatase." Blood **109**(3): 862-867.
- Chan, R. J., Y. Li, M. N. Hass, A. Walter, C. S. Voorhorst, W. C. Shelley, Z. Yang, C. M. Orschell and M. C. Yoder (2006). "Shp-2 heterozygous hematopoietic stem cells

- have deficient repopulating ability due to diminished self-renewal." Exp Hematol **34**(9): 1230-1239.
- Chan, S. M. and R. Majeti (2013). "Role of DNMT3A, TET2, and IDH1/2 mutations in pre-leukemic stem cells in acute myeloid leukemia." Int J Hematol **98**(6): 648-657.
- Choudhary, C., C. Brandts, J. Schwable, L. Tickenbrock, B. Sargin, A. Ueker, F.-D. Boehmer, W. Berdel, C. Mueller-Tidow and H. Serve (2007). "Activation mechanisms of STAT5 by oncogenic Flt3-ITD." Blood **110**(1): 370-374.
- Chowdhury, M., K. Mihara, S. Yasunaga, M. Ohtaki, Y. Takihara and A. Kimura (2007). "Expression of Polycomb-group (PcG) protein BMI-1 predicts prognosis in patients with acute myeloid leukemia." Leukemia **21**(5): 1116-1122.
- Chu, S., D. Heiser, L. Li, I. Kaplan, M. Collector, D. Huso, S. Sharkis, C. Civin and D. Small (2012). "FLT3-ITD Knockin Impairs Hematopoietic Stem Cell Quiescence/Homeostasis, Leading to Myeloproliferative Neoplasm." Cell Stem Cell **11**: 346-358.
- Deschler, B. and M. Lubbert (2006). "Acute myeloid leukemia: epidemiology and etiology." Cancer **107**(9): 2099-2107.
- Ding, L., T. J. Ley, D. E. Larson, C. A. Miller, D. C. Koboldt, J. S. Welch, J. K. Ritchey, M. A. Young, T. Lamprecht, M. D. McLellan, J. F. McMichael, J. W. Wallis, C. Lu, D. Shen, C. C. Harris, D. J. Dooling, R. S. Fulton, L. L. Fulton, K. Chen, H. Schmidt, J. Kalicki-Veizer, V. J. Magrini, L. Cook, S. D. McGrath, T. L. Vickery, M. C. Wendl, S. Heath, M. A. Watson, D. C. Link, M. H. Tomasson, W. D. Shannon, J. E. Payton, S. Kulkarni, P. Westervelt, M. J. Walter, T. A. Graubert, E. R. Mardis, R. K. Wilson and J. F. DiPersio (2012). "Clonal evolution in relapsed acute myeloid leukaemia revealed by whole-genome sequencing." Nature **481**(7382): 506-510.
- Döhner, H., D. J. Weisdorf and C. D. Bloomfield (2015). "Acute Myeloid Leukemia." New England Journal of Medicine **373**(12): 1136-1152.
- Dombret, H. and C. Gardin (2016). "An update of current treatments for adult acute myeloid leukemia." Blood **127**(1): 53-61.
- Doulatov, S., F. Notta, E. Laurenti and J. E. Dick (2012). "Hematopoiesis: a human perspective." Cell Stem Cell **10**(2): 120-136.
- Edgar, K. A., J. J. Wallin, M. Berry, L. B. Lee, W. W. Prior, D. Sampath, L. S. Friedman and M. Belvin (2010). "Isoform-specific phosphoinositide 3-kinase inhibitors exert distinct effects in solid tumors." Cancer Res **70**(3): 1164-1172.
- Estey, E. and H. Döhner (2006). "Acute myeloid leukaemia." The Lancet **368**(9550): 1894-1907.

- Folkes, A. J., K. Ahmadi, W. K. Alderton, S. Alix, S. J. Baker, G. Box, I. S. Chuckowree, P. A. Clarke, P. Depledge, S. A. Eccles, L. S. Friedman, A. Hayes, T. C. Hancox, A. Kugendradas, L. Lensun, P. Moore, A. G. Olivero, J. Pang, S. Patel, G. H. Pergl-Wilson, F. I. Raynaud, A. Robson, N. Saghir, L. Salphati, S. Sohal, M. H. Ultsch, M. Valenti, H. J. Wallweber, N. C. Wan, C. Wiesmann, P. Workman, A. Zhyvoloup, M. J. Zvelebil and S. J. Shuttleworth (2008). "The identification of 2-(1H-indazol-4-yl)-6-(4-methanesulfonyl-piperazin-1-ylmethyl)-4-morpholin-4-yl-thieno[3,2-d]pyrimidine (GDC-0941) as a potent, selective, orally bioavailable inhibitor of class I PI3 kinase for the treatment of cancer." J Med Chem **51**(18): 5522-5532.
- Folkes, A. J., K. Ahmadi, W. K. Alderton, S. Alix, S. J. Baker, G. Box, I. S. Chuckowree, P. A. Clarke, P. Depledge, S. A. Eccles, L. S. Friedman, A. Hayes, T. C. Hancox, A. Kugendradas, L. Lensun, P. Moore, A. G. Olivero, J. Pang, S. Patel, G. H. Pergl-Wilson, F. I. Raynaud, A. Robson, N. Saghir, L. Salphati, S. Sohal, M. H. Ultsch, M. Valenti, H. J. A. Wallweber, N. C. Wan, C. Wiesmann, P. Workman, A. Zhyvoloup, M. J. Zvelebil and S. J. Shuttleworth (2008). "The Identification of 2-(1H-Indazol-4-yl)-6-(4-methanesulfonyl-piperazin-1-ylmethyl)-4-morpholin-4-yl-thieno[3,2-d]pyrimidine (GDC-0941) as a Potent, Selective, Orally Bioavailable Inhibitor of Class I PI3 Kinase for the Treatment of Cancer." Journal of Medicinal Chemistry **51**: 5522-5532.
- Goodwin, C. B., X. J. Li, R. S. Mali, G. Chan, M. Kang, Z. Liu, B. Vanhaesebroeck, B. G. Neel, M. L. Loh, B. J. Lannutti, R. Kapur and R. J. Chan (2014). "PI3K p110delta uniquely promotes gain-of-function Shp2-induced GM-CSF hypersensitivity in a model of JMML." Blood.
- Greenblatt, S., L. Li, C. Slape, B. Nguyen, R. Novak, A. Duffield, D. Huso, S. Desiderio, M. Borowitz, P. Aplan and D. Small (2012). "Knock-in of a FLT3/ITD mutation cooperates with a NUP98-HOXD13 fusion to generate acute myeloid leukemia in a mouse model." Blood **119**: 2883-2894.
- Griffith, J., J. Black, C. Faerman, L. Swenson, M. Wynn, F. Lu, J. Lippke and K. Saxena (2004). "The structural basis for autoinhibition of FLT3 by the juxtamembrane domain." Mol Cell **13**(2): 169-178.
- Guney, I., S. Wu and J. M. Sedivy (2006). "Reduced c-Myc signaling triggers telomere-independent senescence by regulating Bmi-1 and p16(INK4a)." Proc Natl Acad Sci U S A **103**(10): 3645-3650.
- Gwin, K. A., M. B. Shapiro, J. J. Dolence, Z. L. Huang and K. L. Medina (2013). "Hoxa9 and Flt3 signaling synergistically regulate an early checkpoint in lymphopoiesis." J Immunol **191**(2): 745-754.

- Hahn, C. K., J. E. Berchuck, K. N. Ross, R. M. Kakoza, K. Clauser, A. C. Schinzel, L. Ross, I. Galinsky, T. N. Davis, S. J. Silver, D. E. Root, R. M. Stone, D. J. DeAngelo, M. Carroll, W. C. Hahn, S. A. Carr, T. R. Golub, A. L. Kung and K. Stegmaier (2009). "Proteomic and genetic approaches identify Syk as an AML target." Cancer Cell **16**(4): 281-294.
- Hanafusa, H., S. Torii, T. Yasunaga, K. Matsumoto and E. Nishida (2004). "Shp2, an SH2-containing protein-tyrosine phosphatase, positively regulates receptor tyrosine kinase signaling by dephosphorylating and inactivating the inhibitor Sprouty." J Biol Chem **279**(22): 22992-22995.
- Hayakawa, F., M. Towatari, H. Kiyoi, M. Tanimoto, T. Kitamura, H. Saito and T. Naoe (2000). "Tandem-duplicated Flt3 constitutively activates STAT5 and MAP kinase and introduces autonomous cell growth in IL-3-dependent cell lines." Oncogene **19**(5): 624-631.
- Heiss, E., K. Masson, C. Sundberg, M. Pedersen, J. Sun, S. Bengtsson and L. Ronnstrand (2006). "Identification of Y589 and Y599 in the juxtamembrane domain of Flt3 as ligand-induced autophosphorylation sites involved in binding of Src family kinases and the protein tyrosine phosphatase SHP2." Blood **108**(5): 1542-1550.
- Jacobs, J., K. Kieboom, S. Marino, R. DePinho and M. Van Lohuizen (1999). "The oncogene and Polycomb-group gene bmi-1 regulates cell proliferation and senescence through the ink4a locus." Nature **397**(6715): 164-168.
- Janke, H., F. Pastore, D. Schumacher, T. Herold, K.-P. Hopfner, S. Schneider, W. E. Berdel, T. Büchner, B. J. Woermann, M. Subklewe, S. K. Bohlander, W. Hiddemann, K. Spiekermann and H. Polzer (2014). "Activating FLT3 Mutants Show Distinct Gain-of-Function Phenotypes In Vitro and a Characteristic Signaling Pathway Profile Associated with Prognosis in Acute Myeloid Leukemia." PLoS ONE **9**(3): e89560.
- Jordan, C. T. and M. L. Guzman (2004). "Mechanisms controlling pathogenesis and survival of leukemic stem cells." Oncogene **23**(43): 7178-7187.
- Kawagoe, H., R. Humphries, A. Blair, H. Sutherland and D. Hogge (1999). "Expression of HOX genes, HOX cofactors, and MLL in phenotypically and functionally defined subpopulations of leukemic and normal human hematopoietic cells." Leukemia **13**(5): 687-698.
- Ke, Y., E. E. Zhang, K. Hagihara, D. Wu, Y. Pang, R. Klein, T. Curran, B. Ranscht and G. S. Feng (2007). "Deletion of Shp2 in the brain leads to defective proliferation and differentiation in neural stem cells and early postnatal lethality." Mol Cell Biol **27**(19): 6706-6717.
- Kelly, L., Q. Liu, J. L. Kutok, I. Williams, C. Boulton and D. Gililand (2001). "FLT3 internal tandem duplication mutations associated with human acute myeloid

- leukemias induce myeloproliferative disease in a murine bone marrow transplant model." Blood **99**(1): 310-318.
- Kim, K. T., K. Baird, J. Y. Ahn, P. Meltzer, M. Lilly, M. Levis and D. Small (2005). "Pim-1 is up-regulated by constitutively activated FLT3 and plays a role in FLT3-mediated cell survival." Blood **105**(4): 1759-1767.
- Kiyoi, H., R. Ohno, R. Ueda, H. Saito and T. Naoe (2002). "Mechanism of constitutive activation of FLT3 with internal tandem duplication in the juxtamembrane domain." Oncogene **21**: 2555-2563.
- Koh, H., H. Nakamae, K. Hagihara, T. Nakane, M. Manabe, Y. Hayashi, M. Nishimoto, Y. Umemoto, M. Nakamae, A. Hirose, E. Inoue, A. Inoue, M. Yoshida, M. Bingo, H. Okamura, R. Aimoto, M. Aimoto, Y. Terada, K. R. Koh, T. Yamane, M. Ohsawa and M. Hino (2011). "Factors that contribute to long-term survival in patients with leukemia not in remission at allogeneic hematopoietic cell transplantation." J Exp Clin Cancer Res **30**: 36.
- Kornblau, S. M., M. Womble, Y. H. Qiu, C. E. Jackson, W. Chen, M. Konopleva, E. H. Estey and M. Andreeff (2006). "Simultaneous activation of multiple signal transduction pathways confers poor prognosis in acute myelogenous leukemia." Blood **108**(7): 2358-2365.
- Kratz, C. P., C. M. Niemeyer, R. P. Castleberry, M. Cetin, E. Bergstrasser, P. D. Emanuel, H. Hasle, G. Kardos, C. Klein, S. Kojima, J. Stary, M. Trebo, M. Zecca, B. D. Gelb, M. Tartaglia and M. L. Loh (2005). "The mutational spectrum of PTPN11 in juvenile myelomonocytic leukemia and Noonan syndrome/myeloproliferative disease." Blood **106**(6): 2183-2185.
- Kumaravelu, P., L. Hook, A. M. Morrison, J. Ure, S. Zhao, S. Zuyev, J. Ansell and A. Medvinsky (2002). "Quantitative developmental anatomy of definitive haematopoietic stem cells/long-term repopulating units (HSC/RUs): role of the aorta-gonad-mesonephros (AGM) region and the yolk sac in colonisation of the mouse embryonic liver." Development **129**(21): 4891-4899.
- Lan, L., J. D. Holland, J. Qi, S. Grosskopf, J. Rademann, R. Vogel, B. Gyorffy, A. Wulf-Goldenberg and W. Birchmeier (2015). "Shp2 signaling suppresses senescence in PyMT-induced mammary gland cancer in mice." Embo j **34**(11): 1493-1508.
- Lee, B. H., Z. Tothova, R. L. Levine, K. Anderson, N. Buza-Vidas, D. E. Cullen, E. P. McDowell, J. Adelsperger, S. Frohling, B. J. Huntly, M. Beran, S. E. Jacobsen and D. G. Gilliland (2007). "FLT3 mutations confer enhanced proliferation and survival properties to multipotent progenitors in a murine model of chronic myelomonocytic leukemia." Cancer Cell **12**(4): 367-380.
- Leischner, H., C. Albers, R. Grundler, E. Razumovskaya, K. Spiekermann, S. Bohlander, L. Ronnstrand, K. Gotze, C. Peschel and J. Duyster (2012). "SRC is a signaling

mediator in FLT3-ITD- but not in FLT3-TKD-positive AML." Blood **119**(17): 4026-4033.

- Lessard, J. and G. Sauvageau (2003). "*Bmi-1* determines the proliferative capacity of normal and leukaemic stem cells." Nature **423**: 255-260.
- Li, W., S. A. Johnson, W. C. Shelley, M. Ferkowicz, P. Morrison, Y. Li and M. C. Yoder (2003). "Primary endothelial cells isolated from the yolk sac and para-aortic splanchnopleura support the expansion of adult marrow stem cells in vitro." Blood **102**(13): 4345-4353.
- Loh, M. L., M. G. Reynolds, S. Vattikuti, R. B. Gerbing, T. A. Alonzo, E. Carlson, J. W. Cheng, C. M. Lee, B. J. Lange and S. Meshinchi (2004). "PTPN11 mutations in pediatric patients with acute myeloid leukemia: results from the Children's Cancer Group." Leukemia **18**(11): 1831-1834.
- Loh, M. L., S. Vattikuti, S. Schubert, M. G. Reynolds, E. Carlson, K. H. Lieu, J. W. Cheng, C. M. Lee, D. Stokoe, J. M. Bonifas, N. P. Curtiss, J. Gotlib, S. Meshinchi, M. M. Le Beau, P. D. Emanuel and K. M. Shannon (2004). "Mutations in PTPN11 implicate the SHP-2 phosphatase in leukemogenesis." Blood **103**(6): 2325-2331.
- Mackarehtschian, K. H., JD; Moore, KA; Boast, S; Goff, SP; Lemischka, IR (1995). "Targeted Disruption of the *flk2/flt3* Gene Leads to Deficiencies in Primitive Hematopoietic Progenitors." Immunity **3**: 147-161.
- Majeti, R. (2014). "Clonal evolution of pre-leukemic hematopoietic stem cells precedes human acute myeloid leukemia." Best Pract Res Clin Haematol **27**(3-4): 229-234.
- Mali, R. S., P. Ma, L. F. Zeng, H. Martin, B. Ramdas, Y. He, E. Sims, S. Nabinger, J. Ghosh, N. Sharma, V. Munugalavadla, A. Chatterjee, S. Li, G. Sandusky, A. W. Craig, K. D. Bunting, G. S. Feng, R. J. Chan, Z. Y. Zhang and R. Kapur (2012). "Role of SHP2 phosphatase in KIT-induced transformation: identification of SHP2 as a druggable target in diseases involving oncogenic KIT." Blood **120**(13): 2669-2678.
- Masson, K., T. Liu, R. Khan, J. Sun and L. Ronnstrand (2009). "A role of Gab2 association in Flt3 ITD mediated Stat5 phosphorylation and cell survival." Br J Haematol **146**(2): 193-202.
- Mead, A. J., S. Kharazi, D. Atkinson, I. Macaulay, C. Pecquet, S. Loughran, M. Lutteropp, P. Woll, O. Chowdhury, S. Luc, N. Buza-Vidas, H. Ferry, S. A. Clark, N. Goardon, P. Vyas, S. N. Constantinescu, E. Sitnicka, C. Nerlov and S. E. Jacobsen (2013). "FLT3-ITDs instruct a myeloid differentiation and transformation bias in lymphomyeloid multipotent progenitors." Cell Rep **3**(6): 1766-1776.

- Miller, P. G., F. Al-Shahrour, K. A. Hartwell, L. P. Chu, M. Jaras, R. V. Puram, A. Puissant, K. P. Callahan, J. Ashton, M. E. McConkey, L. P. Poveromo, G. S. Cowley, M. G. Kharas, M. Labelle, S. Shterental, J. Fujisaki, L. Silberstein, G. Alexe, M. A. Al-Hajj, C. A. Shelton, S. A. Armstrong, D. E. Root, D. T. Scadden, R. O. Hynes, S. Mukherjee, K. Stegmaier, C. T. Jordan and B. L. Ebert (2013). "In Vivo RNAi screening identifies a leukemia-specific dependence on integrin beta 3 signaling." Cancer Cell **24**(1): 45-58.
- Mizuki, M., R. Fenski, H. Halfter, I. Matsumura, R. Schmidt, C. Mueller, W. Gruening, K. Kratz-Albers, S. Serve, C. Steur, T. Buechner, J. Kienast, Y. Kanakura, W. Berdel and H. Serve (2000). "Flt3 mutations from patients with acute myeloid leukemia induce transformation of 32D cells mediated by the Ras and STAT5 pathways." Blood **96**(12): 3907-3914.
- Mocsai, A., J. Ruland and V. L. Tybulewicz (2010). "The SYK tyrosine kinase: a crucial player in diverse biological functions." Nat Rev Immunol **10**(6): 387-402.
- Mohi, M. G. and B. G. Neel (2007). "The role of Shp2 (PTPN11) in cancer." Curr Opin Genet Dev **17**(1): 23-30.
- Mohi, M. G., I. R. Williams, C. R. Dearolf, G. Chan, J. L. Kutok, S. Cohen, K. Morgan, C. Boulton, H. Shigematsu, H. Keilhack, K. Akashi, D. G. Gilliland and B. G. Neel (2005). "Prognostic, therapeutic, and mechanistic implications of a mouse model of leukemia evoked by Shp2 (PTPN11) mutations." Cancer Cell **7**(2): 179-191.
- Moran-Crusio, K., L. Reavie, A. Shih, O. Abdel-Wahab, D. Ndiaye-Lobry, C. Lobry, M. E. Figueroa, A. Vasanthakumar, J. Patel, X. Zhao, F. Perna, S. Pandey, J. Madzo, C. Song, Q. Dai, C. He, S. Ibrahim, M. Beran, J. Zavadil, S. D. Nimer, A. Melnick, L. A. Godley, I. Aifantis and R. L. Levine (2011). "Tet2 loss leads to increased hematopoietic stem cell self-renewal and myeloid transformation." Cancer Cell **20**(1): 11-24.
- Nabinger, S. C. (2012). Molecular Mechanisms of FLT3-ITD-Induced Leukemogenesis. PhD, Indiana University School of Medicine.
- Nabinger, S. C., X. J. Li, B. Ramdas, Y. He, X. Zhang, L. Zeng, B. Richine, J. D. Bowling, S. Fukuda, S. Goenka, Z. Liu, G. S. Feng, M. Yu, G. E. Sandusky, H. S. Boswell, Z. Y. Zhang, R. Kapur and R. J. Chan (2013). "The protein tyrosine phosphatase, Shp2, positively contributes to FLT3-ITD-induced hematopoietic progenitor hyperproliferation and malignant disease in vivo." Leukemia **27**(2): 398-408.
- Nakao M, Y. S., Iwai T, Kaneko H, Horiike S, Kashima K, Sonoda Y, Fujimoto T, Misawa S. (1996). "Internal tandem duplication of the flt3 gene found in acute myeloid leukemia." Leukemia **10**(12): 1911-1918.

- Neel, B. G., H. Gu and L. Pao (2003). "The 'Shp'ing news: SH2 domain-containing tyrosine phosphatases in cell signaling." Trends Biochem Sci **28**(6): 284-293.
- Nogami, A., G. Oshikawa, K. Okada, S. Fukutake, Y. Umezawa, T. Nagao, T. Kurosu and O. Miura (2015). "FLT3-ITD confers resistance to the PI3K/Akt pathway inhibitors by protecting the mTOR/4EBP1/Mcl-1 pathway through STAT5 activation in acute myeloid leukemia." Oncotarget **6**(11): 9189-9205.
- Oellerich, T., M. F. Oellerich, M. Engelke, S. Munch, S. Mohr, M. Nimz, H. H. Hsiao, J. Corso, J. Zhang, H. Bohnenberger, T. Berg, M. A. Rieger, J. Wienands, G. Bug, C. Brandts, H. Urlaub and H. Serve (2013). "beta2 integrin-derived signals induce cell survival and proliferation of AML blasts by activating a Syk/STAT signaling axis." Blood **121**(19): 3889-3899, s3881-3866.
- Parcells, B. W., A. K. Ikeda, T. Simms-Waldrup, T. B. Moore and K. M. Sakamoto (2006). "FMS-like tyrosine kinase 3 in normal hematopoiesis and acute myeloid leukemia." Stem Cells **24**(5): 1174-1184.
- Park, I., D. Qian, M. Kiel, M. Becker, M. Pihalja, I. Weissman, S. Morrison and M. Clarke (2003). "Bmi-1 is required for maintenance of adult self-renewing haematopoietic stem cells." Nature **423**(6937): 302-305.
- Pratz, K. and M. Levis (2010). "Bench to bedside targeting of flt3 in acute myeloid leukemia." Current Drug Targets **11**(7): 781-789.
- Puissant, A., N. Fenouille, G. Alexe, Y. Pikman, C. F. Bassil, S. Mehta, J. Du, J. U. Kazi, F. Luciano, L. Ronnstrand, A. L. Kung, J. C. Aster, I. Galinsky, R. M. Stone, D. J. DeAngelo, M. T. Hemann and K. Stegmaier (2014). "SYK is a critical regulator of FLT3 in acute myeloid leukemia." Cancer Cell **25**(2): 226-242.
- Quintanar-Audelo, M., P. Yusoff, S. Sinniah, S. Chandramouli and G. R. Guy (2011). "Sprouty-related Ena/vasodilator-stimulated phosphoprotein homology 1-domain-containing protein (SPRED1), a tyrosine-protein phosphatase non-receptor type 11 (SHP2) substrate in the Ras/extracellular signal-regulated kinase (ERK) pathway." J Biol Chem **286**(26): 23102-23112.
- Reilly, J. T. (2002). "Class III receptor tyrosine kinases: role in leukaemogenesis." Br J Haematol **116**(4): 744-757.
- Rizo, A., S. Olthof, L. Han, E. Vellenga, G. de Haan and J. J. Schuringa (2009). "Repression of BMI1 in normal and leukemic human CD34(+) cells impairs self-renewal and induces apoptosis." Blood **114**(8): 1498-1505.
- Rocnik, J. L., R. Okabe, J. C. Yu, B. H. Lee, N. Giese, D. P. Schenkein and D. G. Gilliland (2006). "Roles of tyrosine 589 and 591 in STAT5 activation and transformation mediated by FLT3-ITD." Blood **108**(4): 1339-1345.

- Sarker, D., K. Kristeleit, K. E. Mazina, J. A. Ware, Y. Yan, M. Dresser, M. K. Derynck and J. De-Bono (2009). "A phase I study evaluating the pharmacokinetics (PK) and pharmacodynamics (PD) of the oral pan-phosphoinositide-3 kinase (PI3K) inhibitor GDC-0941." J. Clin. Onc. **27**: abstr 3538.
- Sauvageau, G., P. Lansdorp, C. Eaves, D. Hogge, W. Dragowska, D. Reid, C. Largman, H. Lawrence and R. Humphries (1994). "Differential expression of homeobox genes in functionally distinct CD34+ subpopulations of human bone marrow cells." Cell Biology **91**: 12223-12227.
- Saxton, T. M., M. Henkemeyer, S. Gasca, R. Shen, D. Rossi, F. Shalaby, G. Feng and T. Pawson (1997). "Abnormal mesoderm patterning in mouse embryos mutant for the SH2 tyrosine phosphatase Shp-2." The EMBO Journal **16**(9): 2352-2364.
- Siegel, R. L., K. D. Miller and A. Jemal (2015). "Cancer statistics, 2015." CA Cancer J Clin **65**(1): 5-29.
- Skoda, R. (2007). "The Genetic Basis of Myeloproliferative Disorders." Hematology: 1-10.
- Smith, L. L., J. Yeung, B. B. Zeisig, N. Popov, I. Huijbers, J. Barnes, A. J. Wilson, E. Taskesen, R. Delwel, J. Gil, M. Van Lohuizen and C. W. So (2011). "Functional crosstalk between Bmi1 and MLL/Hoxa9 axis in establishment of normal hematopoietic and leukemic stem cells." Cell Stem Cell **8**(6): 649-662.
- Sparmann, A. and M. van Lohuizen (2006). "Polycomb silencers control cell fate, development and cancer." Nat Rev Cancer **6**(11): 846-856.
- Spiekermann, K., K. Bagrintseva, R. Schwab, K. Schmieja and W. Hiddemann (2003). "Overexpression and constitutive activation of FLT3 induces STAT5 activation in primary acute myeloid leukemia blast cells." Clinical Cancer Research **9**(6): 2140-2150.
- Sprissler, C., D. Belenki, H. Maurer, K. Aumann, D. Pfeifer, C. Klein, T. A. Muller, S. Kissel, J. Hulsdunker, J. Alexandrovski, T. Brummer, H. Jumaa, J. Duyster and C. Dierks (2014). "Depletion of STAT5 blocks TEL-SYK-induced APMF-type leukemia with myelofibrosis and myelodysplasia in mice." Blood Cancer J **4**: e240.
- Tartaglia, M., S. Martinelli, G. Cazzaniga, V. Cordeddu, I. Iavarone, M. Spinelli, C. Palmi, C. Carta, A. Pession, M. Arico, G. Masera, G. Basso, M. Sorcini, B. D. Gelb and A. Biondi (2004). "Genetic evidence for lineage-related and differentiation stage-related contribution of somatic PTPN11 mutations to leukemogenesis in childhood acute leukemia." Blood **104**(2): 307-313.
- Tartaglia, M., C. M. Niemeyer, A. Fragale, X. Song, J. Buechner, A. Jung, K. Hahlen, H. Hasle, J. D. Licht and B. D. Gelb (2003). "Somatic mutations in PTPN11 in

- juvenile myelomonocytic leukemia, myelodysplastic syndromes and acute myeloid leukemia." Nat Genet **34**(2): 148-150.
- Thiede, C., C. Steudel, B. Mohr, M. Schaich, U. Schaekel, U. Platzbecker, M. Wermke, M. Bornhaeuser, M. Ritter, A. Neubauer, G. Ehninger and T. Illmer (2002). "Analysis of FLT3-activating mutations in 979 patients with acute myelogenous leukemia: association with FAB subtypes and identification of subgroups with poor prognosis." Blood **99**(12): 4326-4335.
- Turner, M., P. J. Mee, P. S. Costello, O. Williams, A. A. Price, L. P. Duddy, M. T. Furlong, R. L. Geahlen and V. L. Tybulewicz (1995). "Perinatal lethality and blocked B-cell development in mice lacking the tyrosine kinase Syk." Nature **378**(6554): 298-302.
- Wagner, A. J., D. H. Von Hoff, M. LoRusso, R. Tibes, K. E. Mazina, J. A. Ware, Y. Yan, M. K. Derynck and G. D. Demetri (2009). "A first-in-human phase I study to evaluate the pan-PI3K inhibitor GDC-0941 administered QD or BID in patients with advanced solid tumors." J. Clin. Onc. **27**: 3501.
- Xu, R., Y. Yu, S. Zheng, X. Zhao, Q. Dong, Z. He, Y. Liang, Q. Lu, Y. Fang, X. Gan, X. Xu, S. Zhang, X. Zhang and G. S. Feng (2005). "Overexpression of Shp2 tyrosine phosphatase is implicated in leukemogenesis in adult human leukemia." Blood **106**(9): 3142-3149.
- Yoder, M. C., K. Hiatt and P. Mukherjee (1997). "In vivo repopulating hematopoietic stem cells are present in the murine yolk sac at day 9.0 postcoitus." Proceedings of the National Academy of Sciences of the United States of America **94**(13): 6776-6780.
- You, M., D. H. Yu and G. S. Feng (1999). "Shp-2 tyrosine phosphatase functions as a negative regulator of the interferon-stimulated Jak/STAT pathway." Mol Cell Biol **19**(3): 2416-2424.
- Yu, W. M., H. Daino, J. Chen, K. D. Bunting and C. K. Qu (2006). "Effects of a leukemia-associated gain-of-function mutation of SHP-2 phosphatase on interleukin-3 signaling." J Biol Chem **281**(9): 5426-5434.
- Zhang, E. E., E. Chapeau, K. Hagihara and G. S. Feng (2004). "Neuronal Shp2 tyrosine phosphatase controls energy balance and metabolism." Proc Natl Acad Sci U S A **101**(45): 16064-16069.
- Zhang, S. and H. E. Broxmeyer (1999). "p85 subunit of PI3 kinase does not bind to human Flt3 receptor, but associates with SHP2, SHIP, and a tyrosine-phosphorylated 100-kDa protein in Flt3 ligand-stimulated hematopoietic cells." Biochem Biophys Res Commun **254**(2): 440-445.

- Zhang, S. and H. E. Broxmeyer (2000). "Flt3 ligand induces tyrosine phosphorylation of gab1 and gab2 and their association with shp-2, grb2, and PI3 kinase." Biochem Biophys Res Commun **277**(1): 195-199.
- Zhang, S., C. Mantel and H. E. Broxmeyer (1999). "Flt3 signaling involves tyrosyl-phosphorylation of SHP-2 and SHIP and their association with Grb2 and Shc in Baf3/Flt3 cells." J Leukoc Biol **65**(3): 372-380.
- Zhang, X., Y. He, S. Liu, Z. Yu, Z. X. Jiang, Z. Yang, Y. Dong, S. C. Nabinger, L. Wu, A. M. Gunawan, L. Wang, R. J. Chan and Z. Y. Zhang (2010). "Salicylic acid based small molecule inhibitor for the oncogenic Src homology-2 domain containing protein tyrosine phosphatase-2 (SHP2)." J Med Chem **53**(6): 2482-2493.
- Zhu, H., K. Ji, N. Alderson, Z. He, S. Li, W. Liu, D. Zhang, L. Li and G. Feng (2011). "Kit-Shp2-Kit signaling acts to maintain a functional hematopoietic stem and progenitor cell pool." Blood **117**(20): 5350-5361.

CURRICULUM VITAE

Briana Marie Richine

EDUCATION

- 2016 PhD, Medical and Molecular Genetics, with Minor in Cancer
Biology
Indiana University, Indianapolis, IN
IU Biomedical Gateway Program (IBMG) for PhD Study
- 2011 BS, Chemistry, Cum Laude, with Highest Departmental Honors
Butler University, Indianapolis, IN

AWARDS AND HONORS

- 2015 Awarded Oral Presentation at Midwest Blood Club Symposium,
French Lick, IN
- 2015 Invited to Speak at IUSM Medical and Molecular Genetics
“Introduction to the Department” Seminar
- 2015 Honorable Mention at IU Simon Cancer Center Annual Cancer
Research Day, IUSM, Indianapolis, IN
- 2013 Merit Award Recipient, Awarded Oral Presentation at Midwest
Blood Club Symposium, Cincinnati, OH
- 2013 Honorable Mention at IU Simon Cancer Center Annual Cancer
Research Day, IUSM, Indianapolis, IN
- 2011 B.S. with highest departmental honors and Cum Laude, Butler
University, Indianapolis, IN
- 2011 American Chemical Society Certification
- 2008-09,
2009-10,
2010-11 Dean’s List, Butler University, Indianapolis, IN
- 2007-11 Academic Scholarship, Butler University, Indianapolis, IN

PUBLICATIONS

MANUSCRIPTS:

Nabinger, SC, XJ Li, B Ramdas, Y He, X Zhang, L Zeng, **BM Richine**, JD Bowling, S Fukuda, S Goenka, Z Liu, G-S Feng, M Yu, GE Sandusky, HS Boswell, Z-Y Zhang, R Kapur, RJ Chan. 2012. The Protein Tyrosine Phosphatase, Shp2, Positively Contributes to FLT3-ITD-Induced Hematopoietic Progenitor Hyperproliferation and Malignant Disease *In Vivo*. *Leukemia*, **27**, 398-408.

Li, W, HJ Garringer, CB Goodwin, **B Richine**, A Acton, N VanDuyn, BB Muhoberac, J Irimia-Dominguez, RJ Chan, M Peacock, R Nass, B Ghetti, R Vidal. 2015. Systemic and cerebral iron homeostasis in ferritin knock-out mice. *PLOS One*.

Li, XJ, CB Goodwin, SC Nabinger, **BM Richine**, Z Yang, G Chan, H Hanenberg, H Ohnishi, T Matozaki, BG Neel, GS Feng, RJ Chan. 2015. Protein Tyrosine Phosphatase, Shp2, Positively Regulates Macrophage Oxidative Burst. *JBC*.

ORAL PRESENTATIONS:

Richine, BM, SC Nabinger, Y Liu, RJ Chan. 2015. Regulation of senescence in FLT3-ITD-expressing cells by the protein tyrosine phosphatase, Shp2. MWBC, French Lick, IN, October 10-13, 2015.

Richine, BM, SC Nabinger, R Gao, Y Liu, and RJ Chan. 2013. Regulation of senescence in FLT3-ITD-expressing cells by the protein tyrosine phosphatase, Shp2. MWBC, Cincinnati, OH, September 19-20, 2013. ***Merit Award Recipient***

ABSTRACTS:

Richine, BM, SC Nabinger, Y Liu, RJ Chan. 2015. Regulation of senescence in FLT3-ITD-expressing cells by the protein tyrosine phosphatase, Shp2. MWBC, French Lick, IN, October 10-13, 2015.

Richine, BM, SC Nabinger, Y Liu, RJ Chan. 2015. Regulation of senescence in FLT3-ITD-expressing cells by the protein tyrosine phosphatase, Shp2. IUSCC Cancer Research Day, Indianapolis, IN, May 21, 2015. ***Honorable Mention***

Richine, BM, SC Nabinger, J Bowling, and RJ Chan. 2014. Shp2 Tyrosine Phosphatase Cooperates with Src and Syk Tyrosine Kinases to Promote FLT3-ITD-Induced Acute Myeloid Leukemia. IUSCC Cancer Research Day, Indianapolis, IN, May 19, 2014.

Richine, BM, SC Nabinger, R Gao, Y Liu, and RJ Chan. 2013. Regulation of senescence in FLT3-ITD-expressing cells by the protein tyrosine phosphatase, Shp2. MWBC, Cincinnati, OH, September 19-20, 2013. ***Merit Award Recipient***

Richine, BM, SC Nabinger, R Gao, Y Liu, and RJ Chan. 2013. Regulation of senescence in FLT3-ITD-expressing cells by the protein tyrosine phosphatase, Shp2. IUSCC Cancer Research Day, Indianapolis, IN, May 22, 2013. ***Honorable Mention***

Nabinger, SC, XJ Li, B Ramdas, Y He, X Zhang, **BM Richine**, JD Bowling, S Fukuda, S Goenka, Z Liu, G-S Feng, M Yu, GE Sandusky, HS Boswell, Z-Y Zhang, R Kapur, RJ Chan. 2013. The Protein Tyrosine Phosphatase, Shp2, Positively Contributes to FLT3-ITD-Induced Malignant Disease *In Vivo* and Co-Localizes with Nuclear Phospho-STAT5 in FLT3-ITD-Expressing Leukemic Cells. Annual Meeting of the American Society of Hematology, Atlanta, Georgia. December 8-11, 2012.

Richine, BM, G Hoops. Determination of Cytochrome *c*'s Affinity towards Various Chemically Modified Silica Surfaces via Attenuated Total Reflection Spectroscopy. Butler University Undergraduate Research Conference, April 16, 2010.

Hoops, G, and **BM Richine**: "Cytochrome *c* adsorption to chemically modified silica surfaces" 2010 International Chemical Congress of Pacific Basin Societies (*a.k.a.* Pacifichem). Honolulu, Hawaii. December 15-20, 2010.

GRANTS

- | | |
|-----------|---|
| 2015-2017 | Pre-Doctoral Individual National Cancer Institute Award, F31 CA183342-01A1 |
| 2014-2015 | Cancer Biology Training Program Fellowship, IUSCC, IUSM, Indianapolis, IN |
| 2013-2014 | T32 HL007910, "Basic Science Studies on Gene Therapy of Blood Diseases", IUSM, Indianapolis, IN |